AD NUMBER
AD477070
LIMITATION CHANGES

TO:

Approved for public release; distribution is unlimited. Document partially illegible.

FROM:

Distribution authorized to U.S. Gov't. agencies and their contractors; Critical Technology; DEC 1965. Other requests shall be referred to Air Force Rome Air Development Center, EMASP, Griffiss AFB, NY. Document partially illegible. This document contains export-controlled technical data.

AUTHORITY

RADC USAE ltr 17 Sep 1971

EXPERIMENTAL AND ANALYTICAL INVESTIGATION
OF TARGET SCATTERING MATRICES

C. C. Freeny
General Dynamics/Fort Worth

Space Surveillance and Instrumentation Branch
Rome Air Development Center
Research and Technology Division
Air Force Systems Command
Griffiss Air Force Base, New York

DISCLAIMER NOTICE

THIS DOCUMENT IS BEST QUALITY AVAILABLE. THE COPY FURNISHED TO DTIC CONTAINED A SIGNIFICANT NUMBER OF PAGES WHICH DO NOT REPRODUCE LEGIBLY.

EXPERIMENTAL AND ANALYTICAL INVESTIGATION
OF TARGET SCATTERING MATRICES

C. C. Freeny
General Dynamics/Fort Worth

FOREWORD

This report was sponsored by the Space Surveillance and Instrumentation Branch of Rome Air Development Center. The report is a documentation of an experimental investigation of target scattering matrices conducted by General Dynamics/Fort Worth Division under Contract AF30(602)-3716, Project No. 6512. The work was carried out under the auspices of Mr. D. M. Montana and Capt. J. Fogarty of RADC (EMASP). This report is General Dynamics report No. FZE-473.

This technical report has been reviewed and is approved.

Approved: DONALD M. MONTANA
Program Directors' Office
Space Surveillance and
Instrumentation Branch

Approved: THOMAS S. BOND, JR.
Colonel, USAF
Chief, Surveillance and
Control Division

FOR THE COMMANDER:
IRVING J. GABELMAN
Chief, Advanced Studies Group

ii

RADC-TR-65-298

ABSTRACT

Included in this report are the results of an investigation concerning scattering matrices of several types of targets. The primary purpose of the investigation was to investigate the degradation of data resulting from cross section and phase computations by using a scattering matrix whose elements had been degraded by noise.

A review of the matrix representation of target scattering characteristics is presented along with a discussion of the measurement system and calibration procedure used to obtain the measured data. The measured data was obtained by using an absolute phase measuring radar system operating at 3 gigahertz. The scattering matrix of three targets, designed to exhibit distinctly different scattering characteristics, was measured at various signal-to-noise ratios. The measured data was then used as input data to an IBM 7090 which calculated cross sections and phase at five polarizations. The calculated data was then used to generate degradation curves for each of the three types of targets. In addition, computed versus measured cross section and phase information on each of the three targets is presented for the case of 45-degree linear transmission and reception.

TABLE OF CONTENTS

LIST OF FIGURES

LIST OF FIGURES (Continued)

viii

LIST OF FIGURES (Continued)

LIST OF TABLES

EVALUATION

1. The purpose of this effort was to investigate the degradation of the scattering matrix transformation as a function of the signal-to-noise ratio of the received radar echo. This work was done to determine what signal-to-noise criteria should be used if scattering matrix concepts are to be incorporated in an operational radar.

2. The effort resulted in a report which contains degradation curves for three classes of targets in addition to calculated (via scattering matrix) and measured radar cross section and phase data for various signal-to-noise ratios.

3. In acquiring the data required for the report, the contractor demonstrated that rather precise radar cross section and phase data could be produced via the scattering matrix calculation. The ability to make the scattering matrix calculation is now being incorporated in the RAT SCAT (Radar Target Scatter Site) equipment. When this work is complete, it is expected that RAT SCAT will be able to obtain the scattering matrix of a target and then calculate what that target's radar cross section and phase should be for any arbitrary polarization.

DONALD M. MONTANA
Program Directors' Office
Space Surveillance and
Instrumentation Branch

SECTION I

INTRODUCTION

In general, the scattering matrix of a target contains significantly more information than the cross section of the target obtained at one or several polarizations. In particular, if the scattering matrix of a target is available, the cross section of the target can be computed for every possible polarization combination of a radar transmitter and receiver system.

In addition to the capability just noted, the information contained in the scattering matrix is useful in studies of (1) cross section at other aspect angles, (2) effects of Faraday rotation on target signatures, (3) target signature discrimination, and (4) polarization stepping (analogous to frequency stepping).

In some studies, the accuracy with which the scattering matrix can be obtained is not important, but in others, the accuracy of the data directly influences the results obtained by using the scattering matrix. The primary purpose set for the program being reported was to investigate the degradation of the data obtained via the scattering matrix as a function of the signal-to-noise ratio. Although there are other important degradation parameters which could be investigated, such as phase error and/or aspect error, a common problem associated with the recording of targets is that a significant percent of the time the return signal level is quite close to that of the system sensitivity. In order to investigate the influence of scattering matrix degradation as a function of noise, several types of matrices were used in order to obtain information representative of most types of targets. In particular, the scattering matrices of three targets were used to arrive at the degradation curves presented in this report. The first target was such that the amplitude coefficients of the scattering matrix were nominally of the same value (within 0 to 10 db), that is, the target was of such a nature that it significantly depolarized the illuminating field. The second target was such that the relative phase angles of the scattering matrix covered a significant dynamic range at a significant rate relative to each other. The third target was a "typical" aerospace vehicle in which the frequency-to-size scale factors were compatible with those of full-scale vehicles and operational measurement radars. The matrices of these three types of targets are sufficiently representative that, at least over a limited aspect region, they give degradation information on most targets of interest.

The linear monostatic scattering matrix was measured for each of the targets at 1/10-degree aspect angles for a total of 3600 scattering matrices for each target at each signal-to-noise ratio. This data was then processed in a digital computer where cross section and phase were computed for each of five polarizations. The computed cross section and phase of each target were compared at each of the signal-to-noise ratios with those computed for maximum signal-to-noise; the scattering matrices recorded under maximum signal-to-noise conditions were used to generate reference data for each of the targets. From these comparisons, cross section and phase error cumulative distributions were generated as a function of signal-to-noise.

In addition to the study outlined above, the cross section and phase of each target were measured at a polarization other than the linear polarizations used to obtain the

1

target scattering matrix. The scattering matrix was then used to compute the cross section and phase at the selected measurement polarization, and the results were compared. This experiment was conducted in order to provide data as to the practicality of using the scattering matrix to obtain cross section information rather than provide measurement capability for arbitrary polarization. The results of these experiments were quite positive in that the differences between measured and computed values were in most cases of the same order as the errors caused by cross section and phase measurement limitations. The results were quite good in view of the fact that an absolute phase measuring system, operating at 3 gigahertz, was used to obtain phase information rather than a relative phase measuring system.

A review of the basic concepts of the scattering matrix is presented in Section II, along with a discussion of the factors which must be accounted for in a measurement system in order to measure a target scattering matrix accurately. At the end of the section an amplitude and phase calibration procedure, based on the use of a sphere, is outlined. Section II also contains a brief description of the measurement system used to obtain the data reported.

Section III contains a description of the targets measured, along with their scattering characteristics. The reference used to measure the signal-to-noise (S/N) is discussed, and several patterns obtained at the lower values of S/N are presented for each of the targets. Computed cross sections and phase for 45-degree linear polarization are presented along with measured records of these conditions. The polarizations used in the degradation study are discussed and the degradation curves for phase and cross section are presented.

The results of the program are discussed in Section IV in terms of the requirements imposed on a measurement system designed to obtain the scattering matrix for use in various studies. In conclusion, a discussion is presented on several studies similar to the one reported of other factors which influence the data obtained from a target scattering matrix. Also, several uses of the scattering matrix are discussed, and examples based on the data generated under this study are presented.

2

SECTION II

MATRIX REVIEW AND MEASUREMENT SYSTEM

The scattering matrix is an efficient means of describing the polarization dependence of a target signature. However, the elements of the scattering matrix are in general complex numbers; hence to obtain the matrix, a measurement system capable of measuring both cross section and phase is required. In this section a review of the basic properties of a scattering matrix is presented and is followed by a discussion of the calibration procedure and measurement system used to obtain the results which are reported.

The scattering matrix discussion is limited to the case of monostatic scattering, and it is assumed that the targets scatter in a linear manner. A more detailed discussion of scattering matrix properties and identities is given in Reference 1.

The measurement system used to obtain the matrices reported in this document was of the so-called absolute phase measuring type, which is just one of several techniques that can be used to obtain matrix data (Reference 1 contains a discussion of other techniques). The cross section facility used is a quasi-monostatic ground plane type facility; Reference 2 contains a discussion of the operating principles and typical data obtained from a range of this type. Measurement procedures, system performance, and factors, such as calibration techniques, antenna isolation, bistatic angle, recorder dynamic range, frequency stability, and target motion are all important in a measurement program of this type. Hence, following the review of the scattering matrix, these factors are discussed in terms of their relationship to the measurement system used in this program.

Scattering Matrix

In general, a target scattering matrix is dependent upon the bistatic angle between the transmitter and receiver. However, the only basic difference between the bistatic matrix and monostatic matrix is that the monostatic matrix is generally symmetrical (except possibly in the case of nonlinear scatterers). In the following discussion, the conditions will be restricted to monostatic scattering and linear scatterers.

The principle of superposition is a physical basis for explaining the fact that a set of cross section and phase measurements obtained at two orthogonal polarizations suffice to compute the cross section and phase at all polarizations. In other words, all possible polarizations which a transmitter and receiver can produce and see in the far field can be derived from a set of two vectors of diminsion two. Hence, given the cross section and phase of each of the components of the two vectors, the cross section and phase of any other polarization can be expressed in terms of these four cross sections and phases. This concept is expressed compactly in matrix notation in Equation 1 where the amplitude dependence on range has been neglected.

3

$$\sqrt{\sigma}_{tr}\,\epsilon^{i\phi_{tr}} = \left[\,\mathrm{Sin}\,\gamma_r,\ \mathrm{Cos}\,\gamma_r\,\epsilon^{i\delta_r}\right]$$

$$\begin{bmatrix} \sqrt{\sigma\pi/2,\ \pi/2}\,\epsilon^{i\phi\pi/2,\ \pi/2} & \sqrt{\sigma o,\ \pi/2}\,\epsilon^{i\phi o,\ \pi/2} \\[2ex] \sqrt{\sigma\pi/2,\ o}\,\epsilon^{i\phi\pi/2,\ 0} & \sqrt{\sigma o,\ o}\,\epsilon^{i\phi_{o,\,o}} \end{bmatrix} \begin{bmatrix} \mathrm{Sin}\,\gamma_t \\[2ex] \mathrm{Cos}\,\gamma_t\,\epsilon^{i\delta_t} \end{bmatrix}$$

(1)

$\sqrt{\sigma}_{tr}\,\epsilon^{i\phi_{tr}}$ = square root of cross section and phase at the transmitter polarization condition (t) and the receiver polarization condition (r).

$(\mathrm{Sin}\,\gamma_r,\ \mathrm{Cos}\,\gamma_r\,\epsilon^{i\delta_r})$ = a complex vector of dimension two which represents the possible polarization conditions of the radar receiver

$(\mathrm{Sin}\,\gamma_t,\ \mathrm{Cos}\,\gamma_t\,\epsilon^{i\delta_t})$ = a complex vector of dimension two which represents the possible polarization conditions of the transmitter

The elements of the two-by-two matrix represent the square root of cross section and the phase at the transmitter and receiver polarization conditions indicated by the subscripts. A common method of identifying the elements of the matrix is to let $\pi/2$ represent vertical polarization and o represent horizontal polarization; this identification will be used in the remainder of the report where the subscript V will denote vertical and H horizontal.

The scattering matrix noted in Equation 1 is called the linear scattering matrix since the elements of the scattering matrix are those corresponding to the four linear conditions "transmit" V, "receive" V (TV, RV), "transmit" V, "receive" H (TV, RH), "transmit" H, "receive" V (TH, RV), and "transmit" H, "receive" H (TH, RH), Other representations, such as a circular polarization scattering matrix, are sometimes used, but any one representation can be transformed to the other by use of a simple transformation which is indicated in the following steps.

4

Starting with Equation 1, the identity matrix is inserted as noted in Equation 2

$$\sqrt{\sigma_{tr}}\,\epsilon^{i\phi_{tr}} = \begin{bmatrix} \mathrm{Sin}\gamma_r, & \mathrm{Cos}\gamma_r\,\epsilon^{i\delta_r} \end{bmatrix} \begin{bmatrix} 1 & 0 \\ 0 & 1 \end{bmatrix}$$

$$\begin{bmatrix} \sqrt{\sigma_{VV}}\,\epsilon^{i\phi_{VV}} & \sqrt{\sigma_{HV}}\,\epsilon^{i\phi_{HV}} \\ \sqrt{\sigma_{VH}}\,\epsilon^{i\phi_{VH}} & \sqrt{\sigma_{HH}}\,\epsilon^{i\phi_{HH}} \end{bmatrix} \begin{bmatrix} 1 & 0 \\ 0 & 1 \end{bmatrix} \begin{bmatrix} \mathrm{Sin}\,\gamma_t \\ \mathrm{Cos}\gamma_t\,\epsilon^{i\delta_t} \end{bmatrix}$$

$$(2)$$

Now the identity matrix is equal to the product of any nonsingular matrix multiplied by its inverse, as indicated in Equation 3.

$$\begin{bmatrix} 1 & 0 \\ 0 & 1 \end{bmatrix} = \begin{bmatrix} a_{11} & a_{12} \\ a_{21} & a_{22} \end{bmatrix} \begin{bmatrix} a_{11} & a_{12} \\ a_{21} & a_{22} \end{bmatrix}^{-1}$$

$$(3)$$

To evaluate the elements of the matrix in Equation 3, another polarization basis can be selected, such as right and left circular or plus 45-degree linear and minus 45-degree linear since these are independent (orthogonal) polarizations. To illustrate the procedure, the linear "transmit" and "receive" polarization vectors of Equation 2 will be transformed to a circular polarization system. Multiplying the linear vector in Equation 2 by the first matrix on the right-hand side of Equation 3 gives the vector of Equation 4.

$$\begin{bmatrix} a_{11}\,\mathrm{Sin}\gamma_r + a_{21}\,\mathrm{Cos}\gamma_r\,\epsilon^{i\delta_r}, & a_{12}\,\mathrm{Sin}\gamma_r + a_{22}\,\mathrm{Cos}\gamma_r\,\epsilon^{i\delta_r} \end{bmatrix}$$

$$(4)$$

To evaluate the a_{ij} elements, it is noted that, in the case of a circular base system, the second component of the vector should be zero when the first component is, say, right circular $(\gamma_r = \pi/4,\ \delta_r = -\pi/2)$, and the first component squared should be 1 at this same condition. This latter condition insures that the vector "length", which corresponds to field intensity, is maintained the same before and after the transformation (i.e., conservation of power). A similar set of conditions for left circular $(\gamma_r = \pi/4,\ \delta_r = \pi/2)$ gives another two relationships from which the four a_{ij} values

5

are determined as $a_{11} = 1/\sqrt{2}$, $a_{21} = 1/\sqrt{2}$, $a_{12} = 1/\sqrt{2}$, $a_{22} = -1/\sqrt{2}$. Use of these values for a_{ij} to transform the receiver vector and a similar set determined by operating on the transmitter vector gives

$$\sqrt{\sigma_{tr}}\,\epsilon^{i\phi_{tr}} = 1/4 \left[\sin\gamma_r + i\cos\gamma_r\,\epsilon^{i\delta_r},\ \sin\gamma_r - i\cos\gamma_r\,\epsilon^{i\delta_r} \right]$$

$$\begin{bmatrix} 1 & -i \\ i & 1 \end{bmatrix}$$

right circular

$$\frac{a_{11}^2}{2} - a_{11}a_{21}i - \frac{a_{21}^2}{2} = 1$$

$$\frac{a_{12}}{\sqrt{2}} - \frac{a_{22}}{\sqrt{2}}i = 0$$

left circular

$$\frac{a_{12}^2}{2} + a_{12}a_{22}i - \frac{a_{22}^2}{2} = 1$$

$$\frac{a_{11}}{\sqrt{2}} + \frac{a_{21}}{\sqrt{2}}i = 0$$

$$\begin{bmatrix} \sqrt{\sigma_{VV}}\,\epsilon^{i\phi_{VV}} & \sqrt{\sigma_{HV}}\,\epsilon^{i\phi_{HV}} \\ \sqrt{\sigma_{VH}}\,\epsilon^{i\phi_{VH}} & \sqrt{\sigma_{HH}}\,\epsilon^{i\phi_{HH}} \end{bmatrix} \begin{bmatrix} 1 & 1 \\ -i & +i \end{bmatrix} \begin{bmatrix} \sin\gamma_t + i\cos\gamma_t\,\epsilon^{i\delta_t} \\ \sin\gamma_t - i\cos\gamma_t\,\epsilon^{i\delta_t} \end{bmatrix}$$

(5)

6

Performing the multiplication indicated in Equation 5 on the linear scattering matrix gives the circular scattering matrix in Equation 6.

$$\sqrt{\sigma_{tr}}\,\epsilon^{i\phi_{tr}} = 1/4 \left[\sin\gamma_r + i\cos\gamma_r\,\epsilon^{i\delta_r},\;\; \sin\gamma_r - i\cos\gamma_r\,\epsilon^{i\delta_r} \right]$$

$$\begin{bmatrix} \sqrt{\sigma_{RR}}\,\epsilon^{i\phi_{RR}} & \sqrt{\sigma_{LR}}\,\epsilon^{i\phi_{LR}} \\ \\ \sqrt{\sigma_{RL}}\,\epsilon^{i\phi_{RL}} & \sqrt{\sigma_{LL}}\,\epsilon^{i\phi_{LL}} \end{bmatrix} \begin{bmatrix} \sin\gamma_t + i\cos\gamma_t\,\epsilon^{i\delta_t} \\ \\ \sin\gamma_t - i\cos\gamma_t\,\epsilon^{i\delta_t} \end{bmatrix}$$

$$\text{(6)}$$

$$\sqrt{\sigma_{RR}}\,\epsilon^{i\phi_{RR}} = \sqrt{\sigma_{VV}}\,\epsilon^{i\phi_{VV}} - \sqrt{\sigma_{HH}}\,\epsilon^{i\phi_{HH}} - i\,(\sqrt{\sigma_{VH}}\,\epsilon^{i\phi_{VH}} + \sqrt{\sigma_{HV}}\,\epsilon^{i\phi_{HV}})$$

$$\sqrt{\sigma_{RL}}\,\epsilon^{i\phi_{RL}} = (\sqrt{\sigma_{VV}}\,\epsilon^{i\phi_{VV}} + \sqrt{\sigma_{HH}}\,\epsilon^{i\phi_{HH}}) + i\,(\sqrt{\sigma_{VH}}\,\epsilon^{i\phi_{VH}} - \sqrt{\sigma_{HV}}\,\epsilon^{i\phi_{HV}})$$

$$\sqrt{\sigma_{LR}}\,\epsilon^{i\phi_{LR}} = (\sqrt{\sigma_{VV}}\,\epsilon^{i\phi_{VV}} + \sqrt{\sigma_{HH}}\,\epsilon^{i\phi_{HH}}) + i\,(\sqrt{\sigma_{HV}}\,\epsilon^{i\phi_{HV}} - \sqrt{\sigma_{VH}}\,\epsilon^{i\phi_{VH}})$$

$$\sqrt{\sigma_{LL}}\,\epsilon^{i\phi_{LL}} = (-\sqrt{\sigma_{HH}}\,\epsilon^{i\phi_{HH}} + \sqrt{\sigma_{VV}}\,\epsilon^{i\phi_{VV}}) + i\,(\sqrt{\sigma_{VH}}\,\epsilon^{i\phi_{VH}} + \sqrt{\sigma_{HV}}\,\epsilon^{i\phi_{HV}})$$

The circular scattering matrix form given in Equation 6 is convenient for recording target scattering characteristics in the case of a radar which operates primarily in the circular polarization modes. As in the linear scattering matrix case, cross sections at other polarizations can be computed by adjusting the parameters γ_r, δ_r, γ_t and δ_t. For example,

$$\sqrt{\sigma_{VV}}\,\epsilon^{i\phi_{VV}}$$

is given by letting $\gamma_r = \gamma_t = \pi/2$ and δ_r and δ_t be arbitrary, and in terms of circular scattering matrix components is given by

$$\sqrt{\sigma_{VV}}\,\epsilon^{i\phi_{VV}} = 1/4\,(\sqrt{\sigma_{RR}}\,\epsilon^{i\phi_{RR}} + \sqrt{\sigma_{LL}}\,\epsilon^{i\phi_{LL}} + \sqrt{\sigma_{LR}}\,\epsilon^{i\phi_{LR}} + \sqrt{\sigma_{RL}}\,\epsilon^{i\phi_{RL}})$$

$$\text{(7)}$$

7

The measurement system used to obtain the data being reported was a linear polariza-
tion system; consequently, throughout the remainder of the report, the discussions
will be based on the linear scattering matrix of Equation 2. Before the calibration
procedures are discussed, the symmetry properties of the scattering matrix are
noted, as well as appropriate comments concerning the polarization convention adopted
in this report and the phase components of the scattering matrix elements.

In the monostatic case, the principle of reciprocity can be used to demonstrate
that

$$\sqrt{\sigma_{VH}}\; \epsilon^{i\phi_{VH}} = \sqrt{\sigma_{HV}}\; \epsilon^{i\phi_{HV}}$$

in the case of linear scatterers. This symmetry condition reduces the number of
measurements required to obtain the matrix elements in Equation 2 from eight to six.
In addition, it is noted that each of the phase terms in Equation 2 included a component
due to the range between the radar and target. Since this range term is a function of time,
it is quite dependent on the measurement conditions, and for this reason phase ϕ_{tr} is
usually referenced to some phase term of the matrix. In the computational equations
used in the study being reported, all computed phases were referenced to the phase
ϕ_{VV}. Hence, to compare measured phase with computed phase, ϕ_{VV} was added to
the computed phases (Section III). In the case of a radar which can receive on two
channels simultaneously, relative phase can be measured directly. Relative phase
measurements versus absolute are discussed in more detail in Section IV.

The polarization conventions which are used throughout this report are defined in
terms of the polarization parameters of the transmitter (γ_t, δ_t) and the receiver
(γ_r, δ_r); the γ parameters determine the space direction of the field and the δ param-
eters denote the time angle between the orthogonal space vectors. Any polarization
can be selected by choosing the correct value of γ and δ from their ranges of
$-\pi/2 \leq (\gamma, \delta) \leq \pi/2$. A negative δ represents a field vector rotating in a clockwise
direction as observed in the case of a wave moving away from the observer, and a
positive δ represents a counterclockwise rotating vector (this convention holds when
$\gamma > 0$; when $\gamma < 0$, the rotations are reversed). The polarizations used in this study
are listed in Table 1 in terms of the polarization parameters and the abbreviations
used to designate these conditions.

Calibration

The scattering matrix noted in Equation 2 represents the ideal case when the
measurement system is calibrated to measure cross section and phase for each of the
conditions (TV, RV), (TV, RH), (TH, RH). In practice, equipment requirements and
calibration procedures must be established in order to approximate the ideal case
sufficiently. Before the system requirements are discussed, consideration will be
given to the calibration procedure used to normalize the cross section to dbsm (decibels
relative to a square meter) and the phase relative to a range term.

The measurement system used in this study was a dual-antenna system, operat-
ing on a ground plane range, as indicated in Figure 1. In Figure 1, the influences of
the antenna system and ground plane are noted by transformation circuits since they
operate on the transmitted and reflected waves to alter the horizontal and vertical
components. In the analysis that follows, it will be assumed that these are linear

8

TABLE 1

POLARIZATION CONDITIONS

| γ_t	δ_t	γ_r	δ_r	Polarization Abbreviations		
				Transmit	Receive	Abbreviation
$\pi/2$	arbitrary	$\pi/2$	arbitrary	Vertical (V)	Vertical (V)	(TV, RV)
$\pi/2$	arbitrary	0	0	Vertical (V)	Horizontal (H)	(TV, RH)
0	0	$\pi/2$	arbitrary	Horizontal (H)	Vertical (V)	(TH, RV)
0	0	0	0	Horizontal (H)	Horizontal (H)	(TH, RH)
$\pi/4$	0	$\pi/4$	0	45 degree	45 degree	(T $\pi/4$, R $\pi/4$)
$\pi/4$	$-\pi/2$	$\pi/4$	$-\pi/2$	Right Circular (R)	Right Circular (R)	(TR, RR)
$\pi/4$	$-\pi/2$	$\pi/4$	$\pi/2$	Right Circular (R)	Left Circular (L)	(TR, RL)
$\pi/4$	$-\pi/2$	$\pi/2$	arbitrary	Right Circular (R)	Vertical (V)	(TR, RV)
$\pi/4$	$-\pi/2$	0	0	Right Circular (R)	Horizontal (H)	(TR, RH)

9
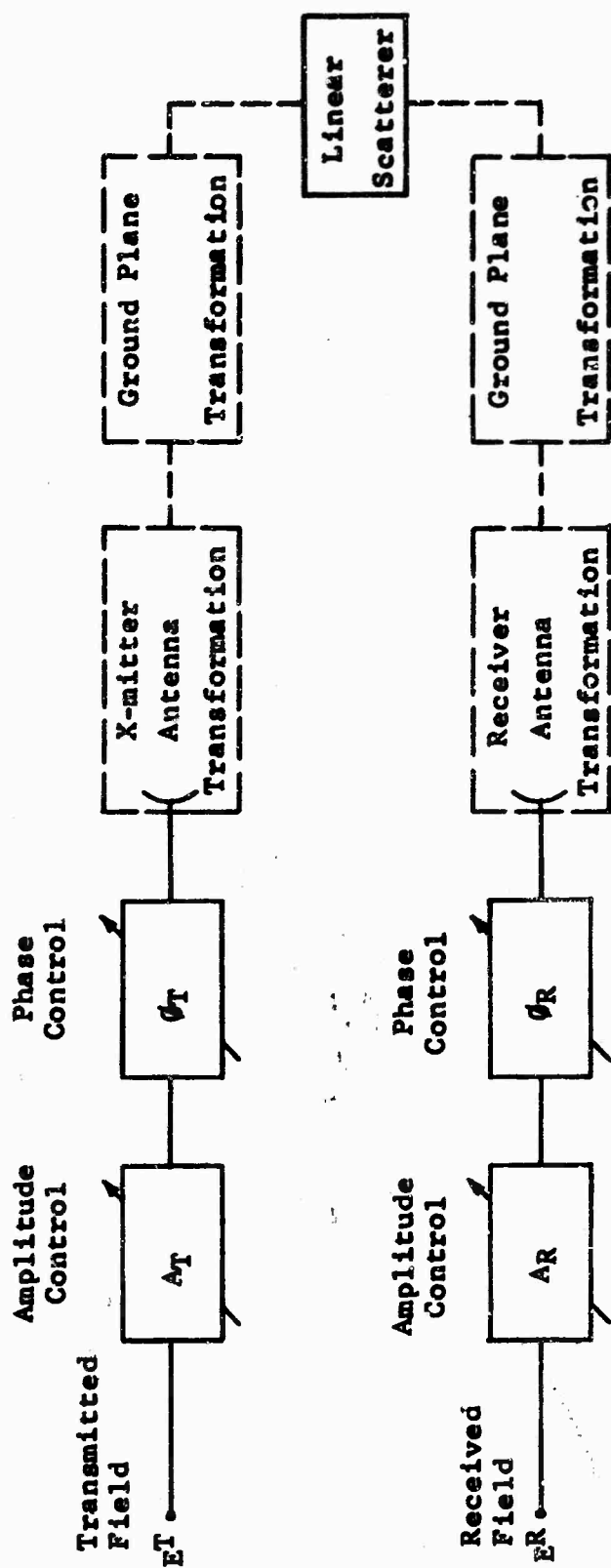
Fig. 1 REPRESENTATION OF DUAL-ANTENNA SYSTEM OPERATING ON GROUND PLANE RANGE

10

operations and that the received field can therefore be related to the incident field as indicated in Equation 8 where α_{RV}, α_{RH}, Γ_{RV}, Γ_{RH}, α_{TV}, α_{TH}, Γ_{TV}, and Γ_{TH} are complex numbers independent of E_T.

$$E^R = E^T A_R \epsilon^{i\phi_R} A_T \epsilon^{i\phi_T} \left[\alpha_{RV} \sin\gamma_r, \ \alpha_{RH} \cos\gamma_r \right] \overbrace{\begin{bmatrix} \Gamma_{RV} & 0 \\ 0 & \Gamma_{RH} \end{bmatrix}}^{\text{Ground plane}}$$

where the bracket $[\alpha_{RV}\sin\gamma_r, \ \alpha_{RH}\cos\gamma_r]$ is labeled "Receive antenna".

$$\begin{bmatrix} \sqrt{\sigma_{VV}}\,\epsilon^{i\phi_{VV}} & \sqrt{\sigma_{VH}}\,\epsilon^{i\phi_{VH}} \\ \sqrt{\sigma_{VH}}\,\epsilon^{i\phi_{VH}} & \sqrt{\sigma_{HH}}\,\epsilon^{i\phi_{HH}} \end{bmatrix} \overbrace{\begin{bmatrix} \Gamma_{TV} & 0 \\ 0 & \Gamma_{TH} \end{bmatrix}}^{\text{Ground plane}} \overbrace{\begin{bmatrix} \alpha_{TV} & \sin\gamma_t \\ \alpha_{TH} & \cos\gamma_t \end{bmatrix}}^{\text{X-mit antenna}}$$

(8)

The α's in Equation 8 denote the gains and phase associated with each of the antenna vertical and horizontal components. (To demonstrate the calibration procedure, it is assumed that the vertical channels can be completely isolated from the horizontal channels by proper selection of γ_r and γ_t.) The Γ's represent the vertical and horizontal reflection coefficients of the ground plane, and under normal conditions, $\Gamma_{RV} = \Gamma_{TV}$, $\Gamma_{RH} = \Gamma_{TH}$. However, since the α's are in general different, differences between the Γ's would be masked as can be seen by combining the ground plane effect with the antenna effect. The result is indicated in Equation 9 where the constant terms of Equation 8 have also been combined.

$$E^R = E^{T'} \left[\rho_{RV} \sin\gamma_r, \ \rho_{RH} \cos\gamma_r \right] \begin{bmatrix} \sqrt{\sigma_{VV}}\,\epsilon^{i\phi_{VV}} & \sqrt{\sigma_{VH}}\,\epsilon^{i\phi_{VH}} \\ \sqrt{\sigma_{VH}}\,\epsilon^{i\phi_{VH}} & \sqrt{\sigma_{HH}}\,\epsilon^{i\phi_{HH}} \end{bmatrix}$$

$$\begin{bmatrix} \rho_{TV} & \sin\gamma_t \\ \rho_{TH} & \cos\gamma_t \end{bmatrix}$$

(9)

11

$$\rho_{ij} = \alpha_{ij} \, \Gamma_{ij}. \qquad\qquad E^{T'} = E^T A_R \, \epsilon^{i\phi R} A_T \, \epsilon^{i\phi T}$$

The calibration procedure is demonstrated only for the case of amplitude since the phase calibration procedure can be demonstrated by using a similar argument. A superscript (S) will be used to denote the measurements of a sphere whose cross section is known and a (T) will be used for a target. To calibrate the (TV, RV) case, $\gamma_r = \gamma_t = \pi/2$, and the measured amplitude of E^R for the sphere is given by

$$\left| E_{RS} \right| = \left| E^{T'} \quad \rho_{RV} \quad \rho_{TV} \right| \sqrt{\sigma_{VV}}^S \tag{10}$$

while that of the target is given by

$$\left| E_{RT} \right| = \left| E^{T'} \quad \rho_{RV} \quad \rho_{TV} \right| \sqrt{\sigma_{VV}}^T \tag{11}$$

Hence

$$\sigma_{VV}^T = \sigma_{VV}^S \left| \frac{E_{VV}^{RT}}{E_{VV}^{RS}} \right|^2 \tag{12}$$

Also, for the (TH, RH) case, σ_{HH}^T is given by

$$\sigma_{HH}^T = \sigma_{HH}^S \left| \frac{E_{HH}^{RT}}{E_{HH}^{RS}} \right|^2 \tag{13}$$

To calibrate σ_{VH}^T, note that the product of $\left| E_{VH}^{RT} \right|$ and $\left| E_{HV}^{RT} \right|$ has the form

$$\left| E_{VH}^{RT} \right| \left| E_{HV}^{RT} \right| = \left| E^{T'} \right|^2 \left| \rho_{RV} \quad \rho_{TH} \right| \left| \rho_{RH} \quad \rho_{TV} \right| \sigma_{VH} \tag{14}$$

12

and the product of $\left| E_{VV}^{RS} \right|$ with $\left| E_{HA}^{RS} \right|$ has the form

$$\left| E_{VV}^{RS} \right| \quad \left| E_{HH}^{RS} \right| = \left| E^{T'} \right|^2 \left| \rho_{RV} \; \rho_{TV} \right| \quad \left| \rho_{TH} \; \rho_{RH} \right| \sigma^S \tag{15}$$

eliminating the common terms in these two expressions gives

$$\sigma_{VH}{}^T = \sigma^S \frac{\left| E_{VH}^{RT} \right| \quad \left| E_{HV}^{RT} \right|}{\left| E_{VV}^{RS} \right| \quad \left| E_{HH}^{RS} \right|} \tag{16}$$

The above demonstration indicates that a sphere can be used to calibrate the system to measure σ_{VV}, σ_{HH}, and σ_{VH}, and a similar argument would show that ϕ_{VV}, ϕ_{HH}, and ϕ_{VH} can be calibrated by using a sphere. In practice, the system is calibrated by using a sphere as a primary standard and a corner as a secondary standard. The secondary standard is located outside the range gate when the gate is centered over the target region. With this arrangement, system calibration can be maintained for long periods of time in a convenient manner. A post calibration is performed by using the sphere in order to provide a safeguard against possible fluctuation caused by changes in the secondary standard. Listed in Table 2 are the records for the precalibration and post calibration of amplitude and phase for the two periods of time used in the measurements.

Included in Table 2 are calibration data for (T $\pi/4$, R $\pi/4$) as well as the principal linear polarizations. To calibrate for (T $\pi/4$, R $\pi/4$), a procedure similar to that outlined for the principal linear conditions was used. However, the accuracy of the calibration is dependent upon how closely the conditions $\rho_{iV} = \rho_{iH}$ are approximated. At the frequency of operation (3 gigahertz), it was estimated that these conditions would be sufficiently approximated in order to measure at (T $\pi/4$, R $\pi/4$), compare these data with computed (T $\pi/4$, R $\pi/4$), and obtain good agreement except possibly over isolated azimuth regions where small errors in the elements of the scattering matrix produce large errors in the resultant cross section and phase. An indication of the validity of the above condition can be obtained by noting the difference in sphere cross section as the antennas are rotated between (TV, RV) and (TH, RH). This difference being small, as was the case in the measurement system used, indicates that $\left| \rho_{iV} \right| = \left| \rho_{iH} \right|$.

Measurement System

In discussing calibration procedures, the measurement system was idealized in that it was assumed that the conditions TV (TH) and RV (RH) could be achieved and the bistatic angle was zero. It was also implicitly assumed that once a calibration level was achieved, cross section and/or phase could be recorded relative to this level in

13

TABLE 2

SECONDARY STANDARD CALIBRATION DATA

	Polarization	Precalibration		Past Calibration	
		Amplitude (dbsm)	Phase (degrees)	Amplitude (dbsm)	Phase (degrees)
Measurement Series 1 (Model 2)	(TV, RV)	- 0.2	53	+ 0.2	49
	(TV, RH)	-10.7	328	-10.7	318
	(TH, RH)	- 2.7	55	- 2.2	55
	(T π/4, R π/4)	- 0.9	32	- 1.2	32
Measurement Series 2 (Models 1 & 3)	(TV, RV)	1.0	350	1.0	0
	(TV, RH)	-12.8	240	-12.2	250
	(TH, RH)	- 2.0	350	- 2.0	0
	(T π/4, R π/4)	- 0.6	340	+ 0.2	340

14

a meaningful manner. The first idealization involves the "purity" of the antenna system and the effect of the bistatic angle while the second involves the accuracy of operating the system over some dynamic range.

The amount of "purity" (isolation) needed in an antenna system in order to measure the elements of the scattering matrix can be estimated by noting the amount of accuracy desired and the relative magnitude between the σ_{VV} (σ_{HH}) cross section and (σ_{VH}). For example, if 1-db accuracy is desired and σ_{VH} is nominally 15 db lower than σ_{VV} and σ_{HH}, then the amount of isolation needed between the transmitted (received) H component is 35 db when the system is supposedly transmitting V (receiving). This isolation can be checked by comparing σ_{VH} and σ_{HV} of a sphere (or other specular reflector) with σ_{VV} or σ_{HH}. Shown in Figure 2 are (1) the isolation test results obtained by using a sphere after aligning the antennas for measurement series 1 and (2) the results obtained by using a flat plate at broadside after aligning the antennas for measurement series 2. The test data indicate that better than 35 db of isolation was achieved with the antenna system used in the measurement program.

The bistatic angle used for the measurement program was approximately 0.25 degree; comparison of σ_{VH} with σ_{HV} shows that the effect of this angle on the data was negligible. Comparisons of σ_{VH} and σ_{HV} for the three models can be made by inspection of Figures 10 through 29. σ_{VH}, ϕ_{VH}, σ_{HV}, and ϕ_{HV} were recorded throughout the measurement program since differences between the appropriate plots would serve as a warning that antenna isolation was degraded.

Another factor which can influence the differences between σ_{VH} and σ_{HV} is the difference in vertical height field patterns between (TV, RV) and (TH, RH). Also, differences in these "transmit" and "receive" field patterns tend to make $|\rho_{iV}| \neq |\rho_{iH}|$. For these reasons, the antennas were adjusted to give field patterns for these conditions as near to optimum as practical. The field patterns obtained are indicated in Figure 3.

The electronic system used to measure the amplitude and phase of the scattering matrix elements is shown in Figure 4. As shown in the figure, this system is operated at the IF level of a range-gated radar. Both the amplitude and phase measuring systems are comparative type circuits which allow cross section to be recorded in dbsm over a 50-db dynamic range by using a linear scale and phase to be recorded from 0 to 360 by using a linear scale. The basic measurement accuracy of the systems (closed loop) are ± .5 db and ± 4 degrees, respectively, in operation over their dynamic ranges. The 50-db dynamic range of the amplitude system can be shifted by adjusting an RF attenuator in the transmitter line (or receiver line), along with making a similar adjustment in the reference line. Hence, once the system is calibrated, measurements can be made over the dynamic range of the radar system.

The signal-to-noise ratios were determined by using the amplitude system to determine the noise floor of the system. The noise floor was determined after adjusting the error detector circuit (Figure 4) to give a zero error when the reference signal was slightly larger than the target signal. This procedure must be used in order to establish a definitive noise floor which is relatively independent of the time on target. That is, in an ideal comparative network, the average error signal is a function of the integration time, and the system will tend to track into the noise if zero error occurs when the reference signal is equal to the target signal. However, if the error circuit is so adjusted that zero error occurs when the reference signal is slightly larger than the target signal, then the system will exhibit a definitive noise floor which is
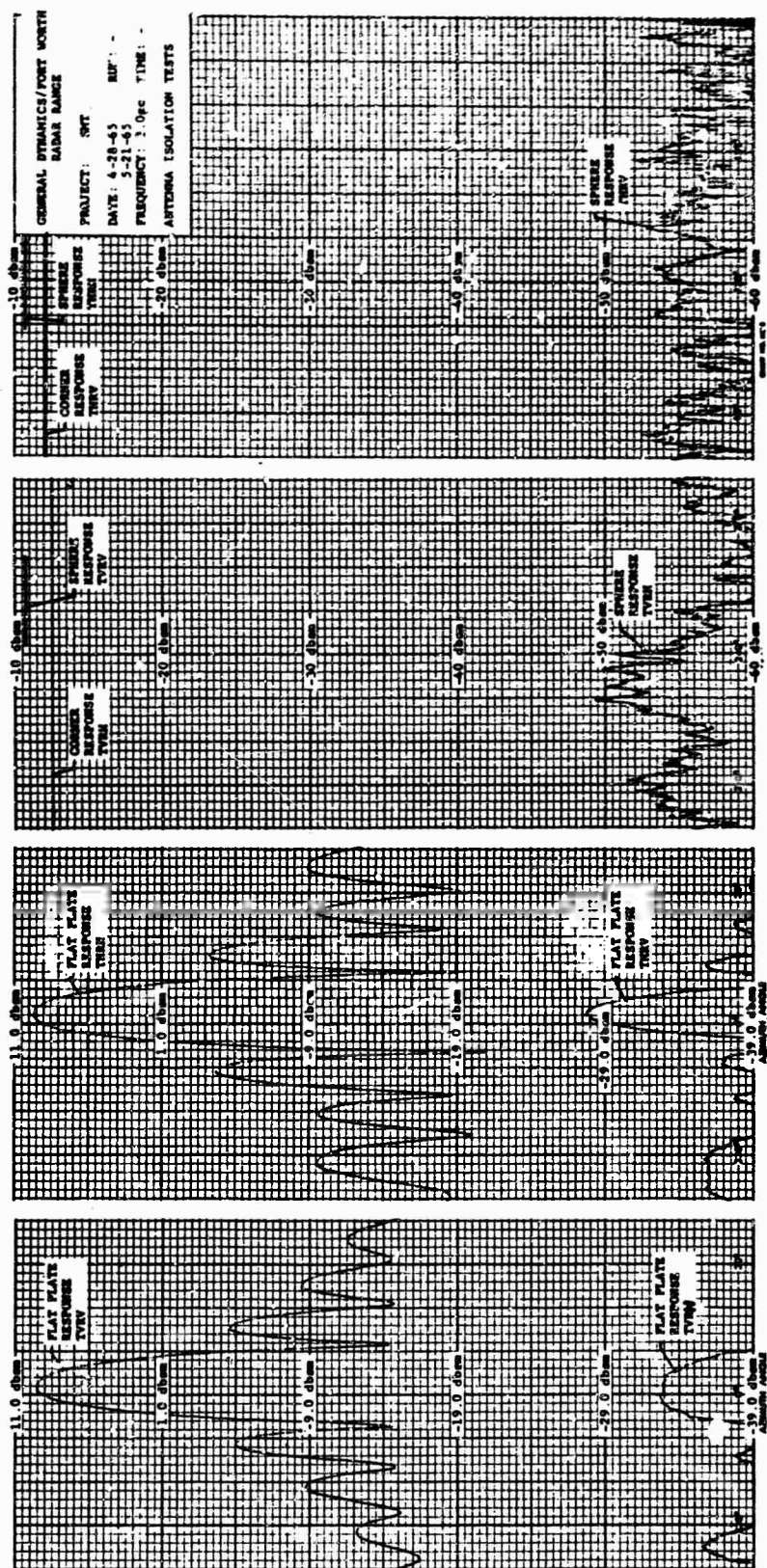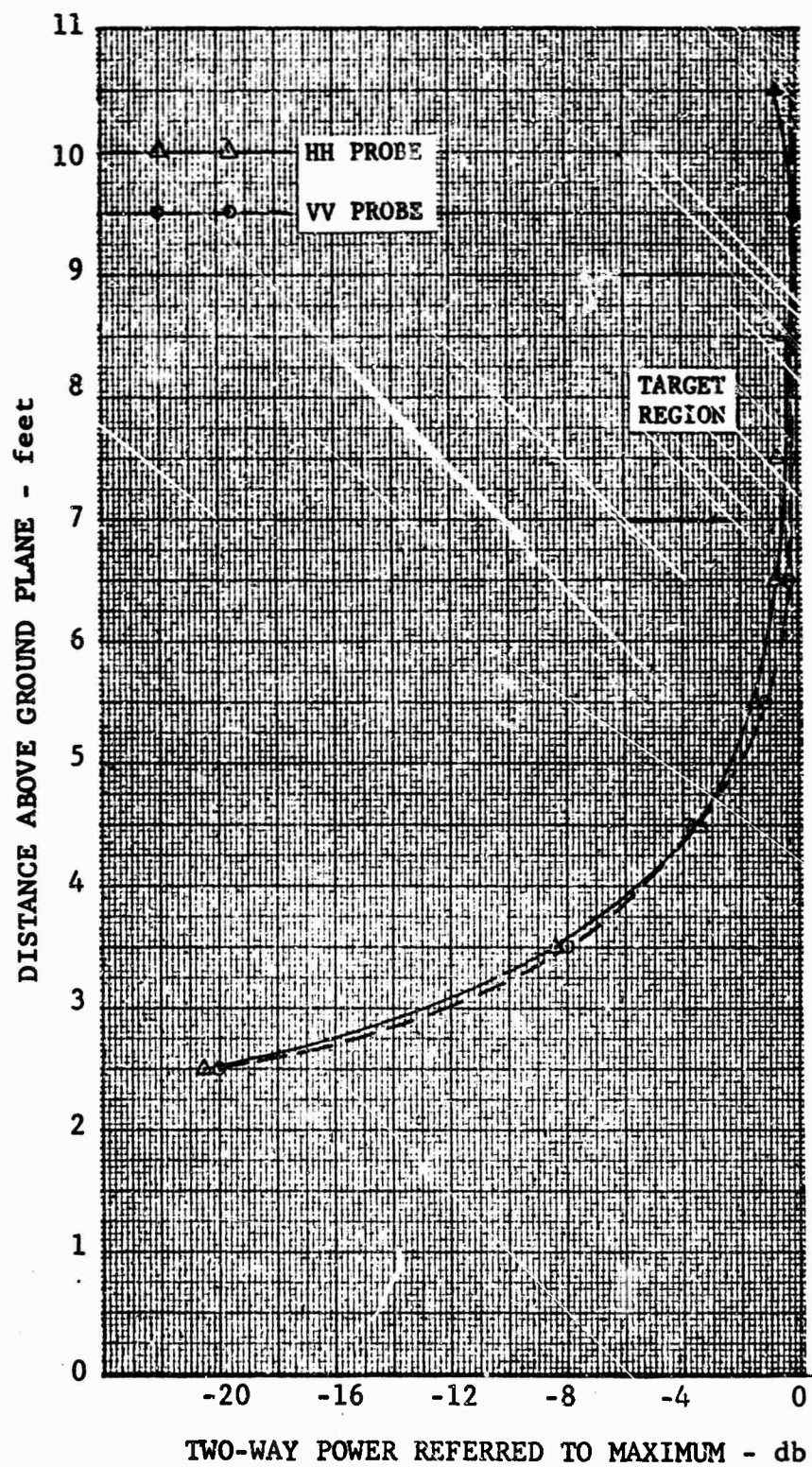
15

Fig. 2 ANTENNA ISOLATION TEST DATA

16
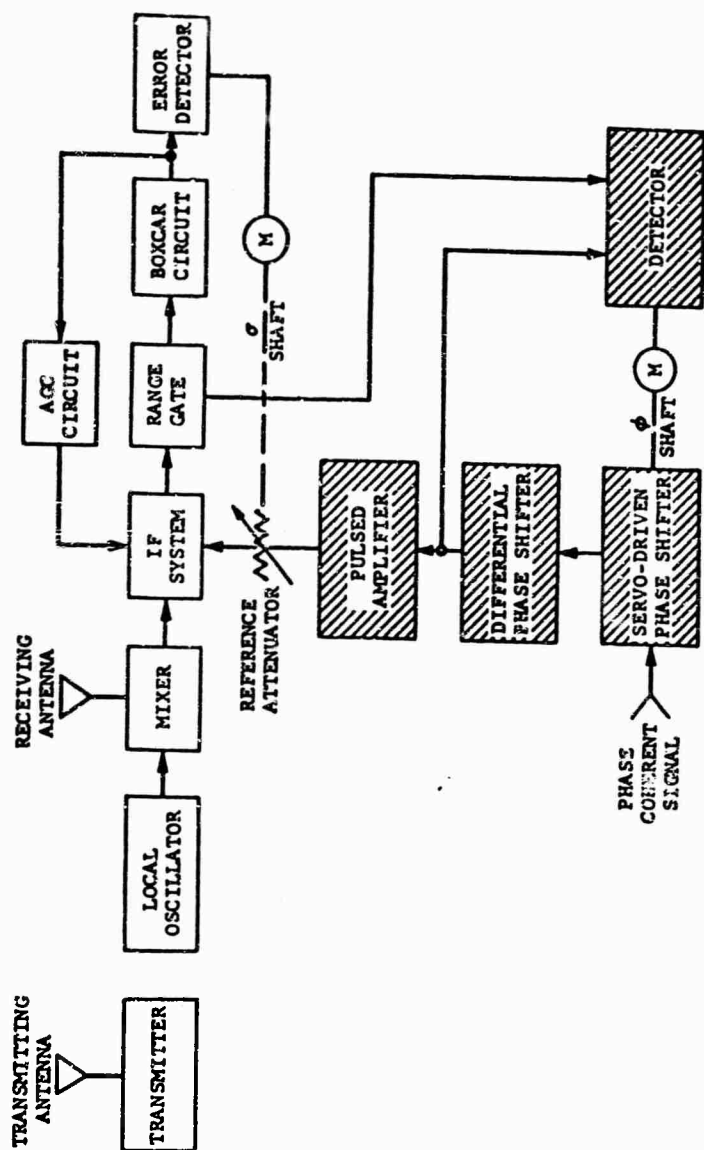
Fig. 3 VERTICAL FIELD PROBE DATA

17

Fig. 4 MEASUREMENT ELECTRONIC SYSTEM BLOCK DIAGRAM

18

relatively independent of the integration time. The level of the noise was determined by plotting the recorded error of cross section as a function of a calibrated attenuator. The noise level was determined by noting the cross section level at which a 3-db error occurred.

This procedure is based on the assumption that, on the average, the noise power σ_N adds to the signal power σ_T so that the measured cross section, σ_M, is given by

$$\sigma_M = \sigma_T + \sigma_N = \sigma_T \left(1 + \frac{\sigma_N}{\sigma_T}\right) \tag{17}$$

By use of Equation 17, it is seen that the error, $E = \sigma_M/\sigma_T$, is 3 db whenever $\sigma_N = \sigma_T$. A plot of the theoretical error and the measured error is shown in Figure 5. To plot the measured data in this figure, the measured errors for the large σ_N/σ_T ratios (i.e., those ≥ 20 db) were used to determine the ratios of σ_N/σ_T at the lower σ_N/σ_T ratios since in these cases 10 Log E is approximately equal to 10 Log σ_N/σ_T. The data plotted in Figure 5 indicates that Equation 17 is representative of the type of error to be expected in the measured cross section as a function of signal-to-noise ratio.

The phase measurement system is described in detail in Reference 3. Basically, the system is an absolute phase measurement system which measures phase by comparing the phase of a reference signal and target signal with that from a coherent oscillator; a voltage which is a function of these phase differences is used to servo a calibrated phase shifter to minimize the difference between the reference signal and the target signal.

The primary error sources associated with an absolute phase measuring system are frequently drift and target motion. The expression for the phase error caused by these factors is indicated in Equation 18.

$$E_\phi = \frac{4\pi\Delta d}{\lambda_0} + \frac{4\pi R \Delta f}{C} + \frac{4\pi\Delta d\,\Delta f}{C} \tag{18}$$

Where

Δd = radial motion due to target

Δf = frequency deviation relative to the calibration frequency f_0

R = range to target

C = 3×10^8 meters/second

The last term on the right of Equation 18 is a second order effect, and only the first two terms need be considered. To demonstrate the requirements placed on target motion during operation at 3 gigahertz, note than when $E_\phi \leq 7.2$ degrees, $\Delta d \leq .1$ centimeter. Also, in the case of the operating range used during the measurement program ($R \approx 800$ feet), $E_\phi \leq 7.2$, $\Delta f \leq 1.25$ kilohertz which is an oscillator stability
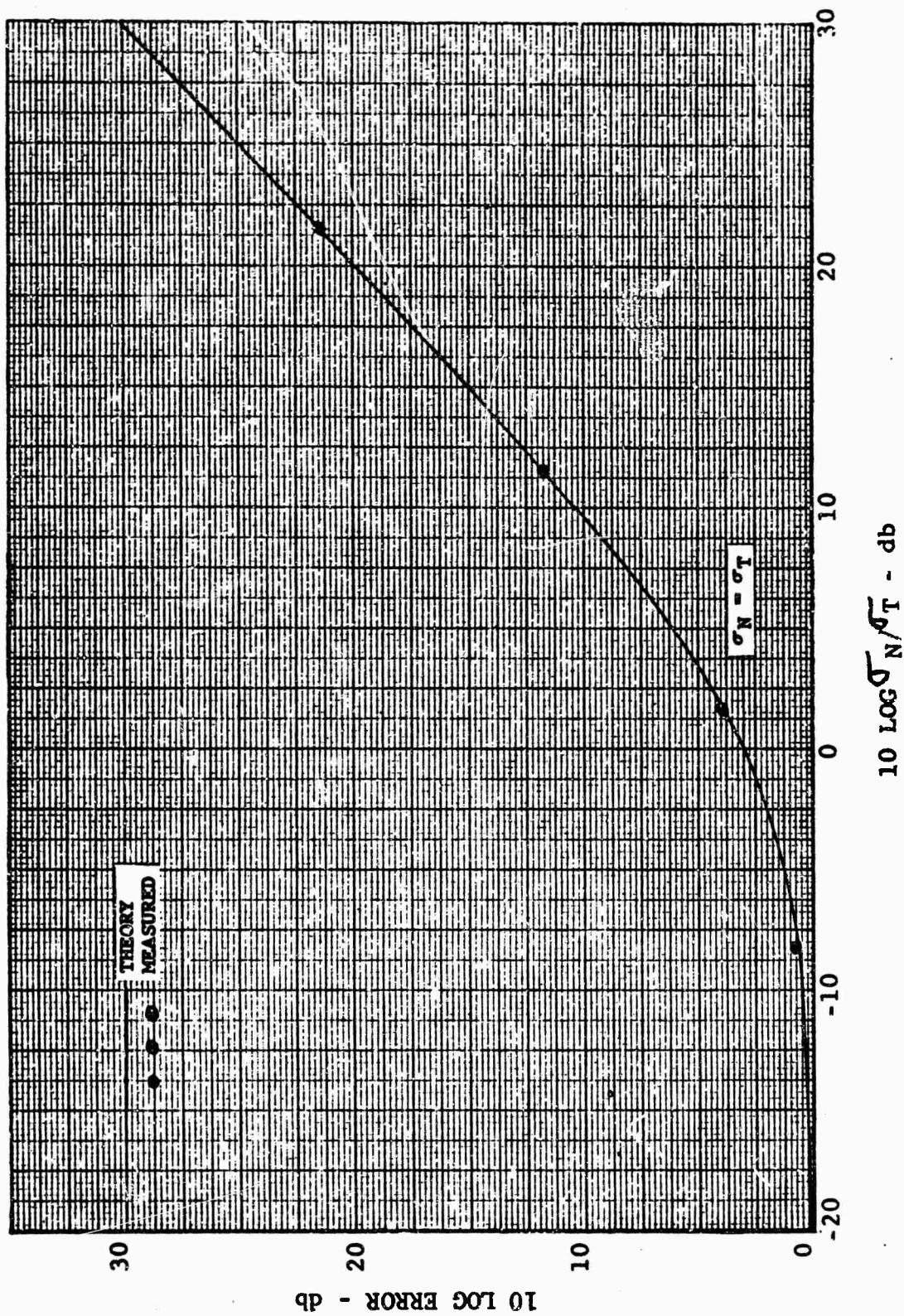
19

Fig. 5 MEASUREMENT ERROR AS FUNCTION OF SIGNAL-TO-NOISE RATIO

20

requirement of better than 1 part in 10^6. The equipment was designed by using a reference oscillator rated at 1 part in 10^7. Several tests were conducted by using the secondary standard (R $\approx$ 1200 feet) for frequency drift in which the phase deviation as a function of time was noted. The maximum deviation noted during these tests was 15 degrees over a time period of 30 minutes; this result indicates a short-term frequency stability of better than 1 part in 10^6.

The long-term stability can be determined by measuring the phase difference between data obtained at the beginning of a measurement series and data on the same target at the end of the measurement series. Since the target has not been moved during this time period (except for minor fluctuations caused by wind), the distances between the radar reference, secondary standard, and target can be considered a constant. Hence, using Equation 18, the frequency drift can be measured by comparing phase data obtained for the same polarization conditions and using the range between the secondary standard and target ($\approx$ 400 feet). (Note that the pre and post calibration data in Table 1 cannot be used for a test of this type since the separation between corner and sphere could have been different in the pre calibration than in post calibration; that is, the sphere was not mounted exactly at the center of rotation of the target rotator. However, care must be taken to note if any constant phase shifts were incurred between the time the range gate was centered over the secondary standard and the time the target was measured. Shifts of this type were noted during the program but were compensated for when processing the data. These shifts were partially correlated with power line transients. In Figure 6, portions of two phase plots of the same target taken 26 hours apart are shown. Comparison of the phase data indicates that on the average the phase is within 6 degrees which indicates a long term frequency stability of approximately 1 part in 10^6. Inspection of data presented in Section III indicates a similar degree of phase stability as indicated above by comparing phase data obtained at the high S/N levels. However, in some cases there are noticeable constant phase shifts caused by system transients as discussed above. The magnitude of phase perturbations caused by target motion are also indicated in Figure 6 although these plots were taken under quite calm wind conditions ($\leq$ 5 knots) which were typical of the conditions present when measurements were obtained.

21

Note: The data obtained on 6-6-65 is shifted one and one half degrees to the left of the data obtained on 6-5-65.
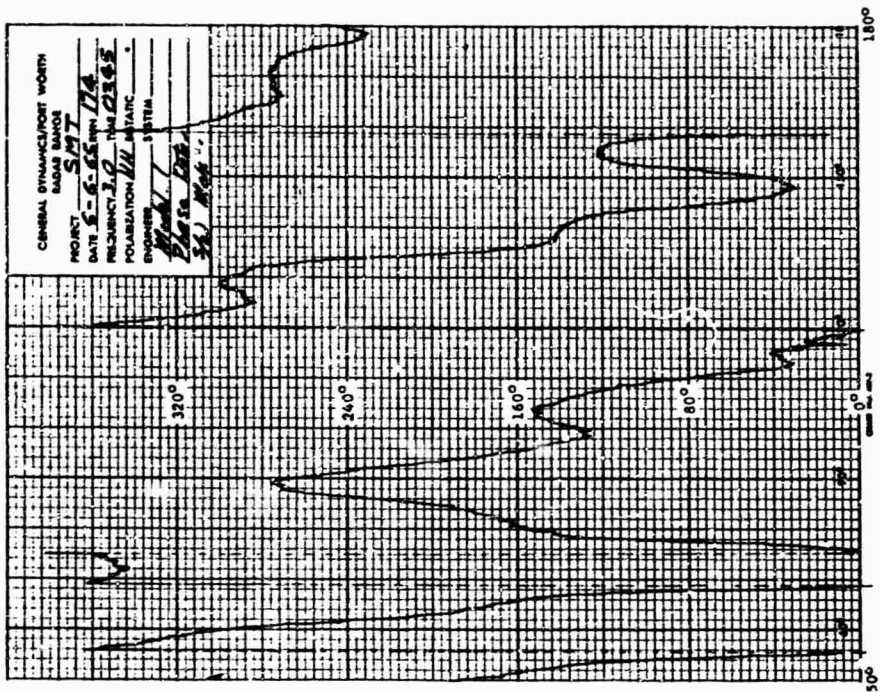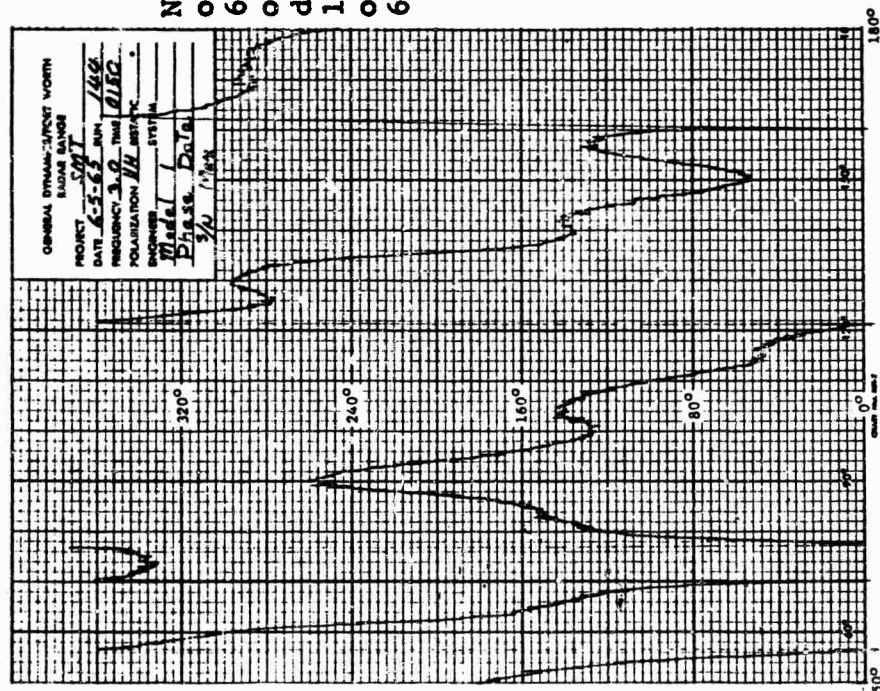
Fig. 6 VEHICLE PHASE DATA RECORDED AT DIFFERENT TIMES

SECTION III

MEASUREMENT AND COMPUTATION PROGRAMS

In order to obtain data pertaining to a large class of targets, the vehicles were selected for measurement on the basis of the type of scattering matrix they would tend to exhibit. The signal-to-noise ratios used in measuring the scattering matrices were selected so that the amplitude elements of the linear scattering matrix varied between no error due to noise and noise alone. This same criterion was applied to all three targets measured in order that the degradation of each target could be compared in terms of S/N.

The effect of noise degradation on scattering matrix usage was measured by computing cross section and phase at selected polarization conditions. The same computations were made for each of the S/N conditions at which the scattering matrix was measured. The computed data obtained by using the matrix which represented the best S/N condition was then used as reference data for generating the errors incurred at the lower S/N conditions. The polarizations used in obtaining cross section and phase were selected to obtain transformation characteristics considered representative of those which would be observed in a general polarization study.

Vehicles Measured

The vehicles measured in this study were chosen in order to obtain three distinct types of matrices. The first model was designed to give a matrix so that the amplitude of its elements would nominally have the same average value but would vary rapidly relative to each other as a function of azimuth. The second model was designed so that the phase of its matrix elements would vary rapidly relative to each other as a function of azimuth. The third model was to exhibit the scattering characteristics of a "typical" aerospace vehicle. Throughout the remainder of the report, the vehicles associated with the above three types of matrices will be referred to as Models 1, 2, and 3, respectively.

The first two types of targets exhibit the characteristics of a complex target which is measured in and/or near the resonance region, that is, a target which has a quite complex current distribution and is quite sensitive to the polarization of the transmitter and receiver. The first target is primarily amplitude sensitive, and the second type is phase (and possibly amplitude) sensitive. The third type of model was also chosen of such a size that would provide a matrix characteristic of a physical optics type scatterer over a substantial azimuth region, i.e., $(\sigma_{VH} \ll \sigma_{VV} \simeq \sigma_{HH})$.

To obtain a matrix of the first type, Model 1 was a torroid constructed of wire mesh and mounted at 45 degrees as indicated in Figure 7 a and b. The dimensions of the torroid and wire mesh were chosen so that the loops of the mesh were resonant (Reference 4) and the torroid cylinder was 5λ in diameter. Use of this design resulted in an extremely polarization-sensitive target which exhibited the desired characteristics.

The matrix of the second type was achieved by adding a vertical dipole to Model 1 as indicated in Figure 7b. The size of the dipole was chosen so that the cross section was as large as or larger than the cross section of Model 1 for the case of (TV, RV). Under these conditions the phase center of the scattered wave will tend to be spatially.
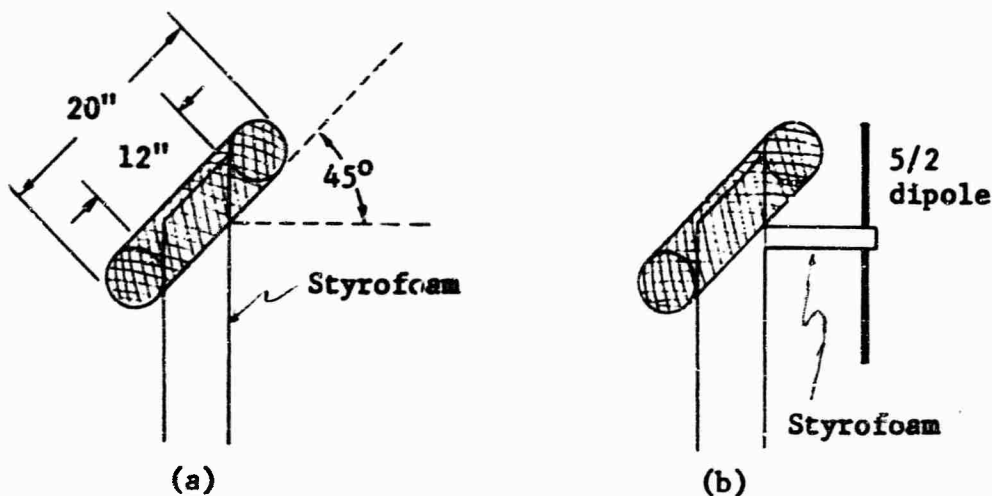
23

Fig. 7 SKETCHES AND ORIENTATION OF MODELS 1 AND 2

located near the dipole whereas in the case of (TH, RH) the phase center will be located inside the torroid as in the case of Model 1. Hence, because of the spatial separation between the dipole and torroid, a large and rapid phase variation between elements of the matrix was anticipated and observed.

The third type of matrix was generated by using a typical aerospace vehicle which, as desired, produced a significant amount of specular reflection in the broadside regions.

Signal-to-Noise Criteria

In order to cover the range from no degradation to complete degradation of the scattering matrix as a function of S/N, the reference used for setting the ratios was the largest cross section of the linear matrix elements. This largest cross section value was obtained under the (TV, RV) conditions for all three models. By use of this reference, the S/N in db was set to obtain data at 0, 3, 6, 12, 24, X, and maximum by adjusting an attenuator placed in the transmitter line. The X-db S/N was determined by inspection of the cross section dynamic range of the matrix elements of each model. The value of X for each model was set to be slightly less than the dynamic range of the matrix elements. In the case of Model 1, X = 35 db, Model 2, X = 42 db and Model 3, X = 52 db. The maximum S/N level in all three cases was greater than or equal to 60 db.

Although the S/N reference criterion outlined above was a practical means of obtaining data at various levels of degradation, from the standpoint of analyzing the

24

data, a more practical criterion was considered to be a reference based on the use of the average cross section level of the largest term of the scattering matrix. In other words, when a radar design is being considered or a measurement criterion is being selected, the average cross section level of a particular class of targets would most likely be chosen rather than the peak cross section. The degradation curves presented later in this report demonstrate the difference between which type of reference is used as a function of the type of model matrix.

Measured Data

The amplitude and phase data was recorded on analog plots and digital tape. The azimuth recording increment of the digital system was 0.1 degree. The resolution of the digital amplitude encoder was 0.1 db and that of the phase encoder was 1 degree. The analog plots of the amplitude and phase of the matrix elements of each of the three models are shown in Figures 8 through 31 for the case of maximum S/N. The amplitude plots read directly in decibels relative to a square meter (dbsm) and the phase plots in degrees.

In Figures 32 through 67 are shown the cross section and phase plots of each model for the case of (TV, RV) as a function of S/N. These plots are typical of the effect of degradation caused by the noise observed on other elements of the matrix. On each of the plots, the noise level is indicated in dbsm. In Figures 8, 16, and 24, the average cross section level is indicated. These average values were used to determine the S/N levels by using an average as reference.

Computed Cross Section and Error

The data, as illustrated in Figures 8 through 67, was used to generate degradation information as a function of S/N and model. In addition, the cross section and phase for the condition (T $\pi/4$, R $\pi/4$) were computed for each model for the case of maximum S/N and compared with data measured for this condition.

The computations were based on the expression for cross section and phase given in Equation 19 which was obtained from Equation 2.

$$\sigma_{tr} = \sigma_{VV} \operatorname{Sin}^2\gamma_t \operatorname{Sin}^2\gamma_r + \sigma_{HH} \operatorname{Cos}^2\gamma_t \operatorname{Cos}^2\gamma_r$$

$$+ \frac{\sqrt{\sigma_{VV}\sigma_{HH}}}{2} \left[\operatorname{Sin} 2\gamma_t \operatorname{Sin} 2\gamma_r \operatorname{Cos} (\psi + \delta_t + \delta_r) \right]$$

$$+ \sigma_{VH} \left[\operatorname{Cos}^2\gamma_t \operatorname{Sin}^2\gamma_r + \operatorname{Sin}^2\gamma_t \operatorname{Cos}^2\gamma_r \right.$$

$$\left. + 1/2 \operatorname{Sin} 2\gamma_t \operatorname{Sin} 2\gamma_r \operatorname{Cos} (\delta_t - \delta_r) \right]$$

25

$$+ \sqrt{\sigma_{VV}\,\sigma_{VH}} \left[\text{Sin } 2\gamma_t \text{ Sin}^2\gamma_r \text{ Cos } (\theta + \delta_t) \right.$$

$$\left. + \text{Sin}^2\gamma_t \text{ Sin } 2\gamma_r \text{ Cos } (\theta + \delta_r) \right]$$

$$+ \sqrt{\sigma_{HH}\,\sigma_{VH}} \left[\text{Sin } 2\gamma_r \text{ Cos}^2\gamma_t \text{ Cos } (\theta - \psi - \delta_r) \right.$$

$$\left. + \text{Cos}^2\gamma_r \text{ Sin } 2\gamma_t \text{ Cos } (\theta - \psi - \delta_t) \right]$$

$$\tag{19}$$

$$\phi'_{tr} = \phi_{tr} - \phi_{VV} = \text{Arg} \left[\sqrt{\sigma}_{tr} - \phi_{VV} \right]$$

$$\psi = \phi_{HH} - \phi_{VV}$$

$$\theta = \phi_{VH} - \phi_{VV}$$

In each of the model studies, a set of reference data was generated by processing the data obtained for the condition of maximum S/N and storing this data on magnetic tape. Cross section and phase were computed for each of the polarizations (TR, RR), (TR, RL), (TR, RV), (TR, RH), and (T $\pi/4$, R $\pi/4$). The data obtained at other S/N ratios was then processed for the same polarization conditions. At each azimuth point the cross section and phase computed for the lower S/N ratios were compared with the reference data, and the differences in | db | and | phase | were stored as error for each of the polarization conditions. As illustrated in Tables 3 through 6, the data was printed out for each of the conditions indicated above. In addition, on the basis of all five polarizations, the error data generated at each S/N condition was used to generate cumulative error curves for phase and amplitude. The cumulative curves were obtained by dividing the dynamic range of the error data into one hundred parts. The dynamic range of the phase error is ≤ 180 degrees, but on amplitude error there is no bound. Hence a bound of 60-db error was used in order to keep the resolution elements of the amplitude cumulative near or less than 0.5 db. Although the number of data points used to obtain each cumulative curve varied somewhat because of the azimuth correlation of the three input tapes needed for each run, on the average, approximately 15,000 data points were used to obtain each cumulative curve.
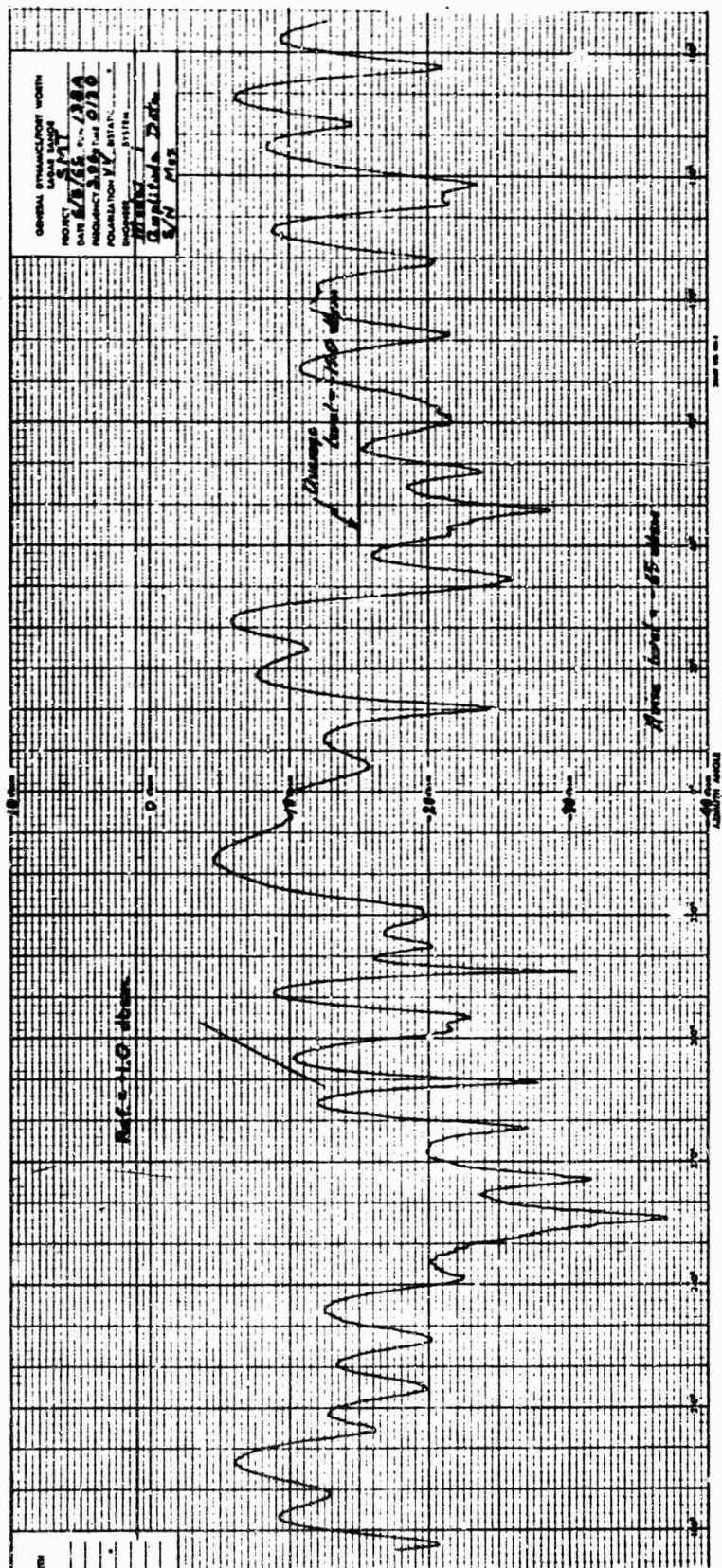
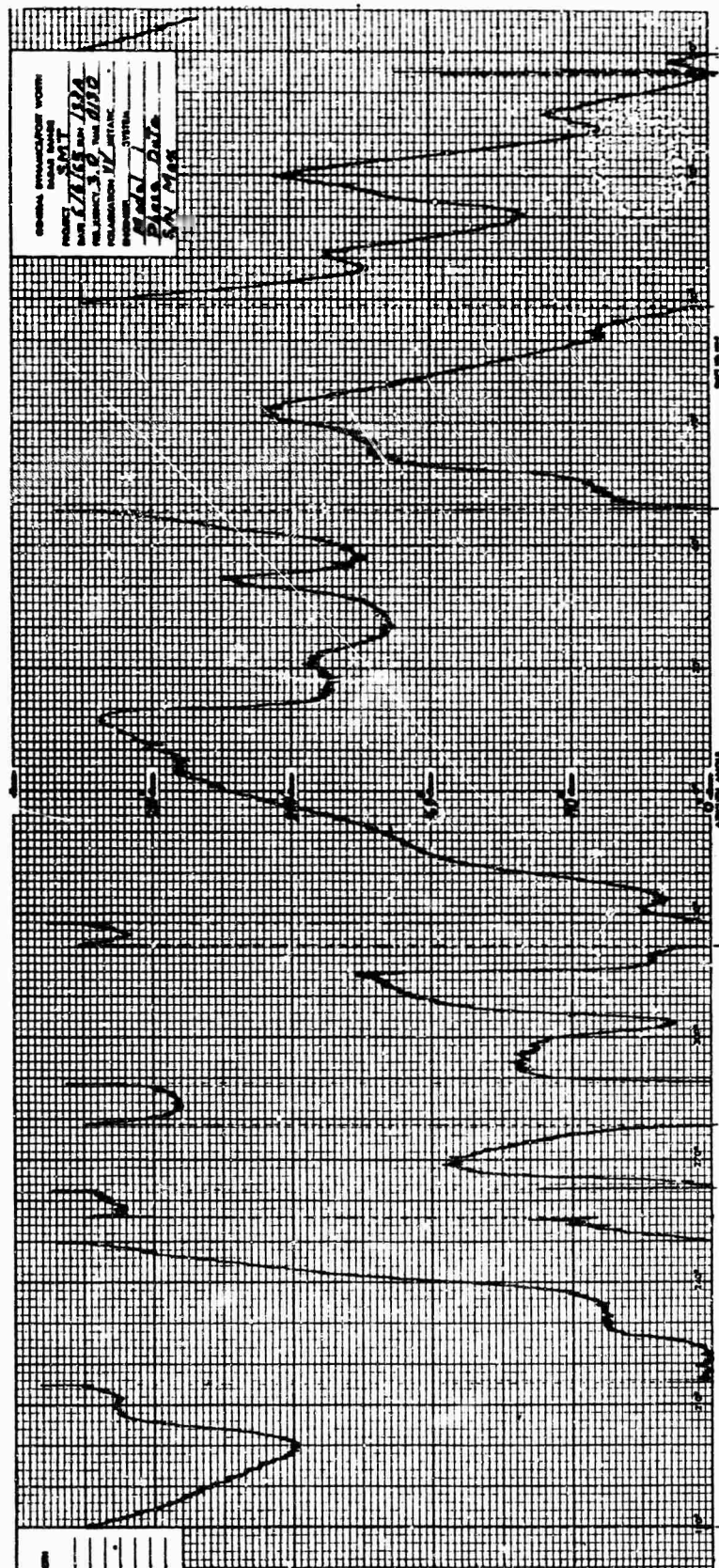Fig. 8 MODEL 1 CROSS SECTION FOR (TV, RV)
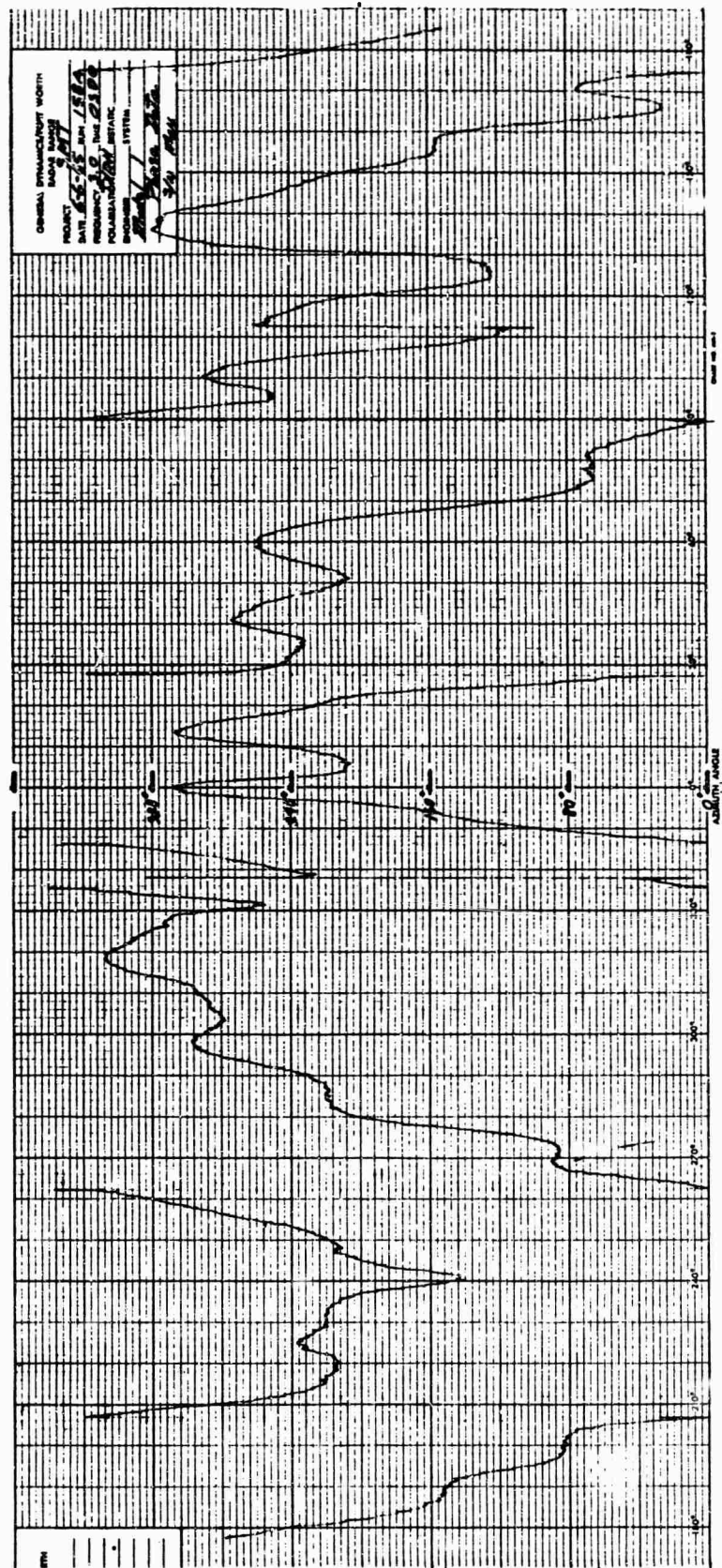
28

Fig. 9 MODEL 1 PHASE FOR (TV, RV)

Fig. 10 MODEL 1 CROSS SECTION FOR (TV, RH)

Fig. 11 MODEL 1 PHASE FOR (TV, RH)
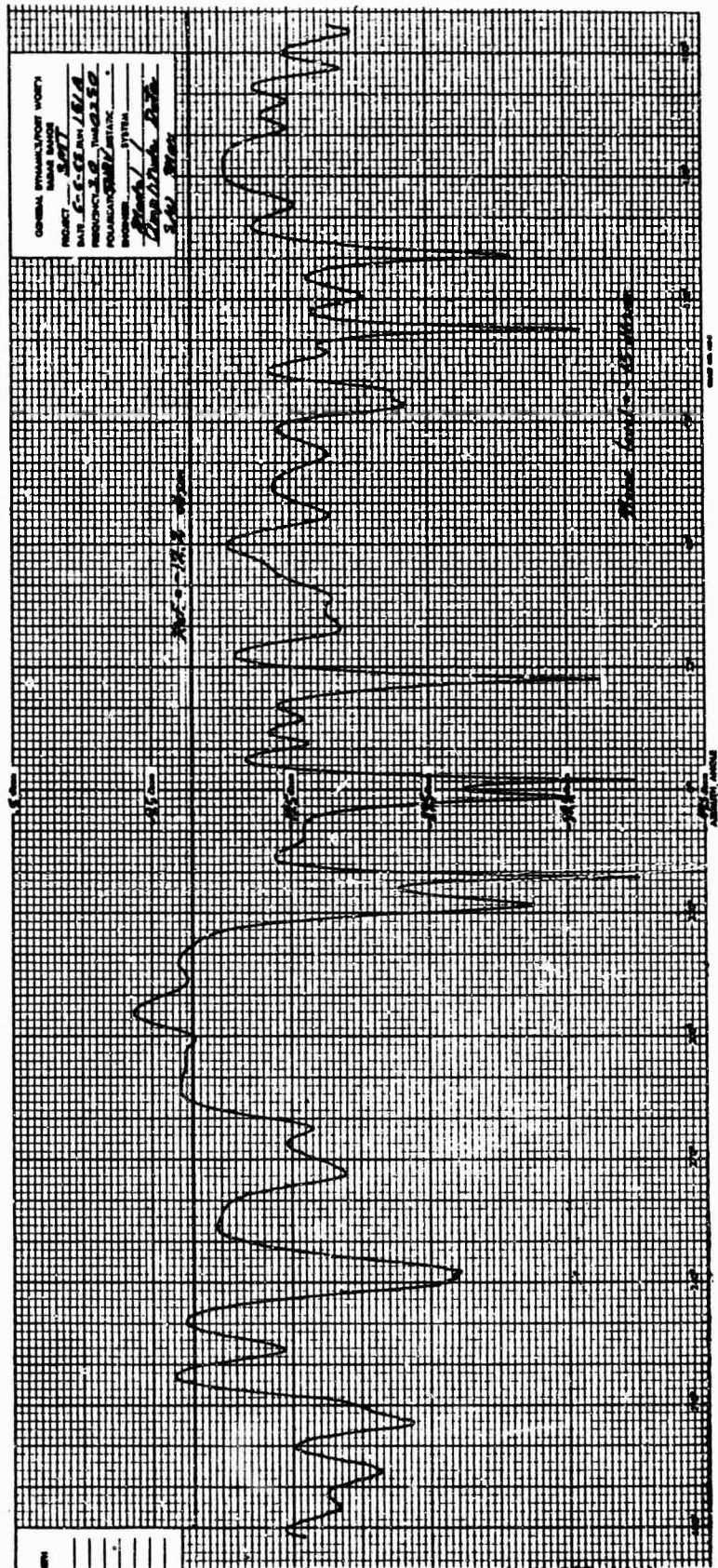
Fig. 12 MODEL 1 CROSS SECTION FOR (TH, RV)
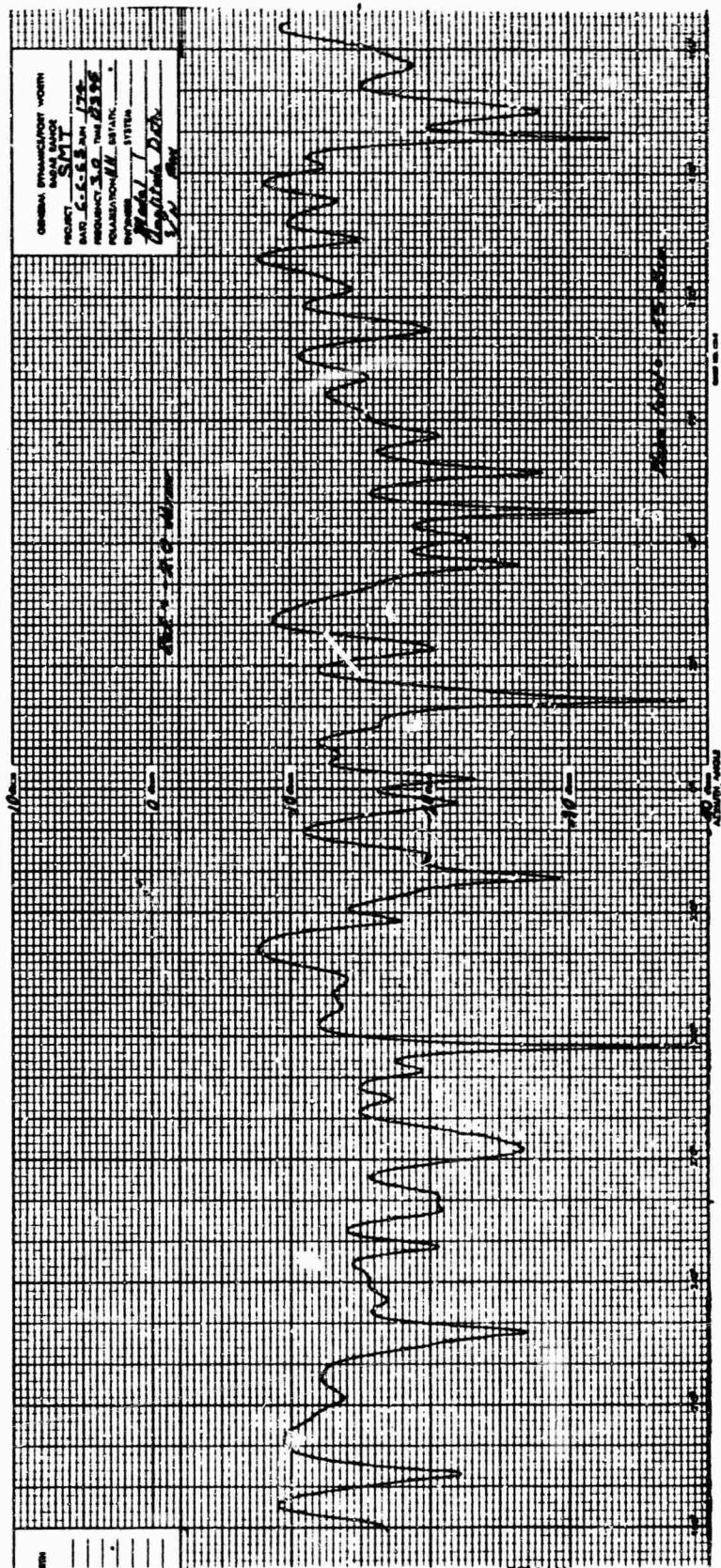
Fig. 13 MODEL 1 PHASE FOR (TH,RV)
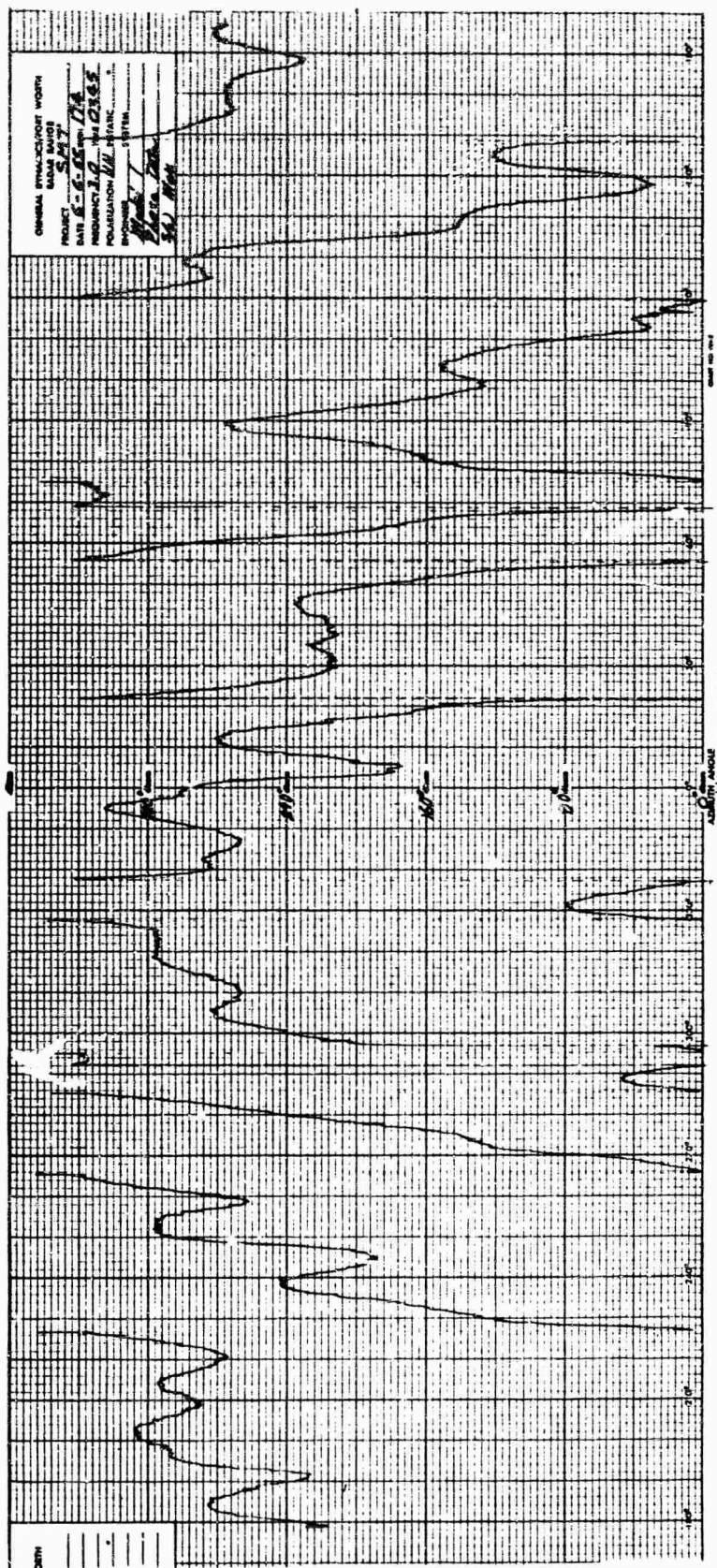
33

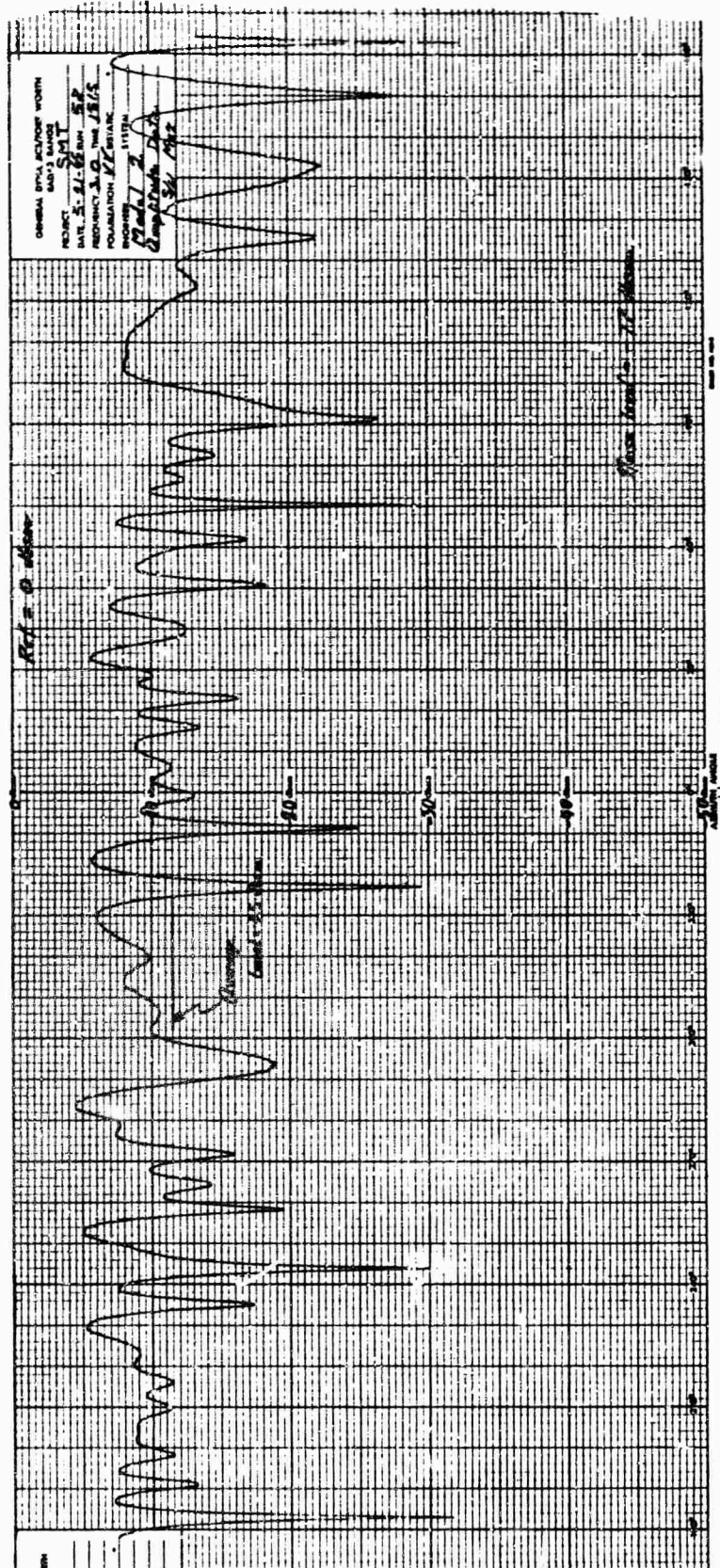Fig. 14 MODEL 1 CROSS SECTION FOR (TH, RH)

Fig. 15 MODEL 1 PHASE FOR (TH,RH)
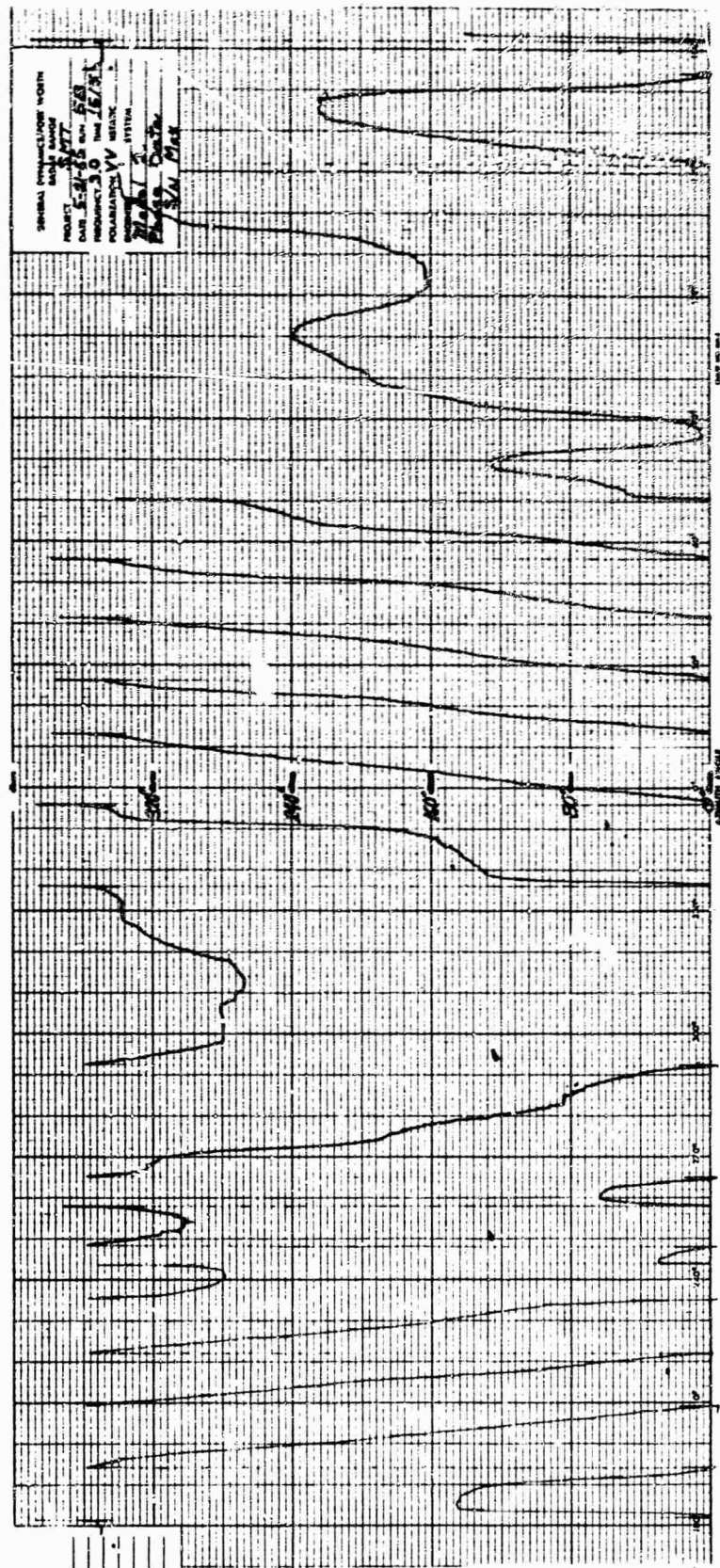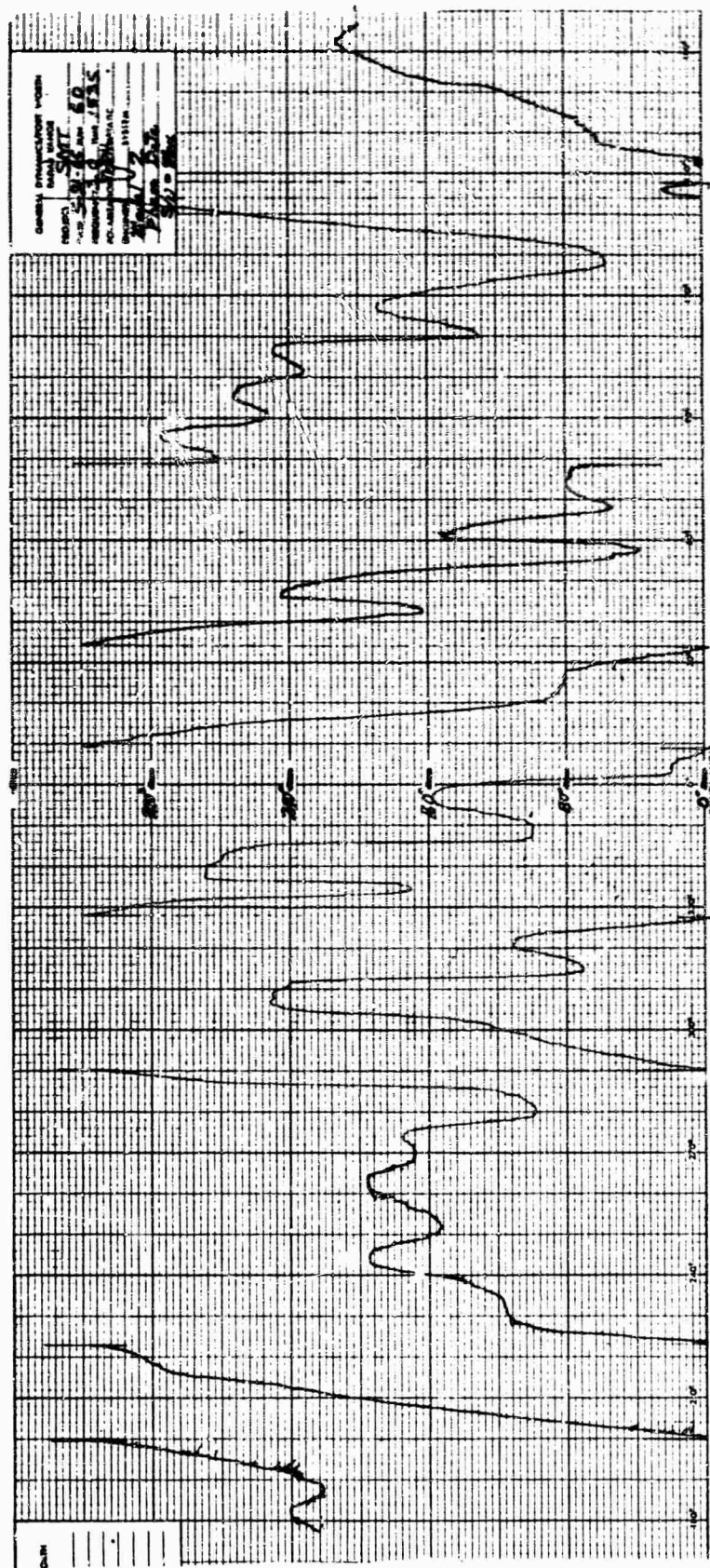
Fig. 16 MODEL 2 CROSS SECTION FOR (TV, RV)

Fig. 17 MODEL 2 PHASE FOR (TV, RV)

Fig. 18 MODEL 2 CROSS SECTION (TV, RH)

Fig. 19 MODEL 2 PHASE FOR (TV, RH)

39

Fig. 20 MODEL 2 CROSS SECTION FOR (TH, RV)

40

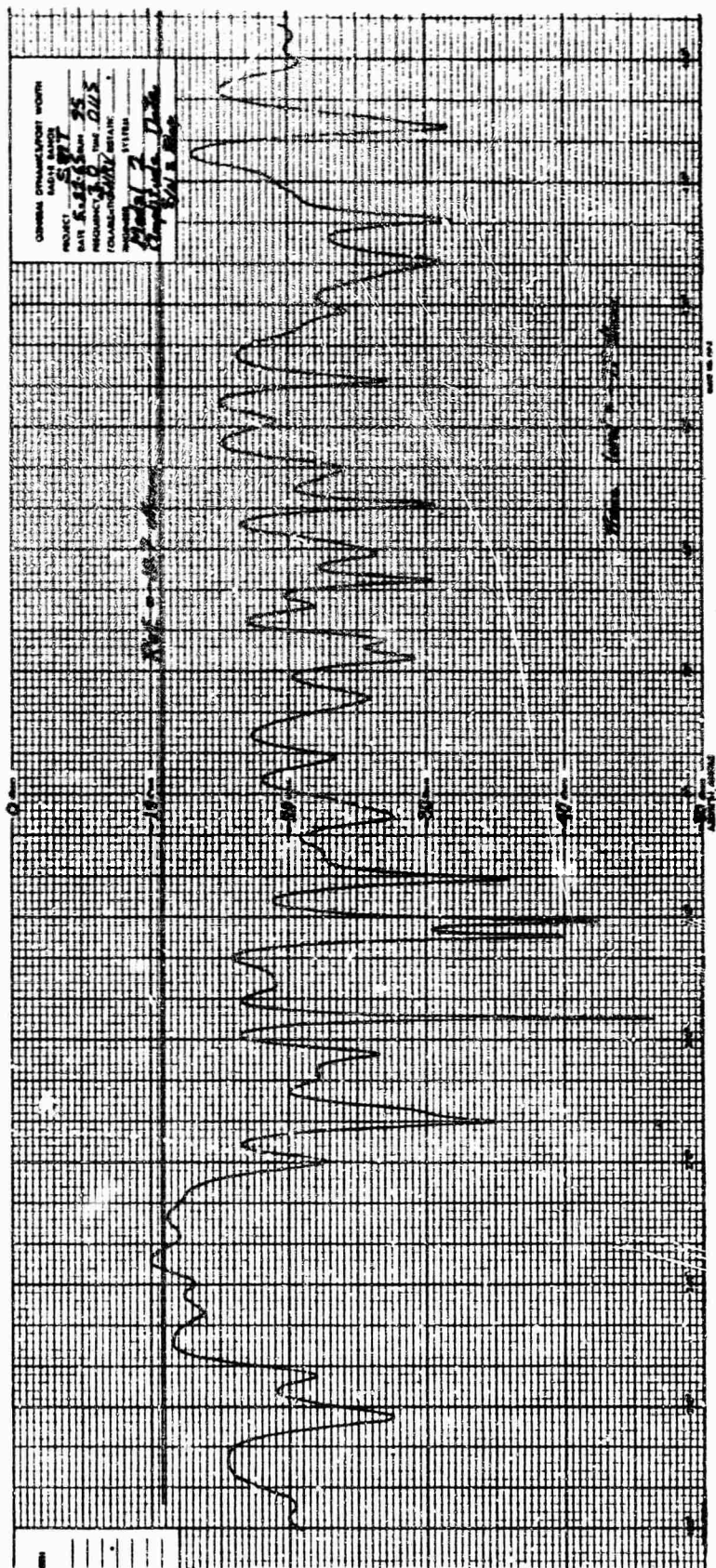Fig. 21 MODEL 2 PHASE FOR (TH, RV)

41

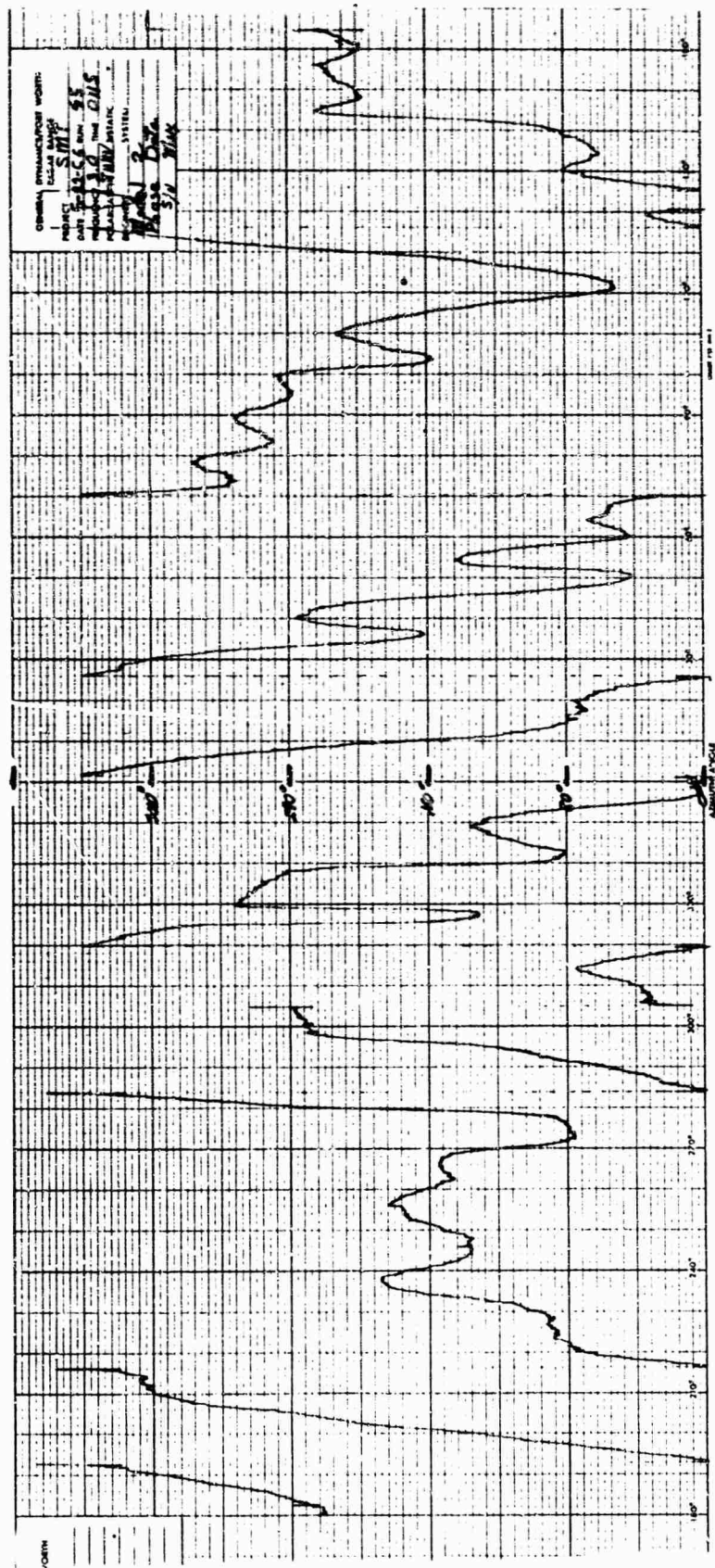Fig. 22 MODEL 2 CROSS SECTION FOR (TH, RH)

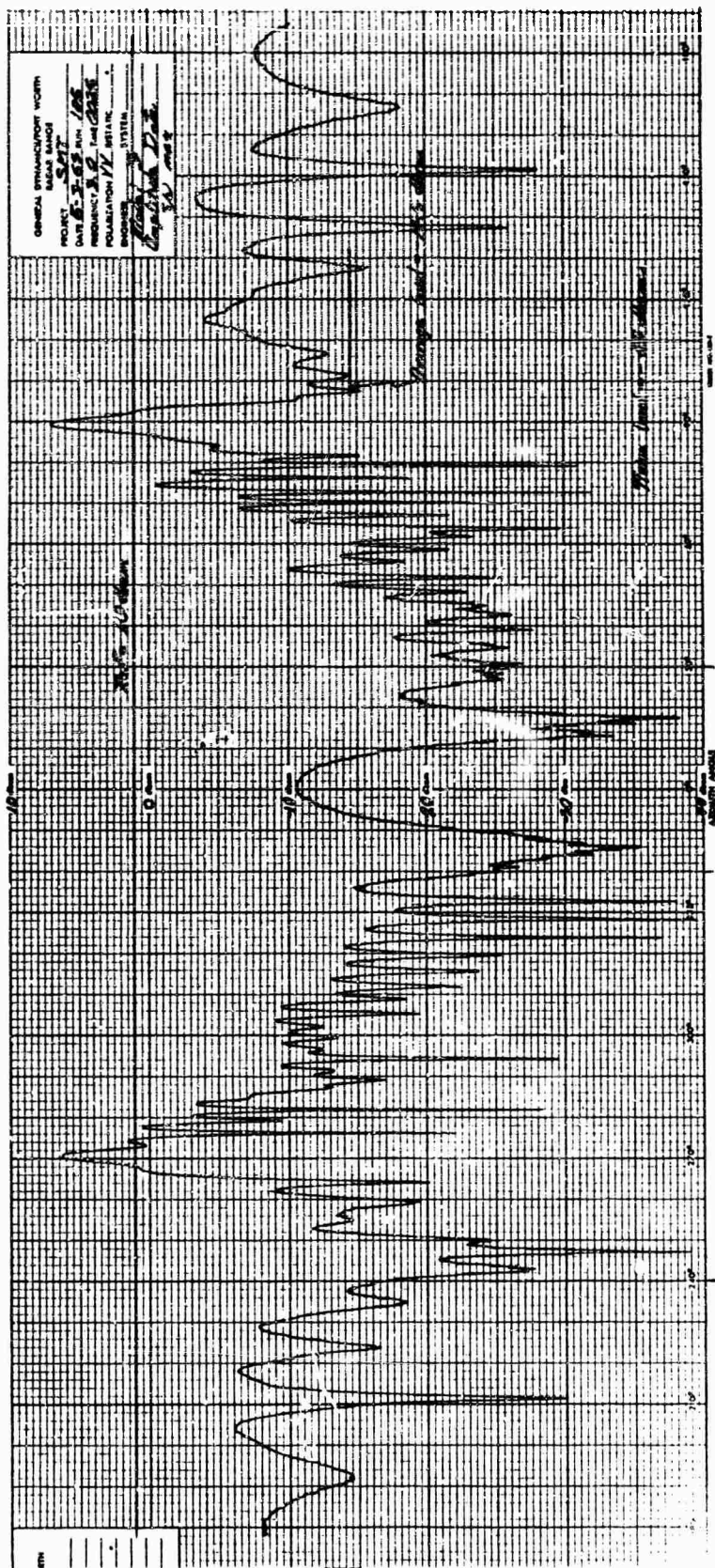Fig. 23 MODEL 2 PHASE FOR (TH, RH)

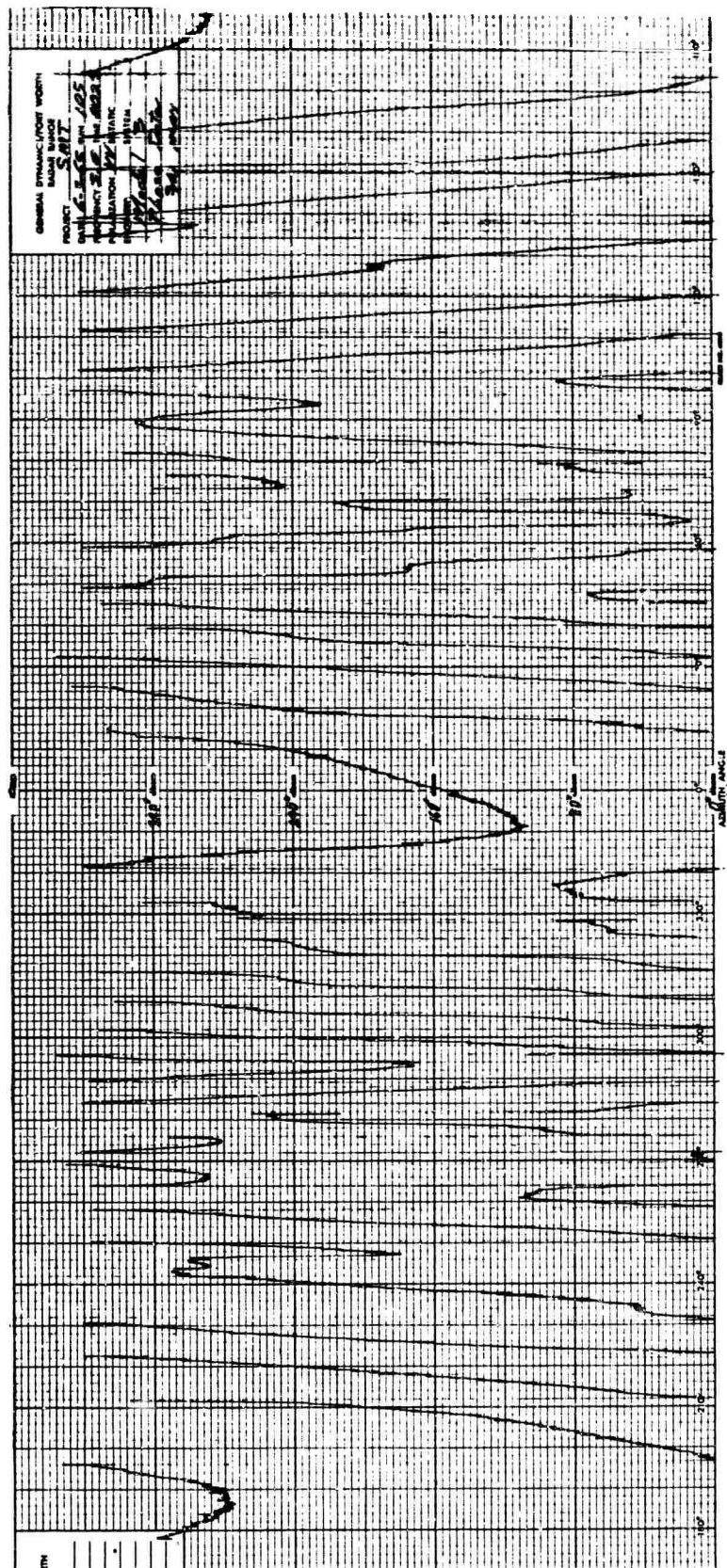Fig. 24 MODEL 3 CROSS SECTION FOR (TV , RV)

44

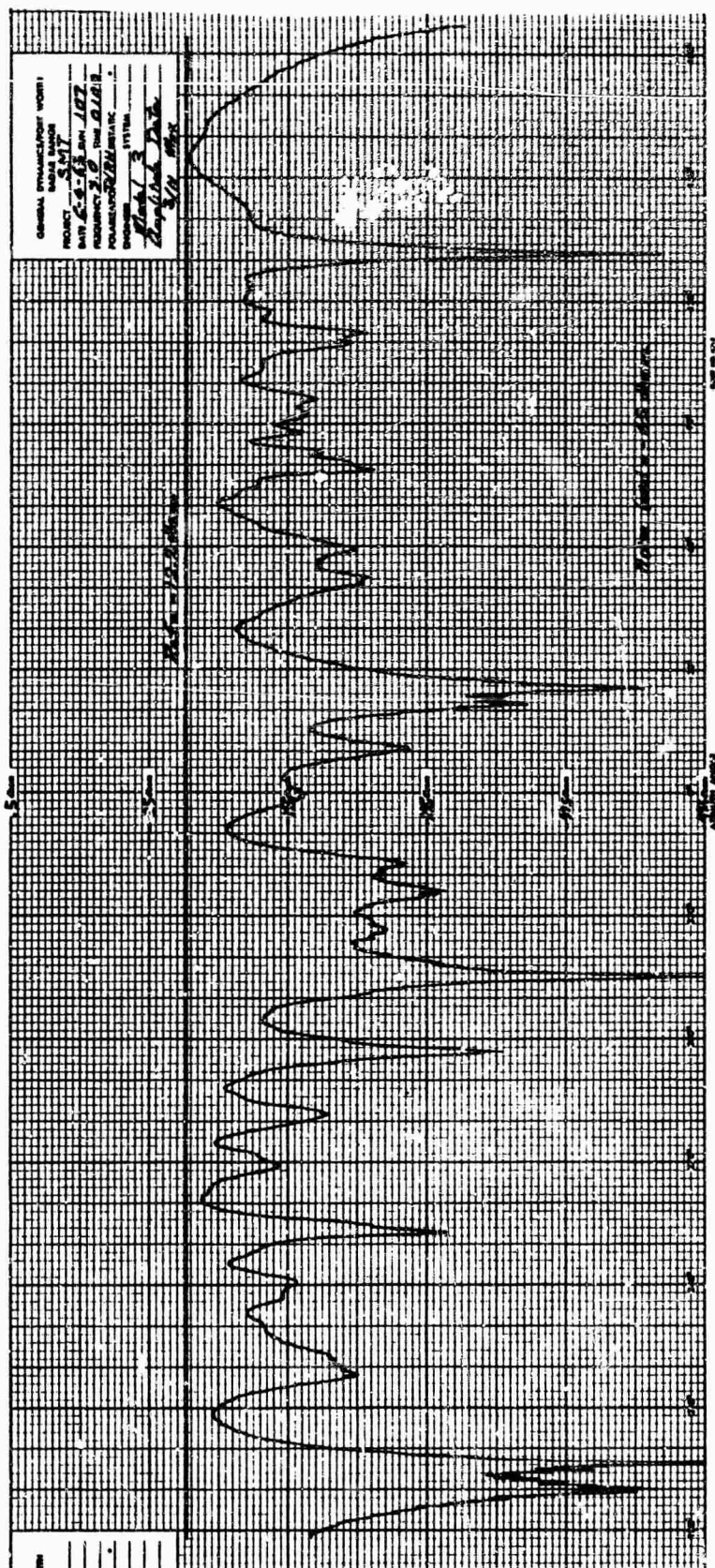Fig. 25 MODEL 3 PHASE FOR (TV, RV)

45

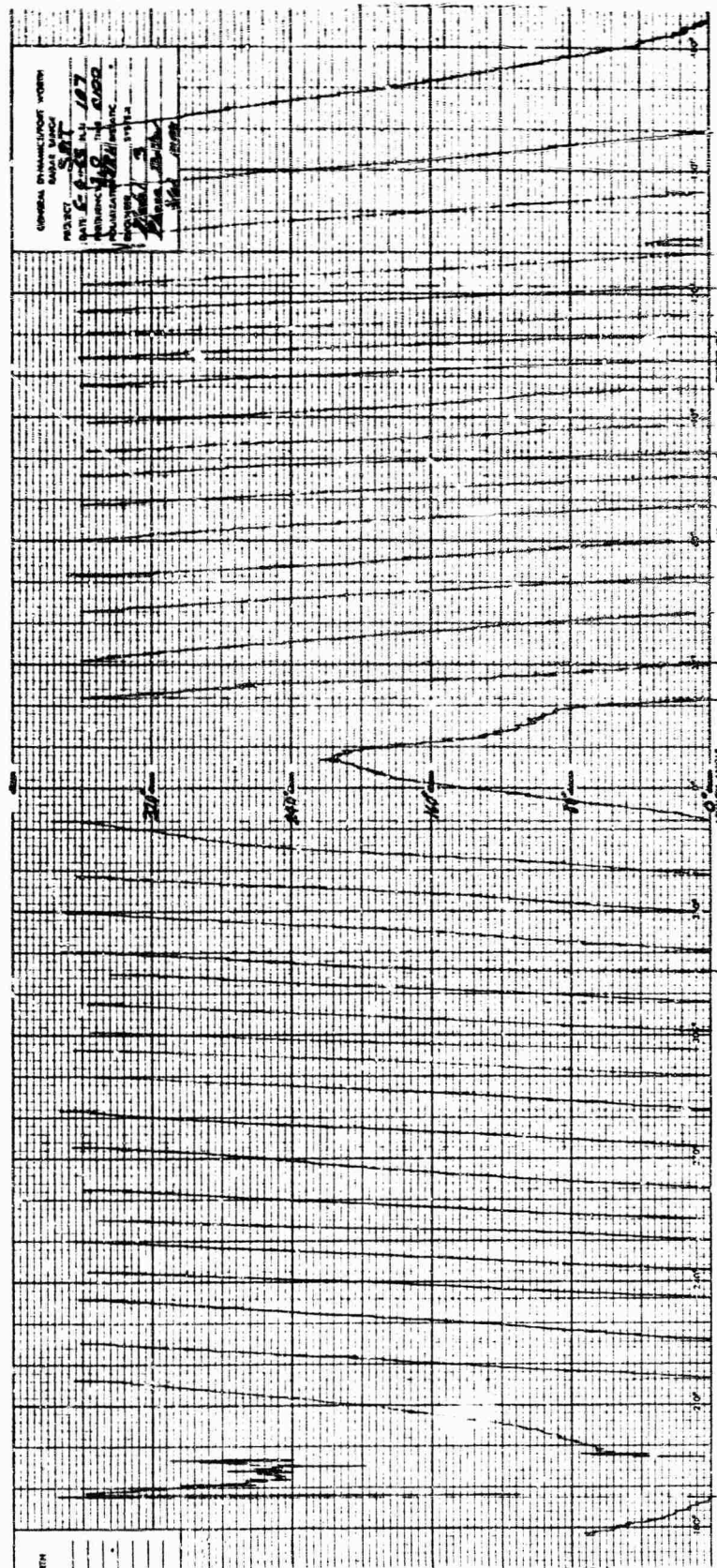Fig. 26 MODEL 3 CROSS SECTION FOR (TV, RH)

Fig. 27 MODEL 3 PHASE FOR (TV, RH)

47

Fig. 28 MODEL 3 CROSS SECTION FOR (TH, RV)

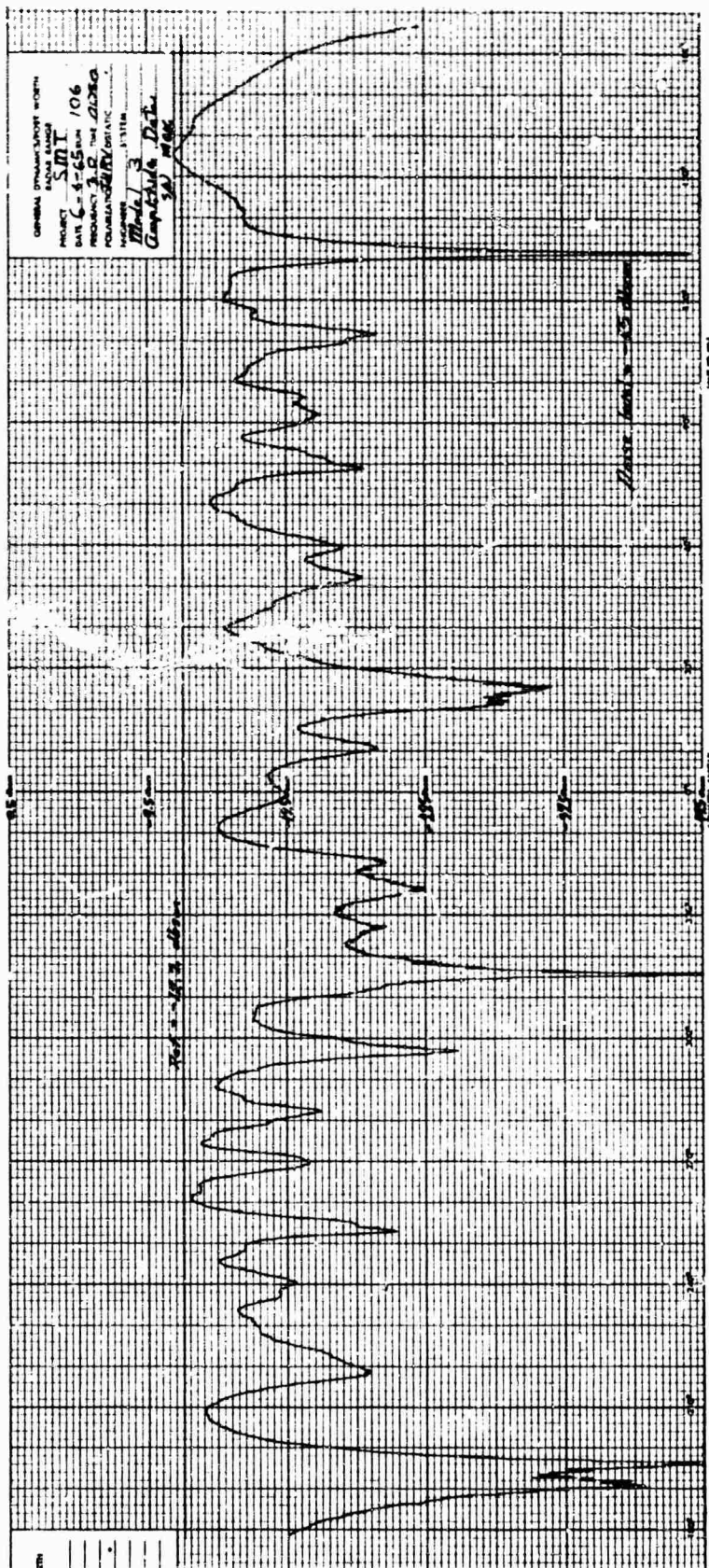Fig. 29 MODEL 3 PHASE FOR (ℓH, RV)

49
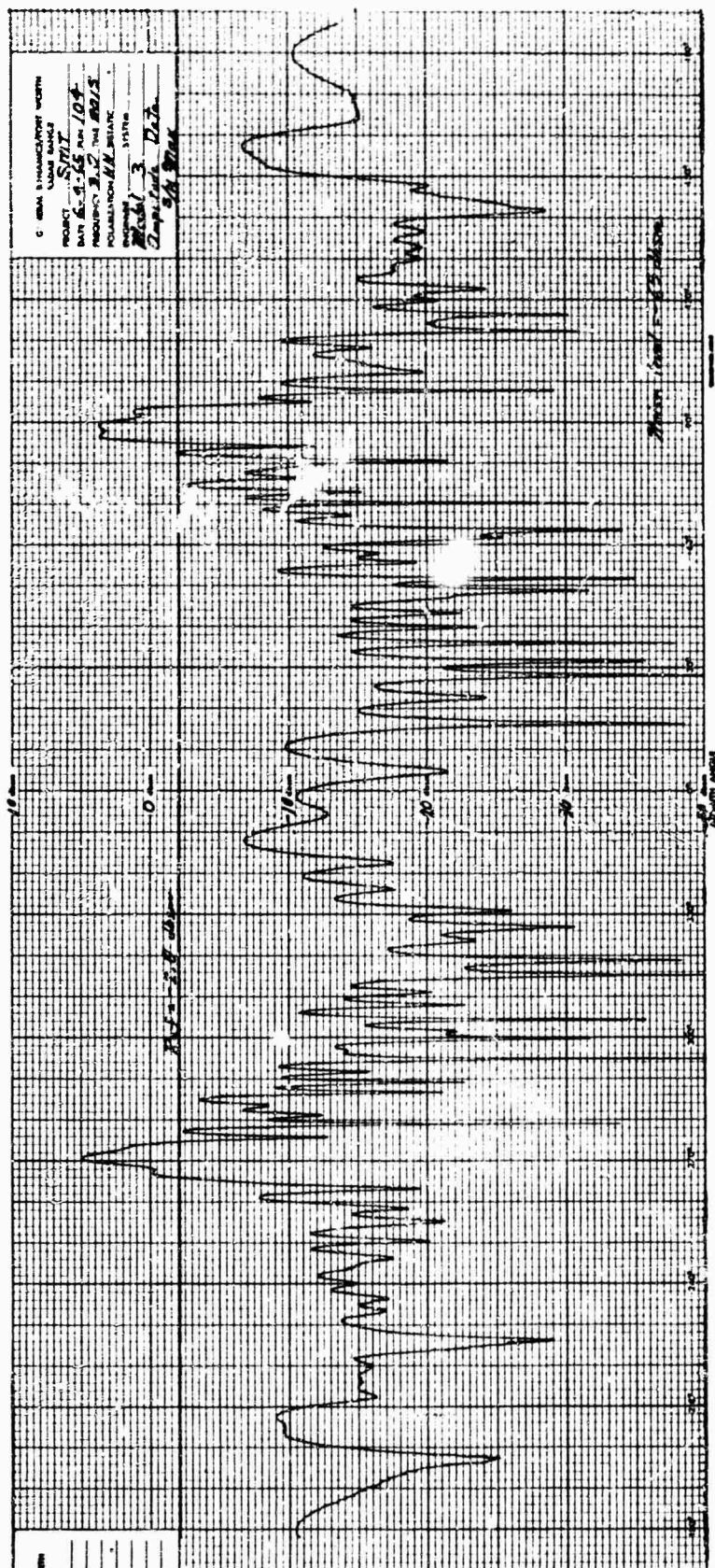
Fig. 30 MODEL 3 CROSS SECTION FOR (TH, RH)
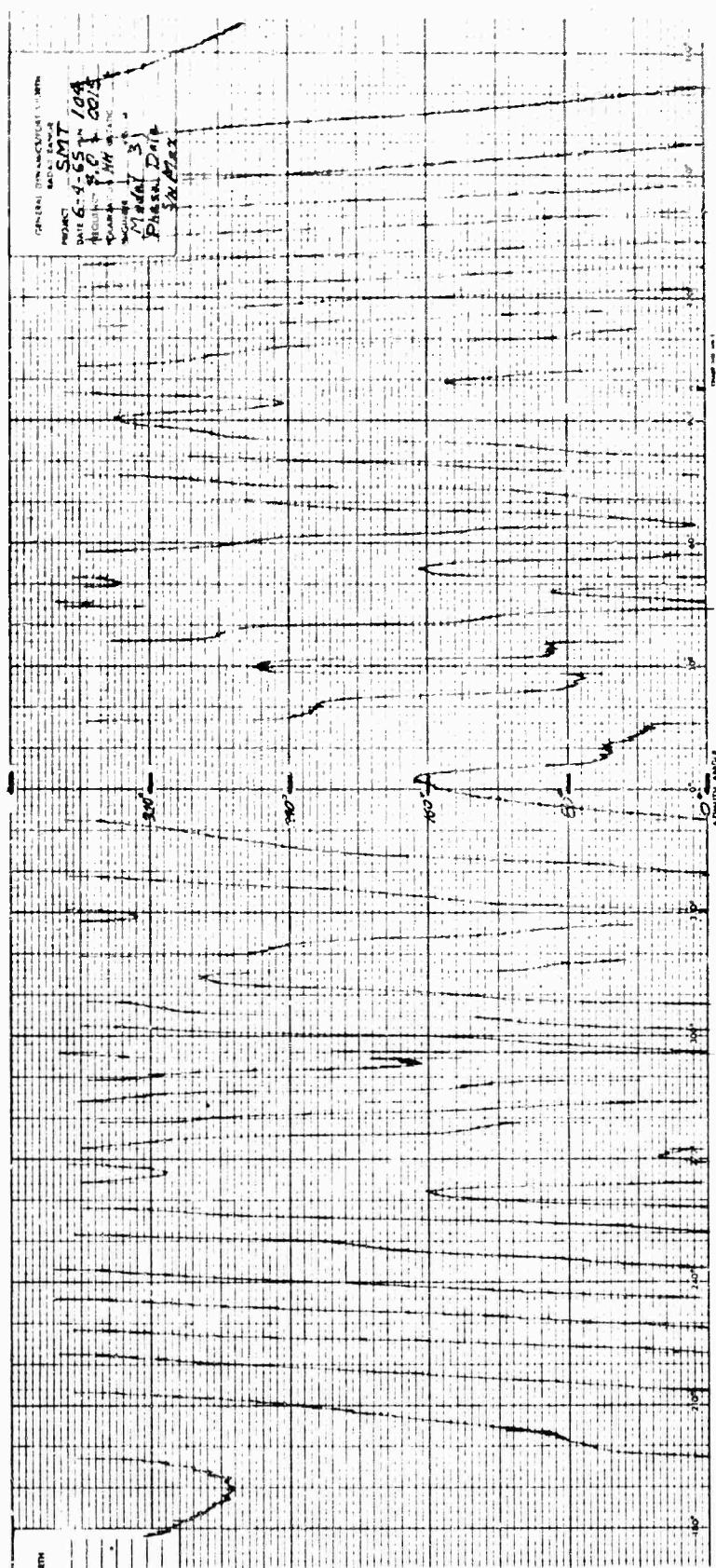
Fig. 31 MODEL 3 PHASE FOR (TH, RH)

51

Fig. 32 MODEL 3 CROSS SECTION FOR S/N = 52 db

Fig. 33 MODEL 3 PHASE FOR S/N = 52 db

53

Fig. 34 MODEL 3 CROSS SECTION FOR S/N = 24 db

54

Fig. 35 MODEL 3 PHASE FOR S/N = 24 db

55
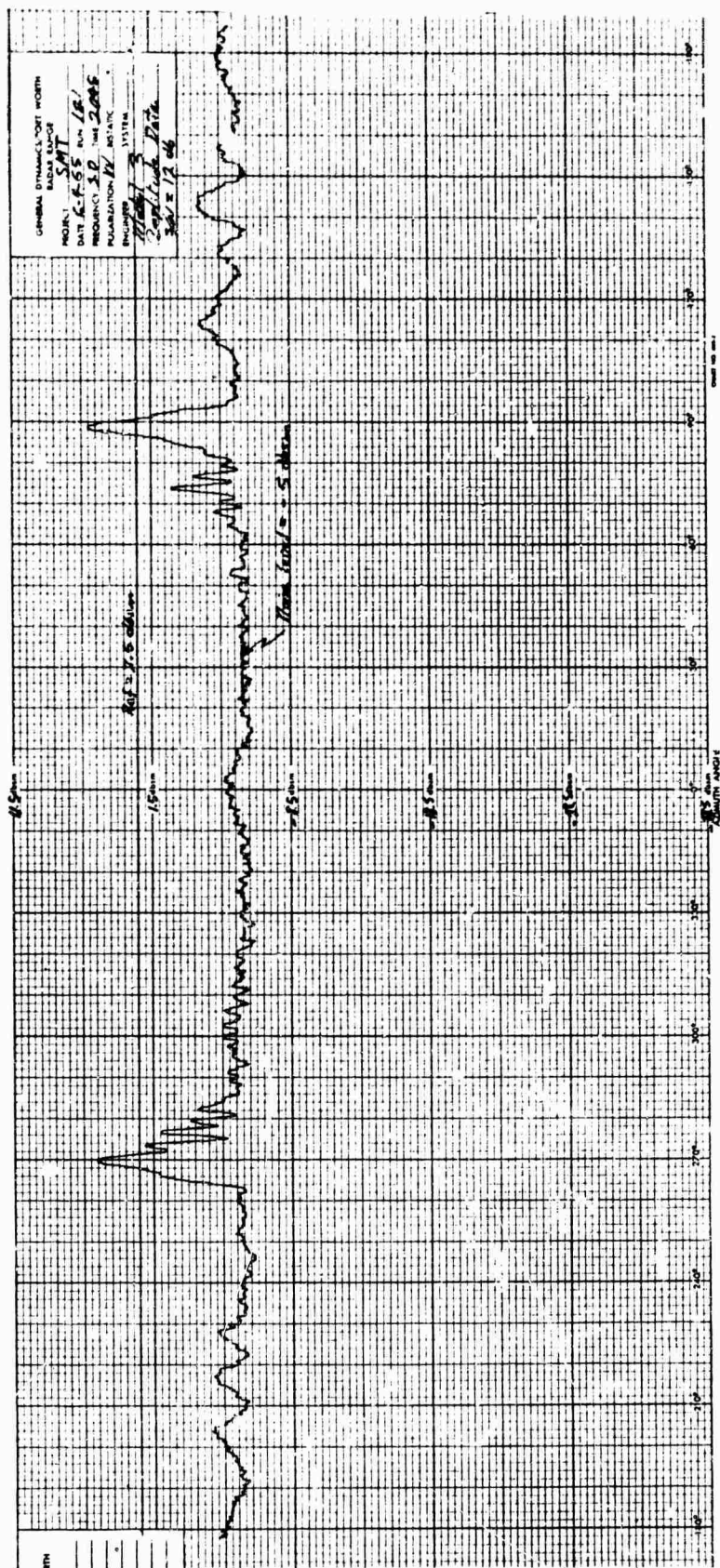
Fig. 36 MODEL 3 CROSS SECTION FOR S/N = 12 db
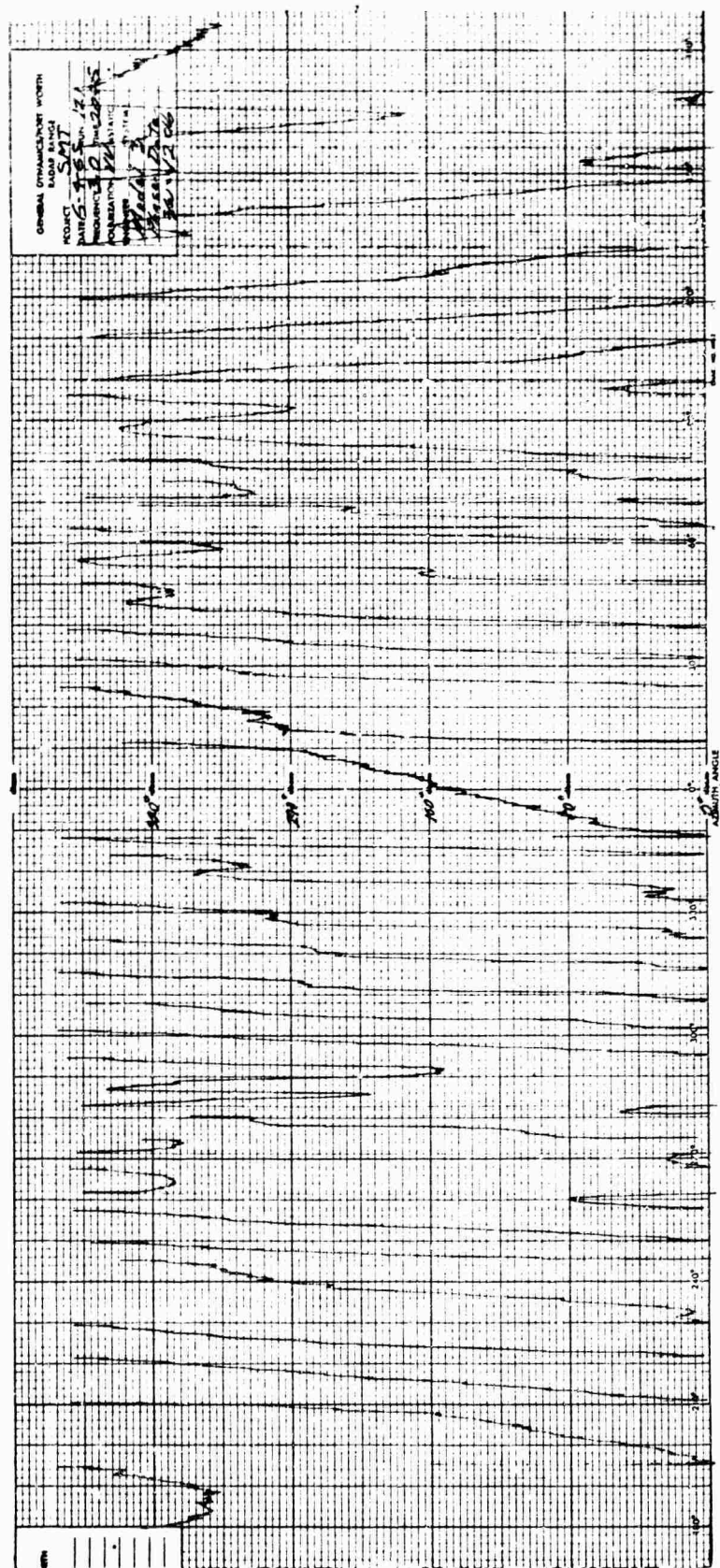
Fig. 37 MODEL 3 PHASE FOR S/N = 12 db

57
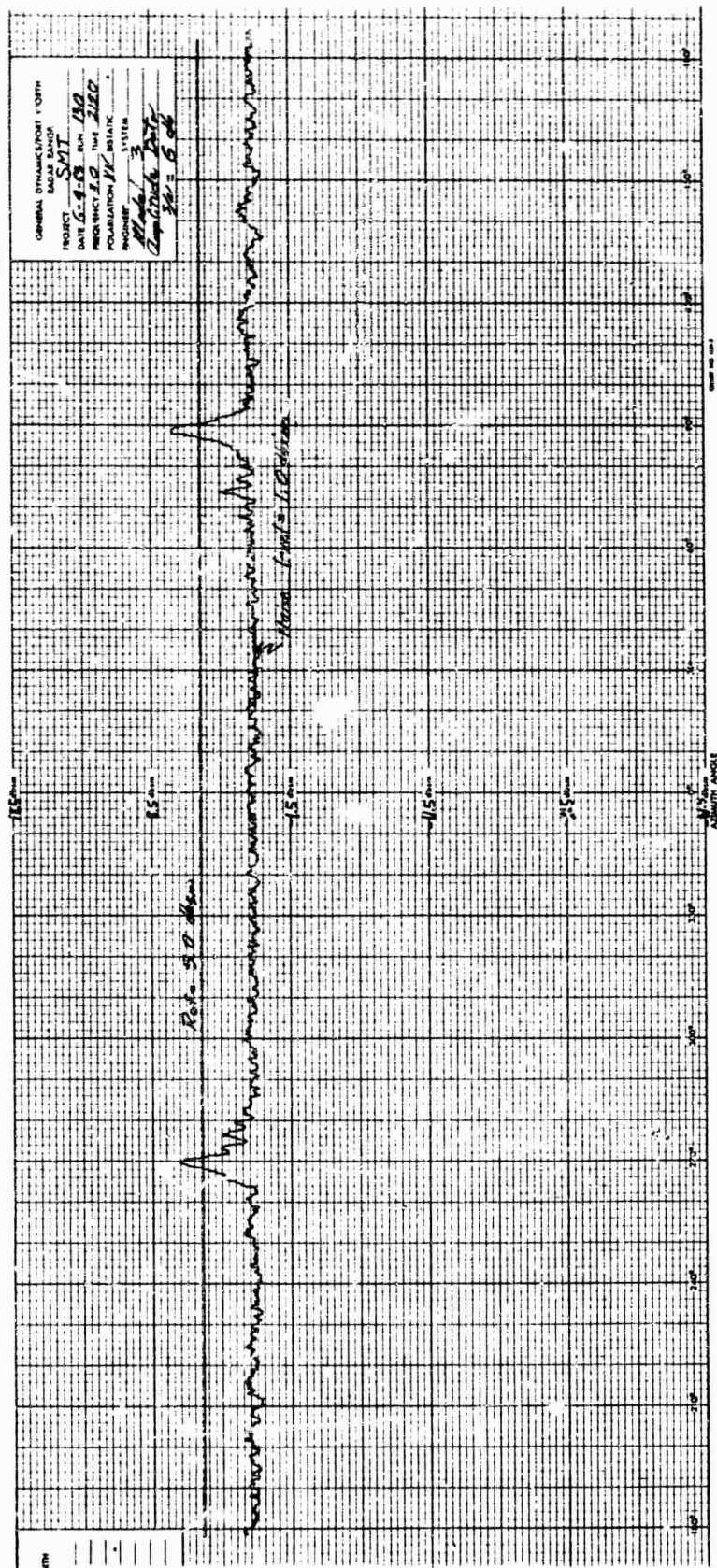
Fig. 38 MODEL 3 CROSS SECTION FOR S/N = 6 db

Fig. 39 MODEL 3 PHASE FOR S/N = 6 db

59

Fig. 40 MODEL 3 CROSS SECTION FOR S/N = 3 db

Fig. 41 MODEL 3 PHASE FOR S/N = 3 db
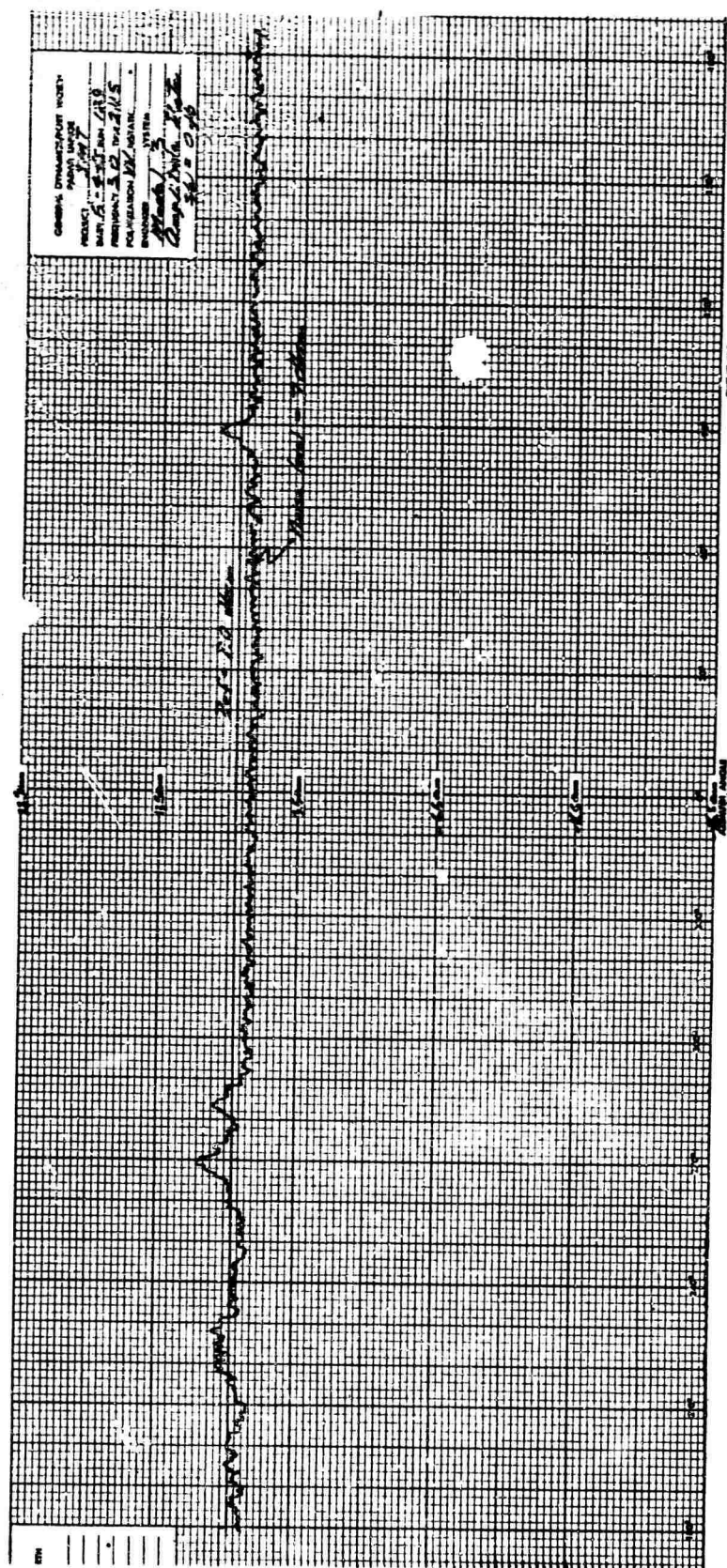
Fig. 42 MODEL 3 CROSS SECTION FOR S/N = 0 db

62

Fig. 43 MODEL 3 PHASE FOR S/N = 0 db

63
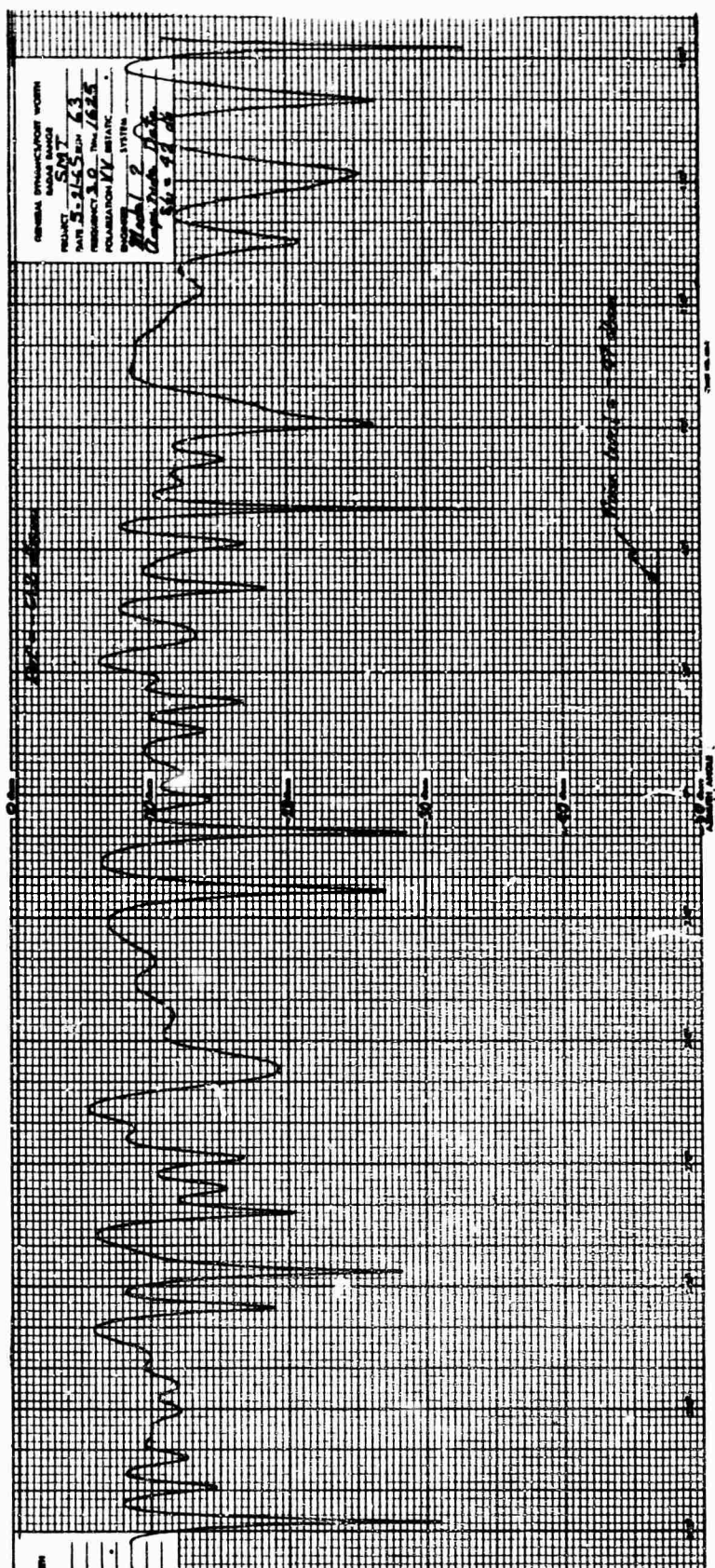
Fig. 44 MODEL 2 CROSS SECTION FOR S/N = 42 db

Fig. 45 MODEL 2 PHASE FOR S/N = 42 db

Fig. 46 MODEL 2 CROSS SECTION FOR S/N = 20 db

Fig. 47 MODEL 2 PHASE FOR S/N = 24 db

Fig. 48 MODEL 2 CROSS SECTION FOR S/N = 12 db

Fig. 49 MODEL 2 PHASE FOR S/N = 12 db

Fig. 50 MODEL 2 CROSS SECTION FOR S/N = 6 db

70

Fig. 51 MODEL 2 PHASE FOR S/N = 6 db
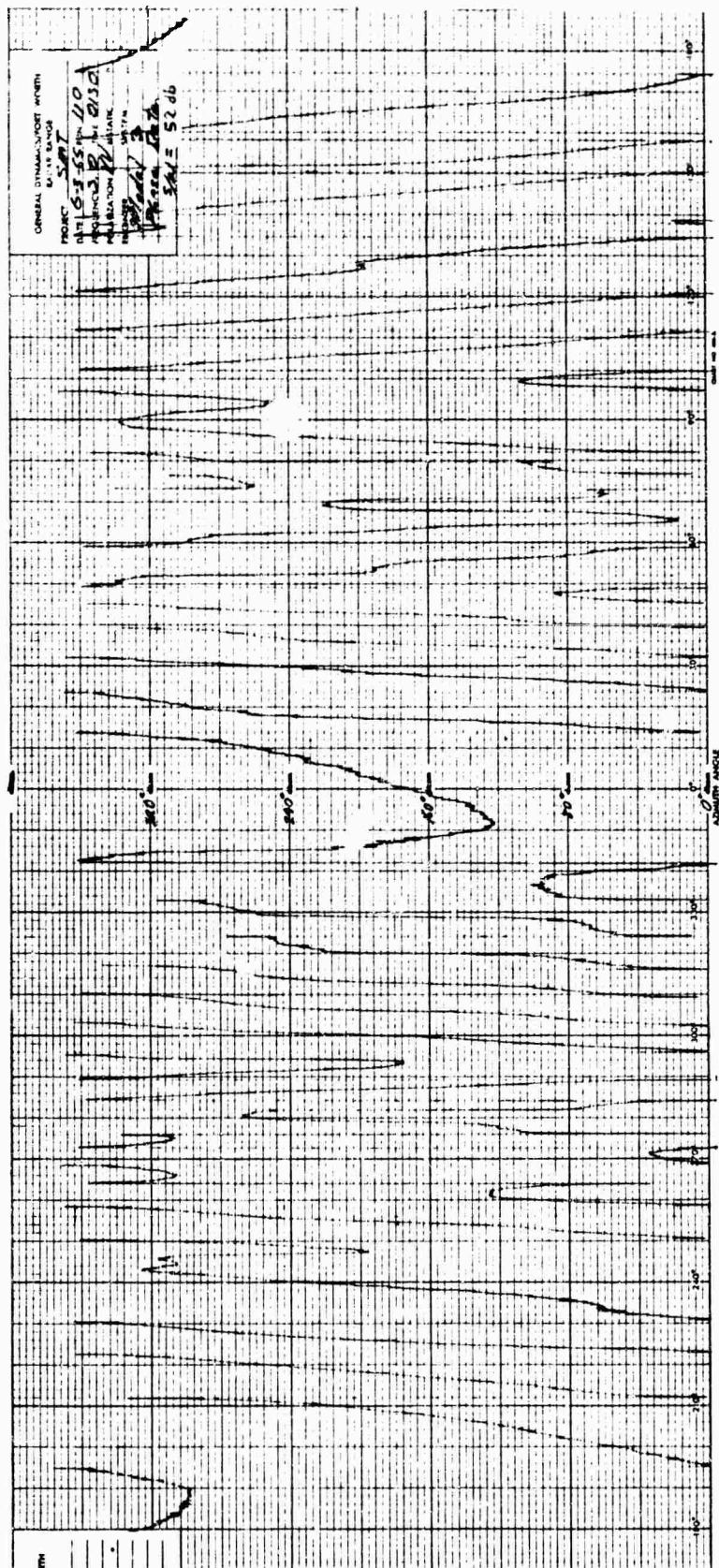
71

Fig. 52 MODEL 2 CROSS SECTION FOR S/N = 3 db

72

Fig. 53   MODEL 2 PHASE FOR S/N = 3 db

Fig. 54 MODEL 2 CROSS SECTION FOR S/N = 0 db
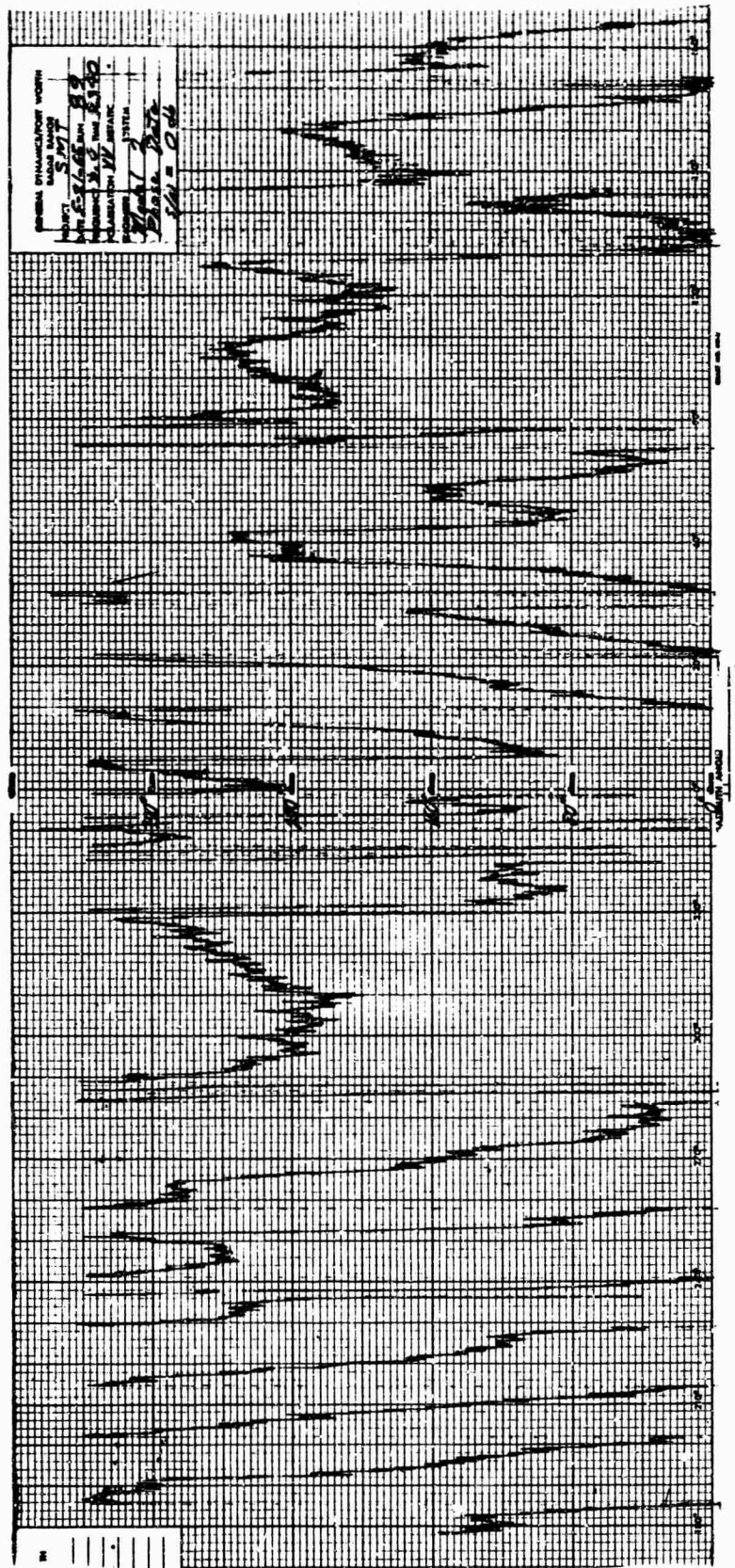
Fig. 55 MODEL 2 PHASE FOR S/N = 0 db

75
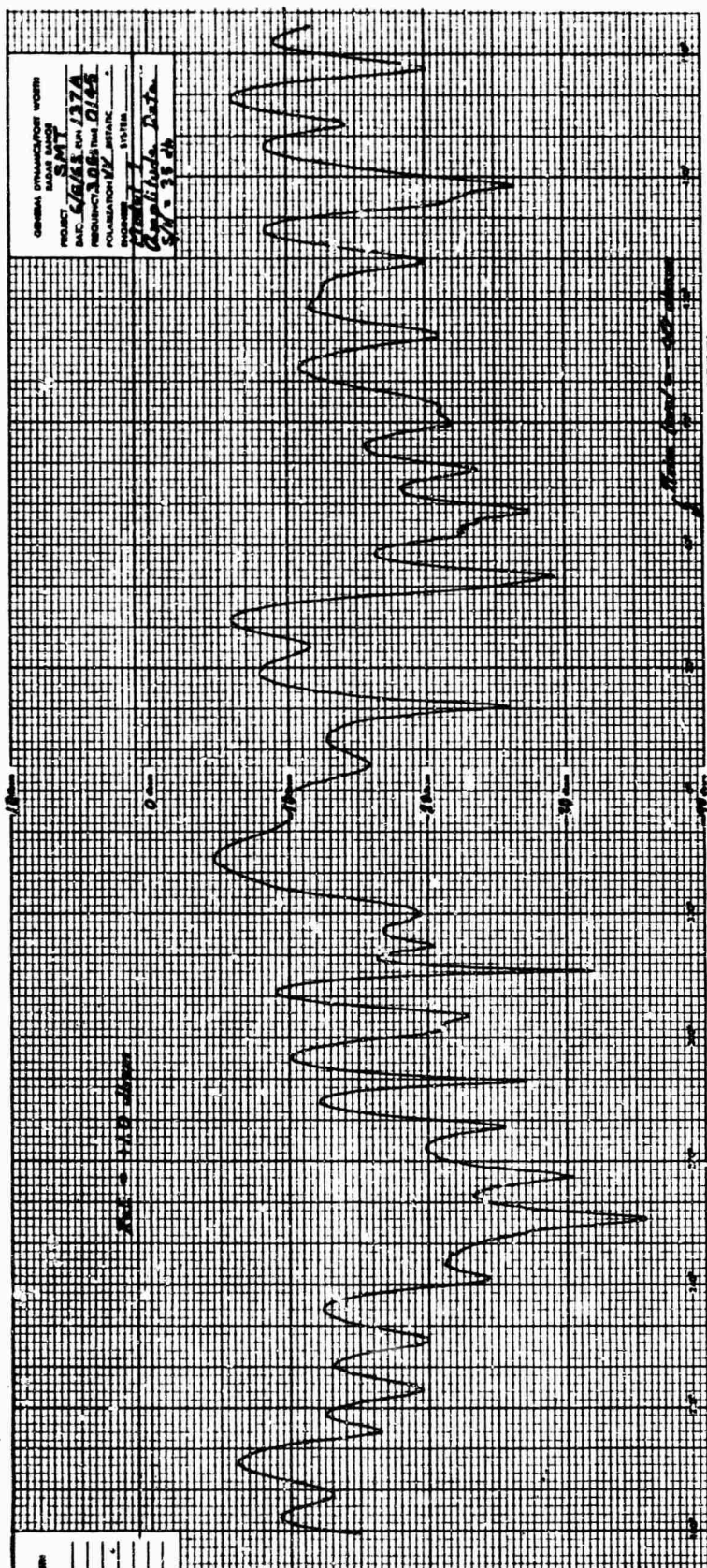
Fig. 56 MODEL 1 CROSS SECTION FOR S/N = 35 db
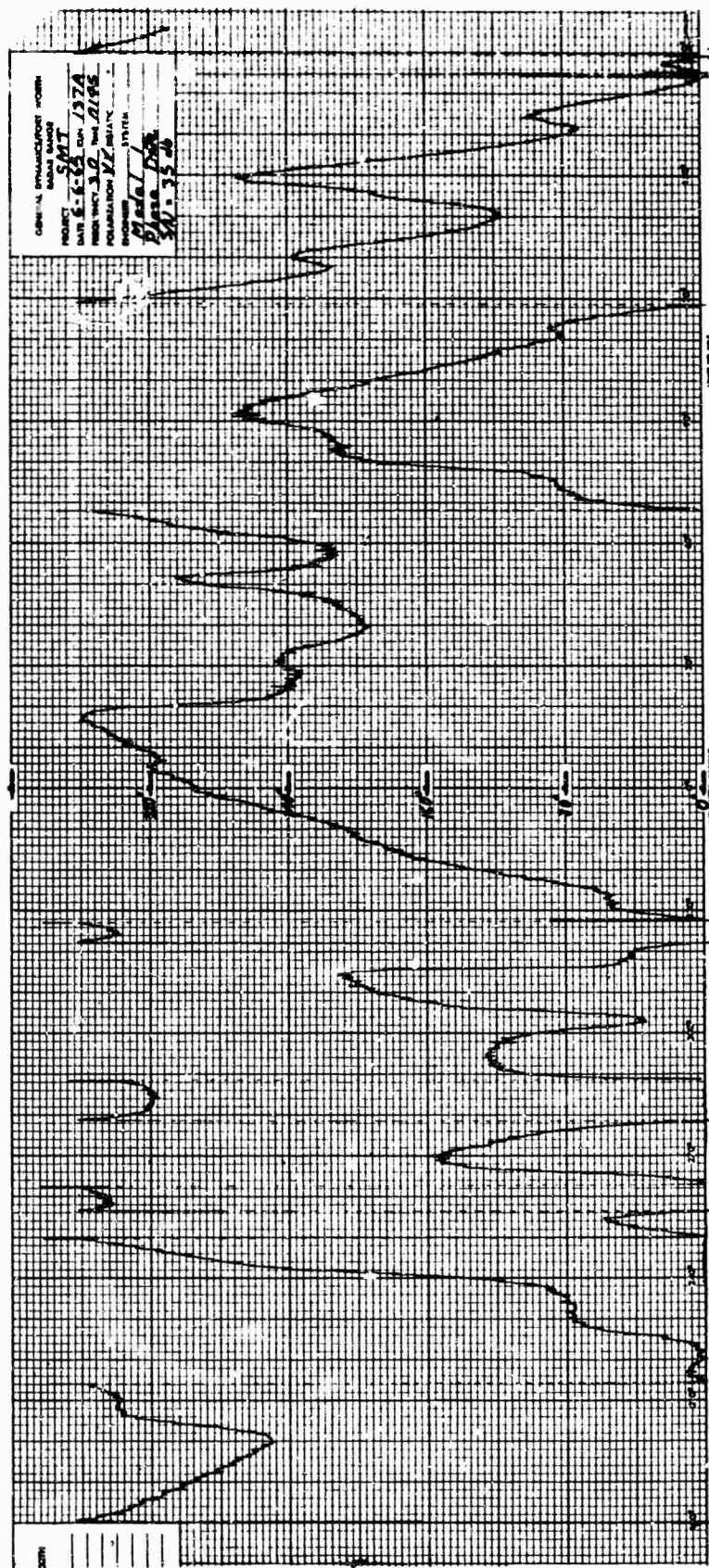
Fig. 57 MODEL 1 PHASE FOR S/N = 35 db
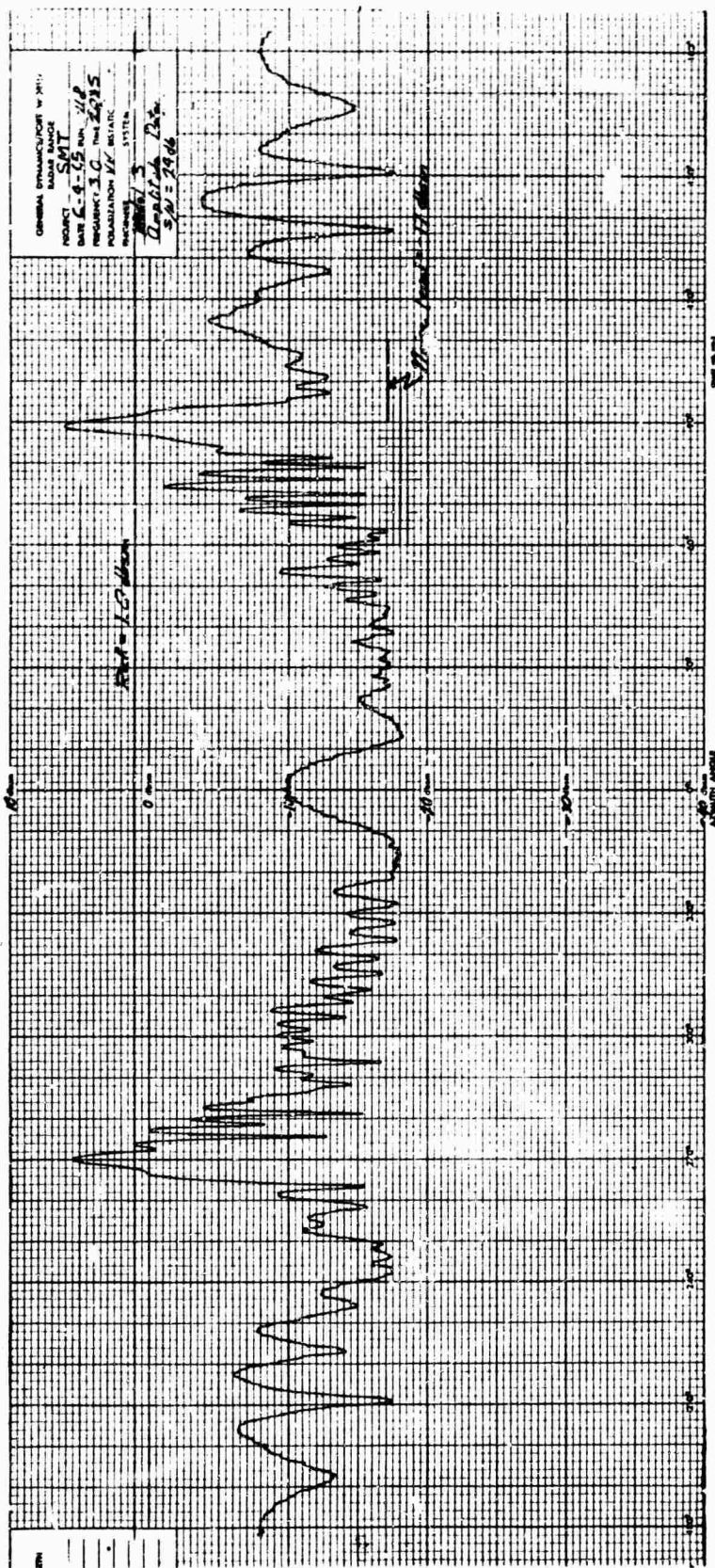
77

Fig. 58 MODEL 1 CROSS SECTION FOR S/N = 24 db

78

Fig. 59 MODEL 1 PHASE FOR S/N = 24 db

Fig. 60 MODEL 1 CROSS SECTION FOR S/N - 12 db
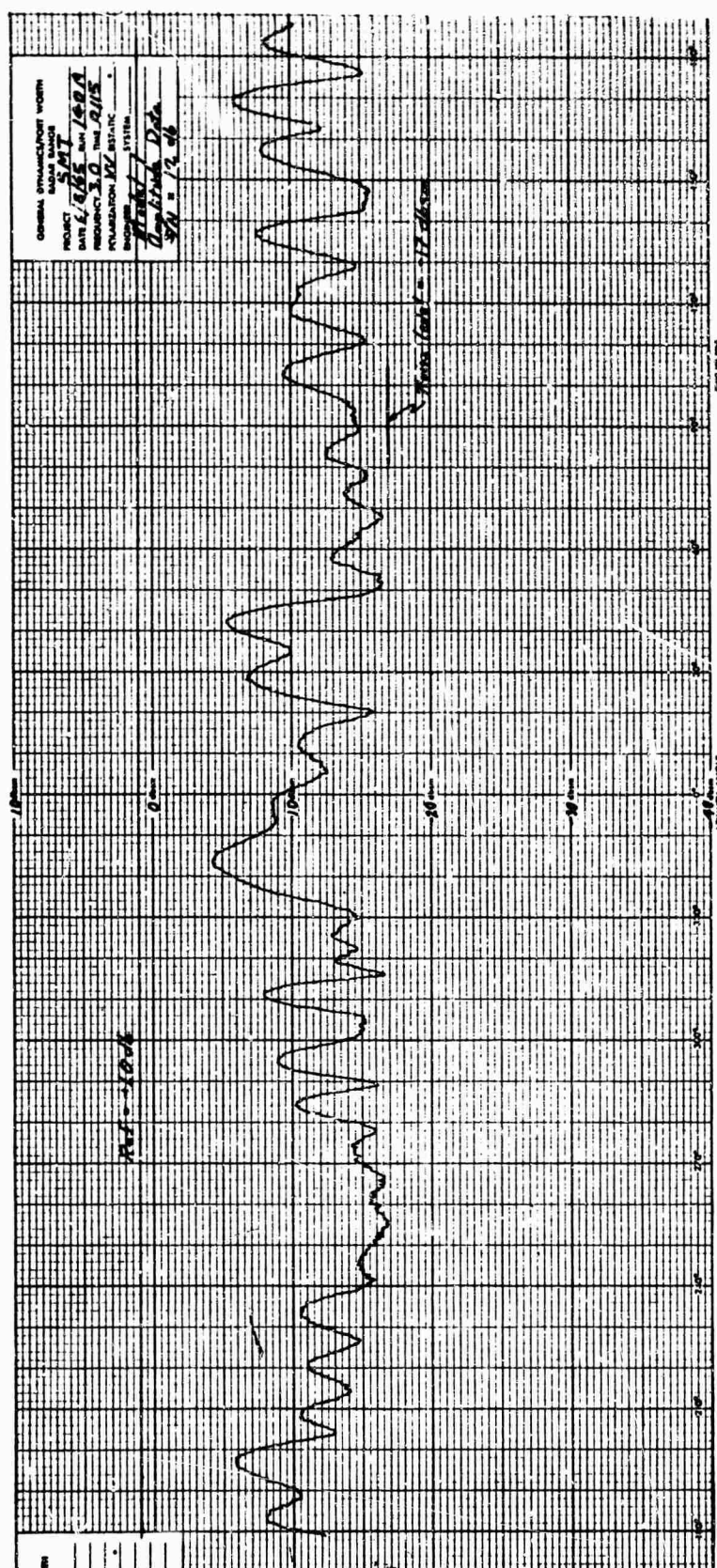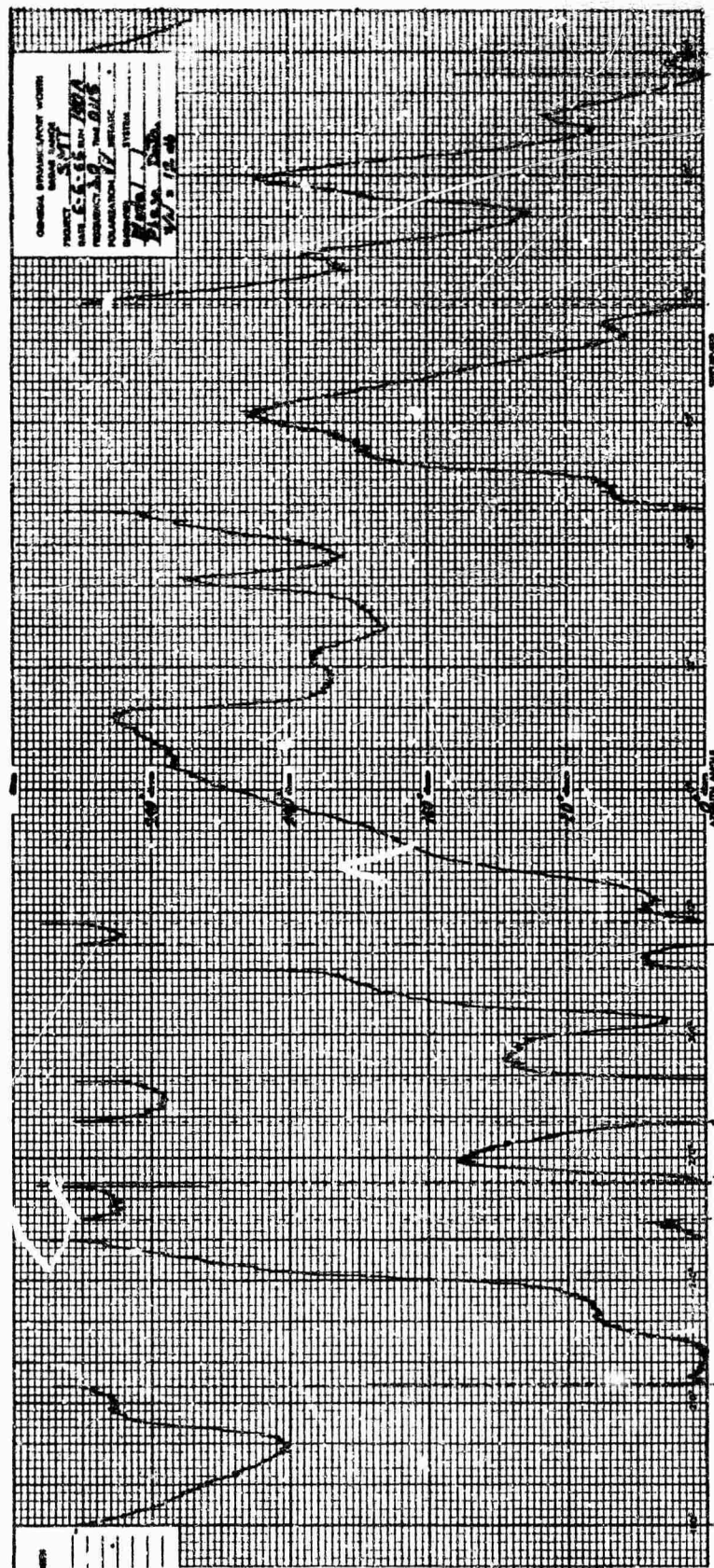
Fig. 61 MODEL 1 PHASE FOR S/N = 12 db

81

Fig. 62 MODEL 1 CROSS SECTION FOR S/N = 6 db
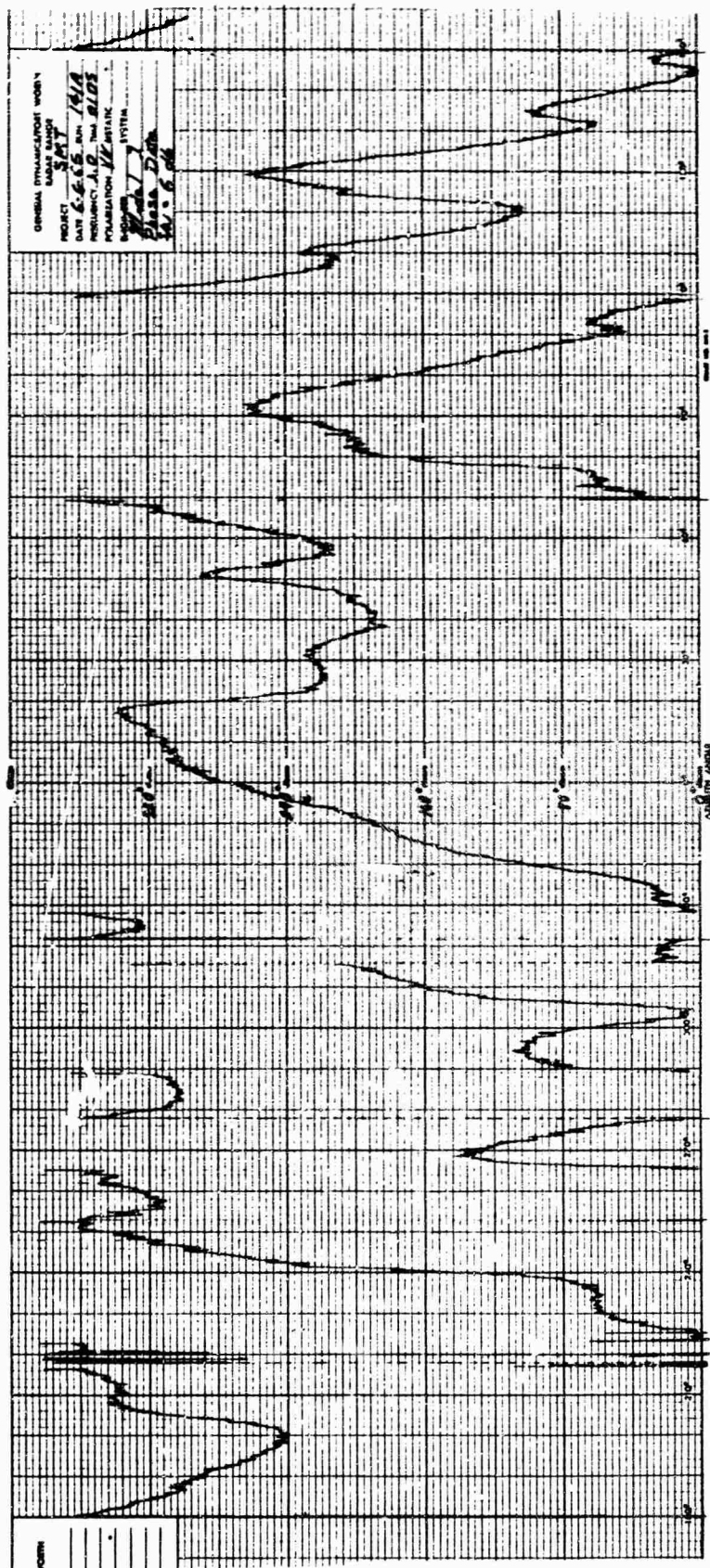
Fig. 63 MODEL 1 PHASE FOR S/N = 6 db

Fig. 64 MODEL 1 CROSS SECTION FOR S/N = 3 db

84
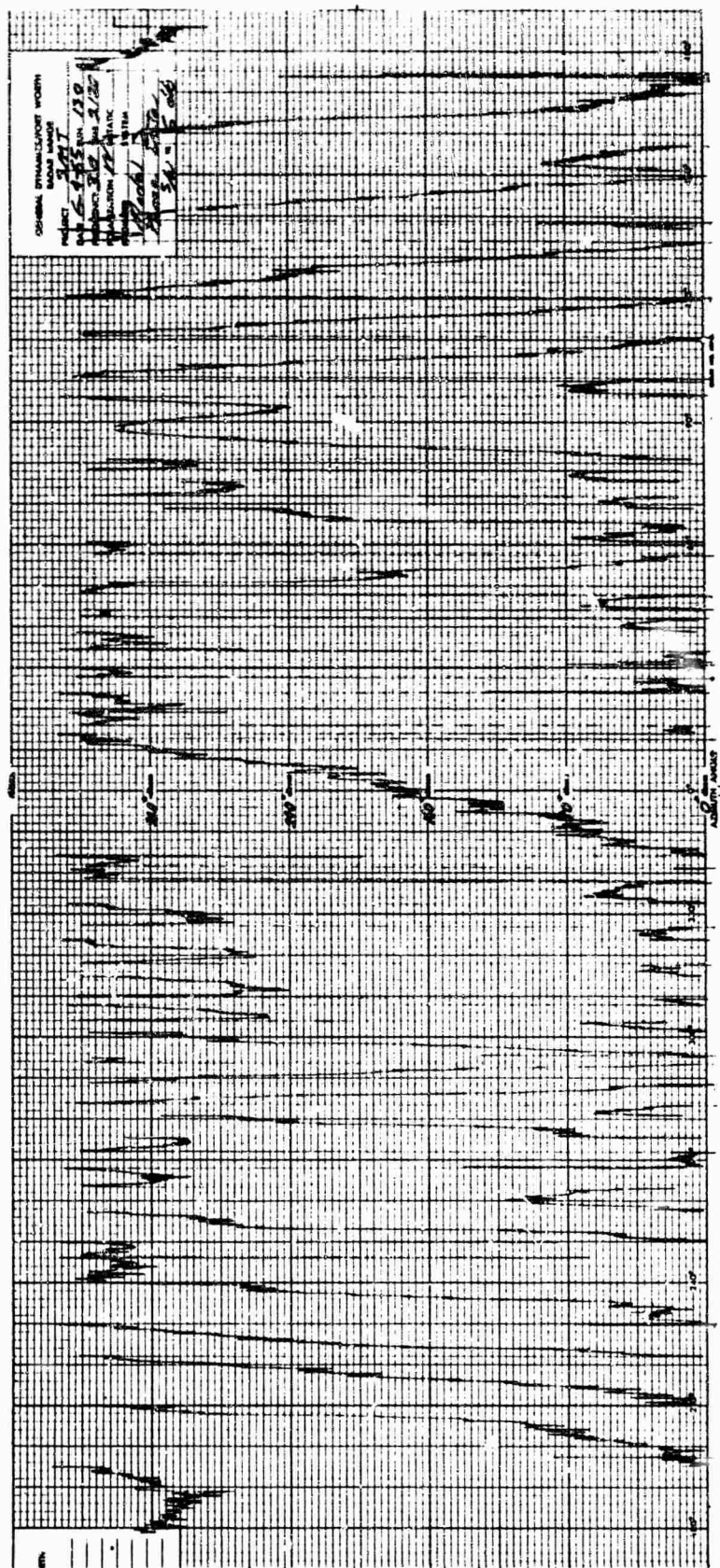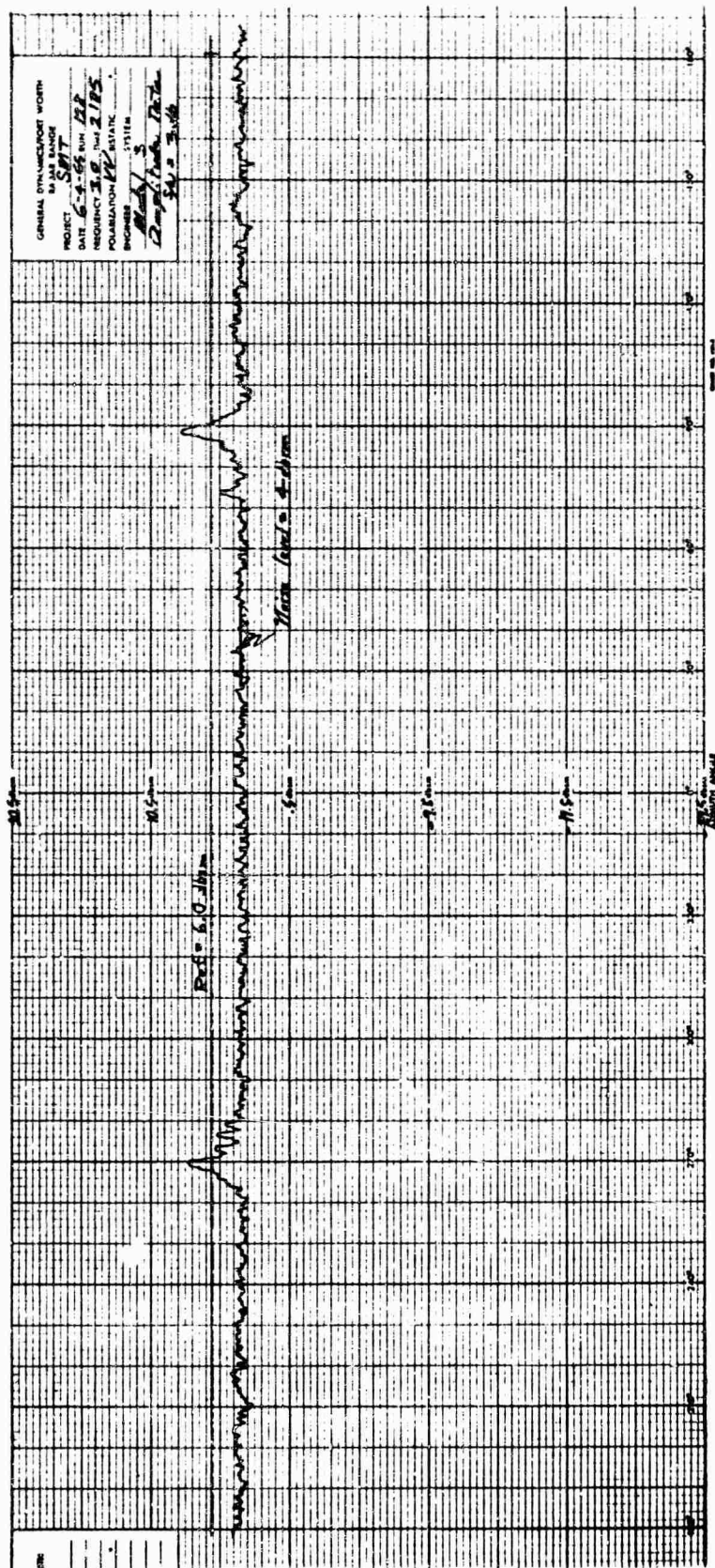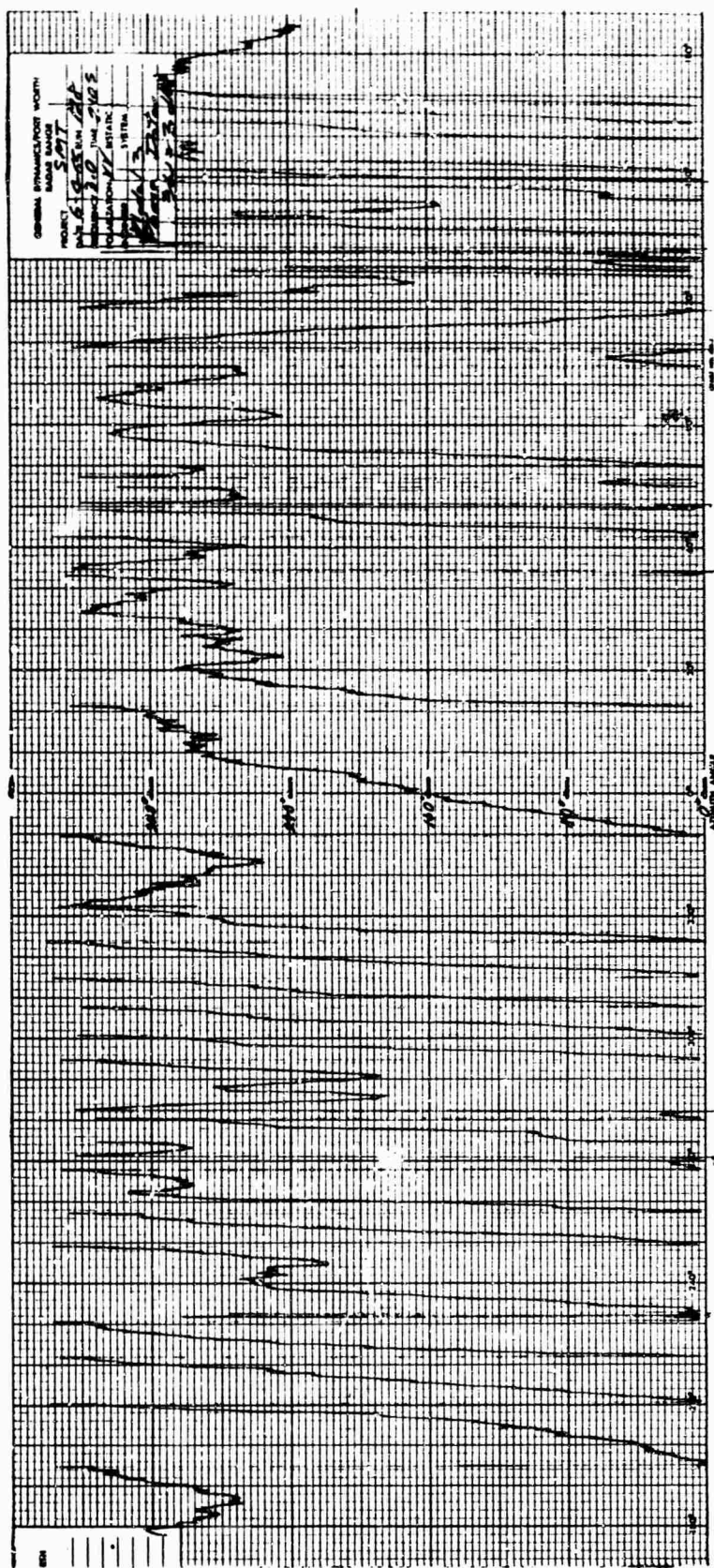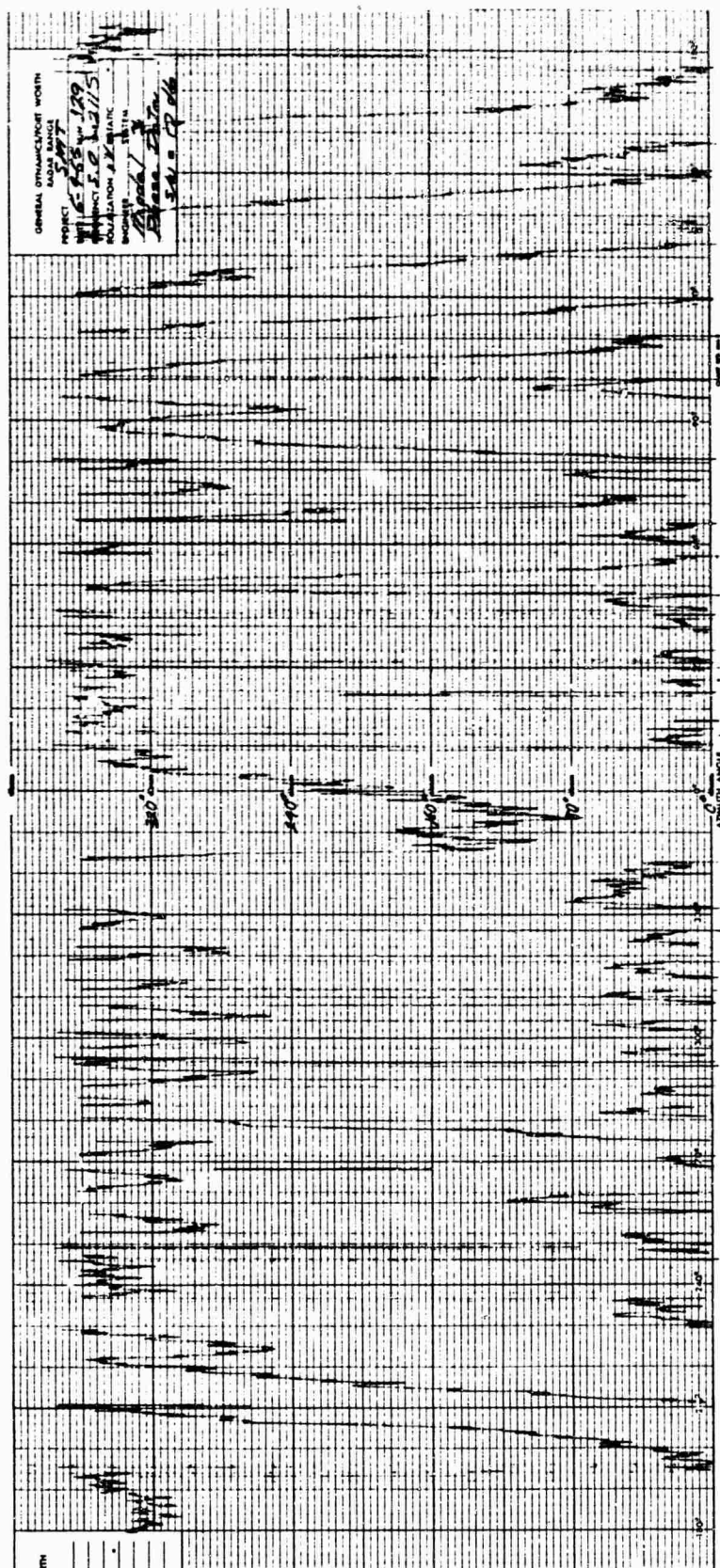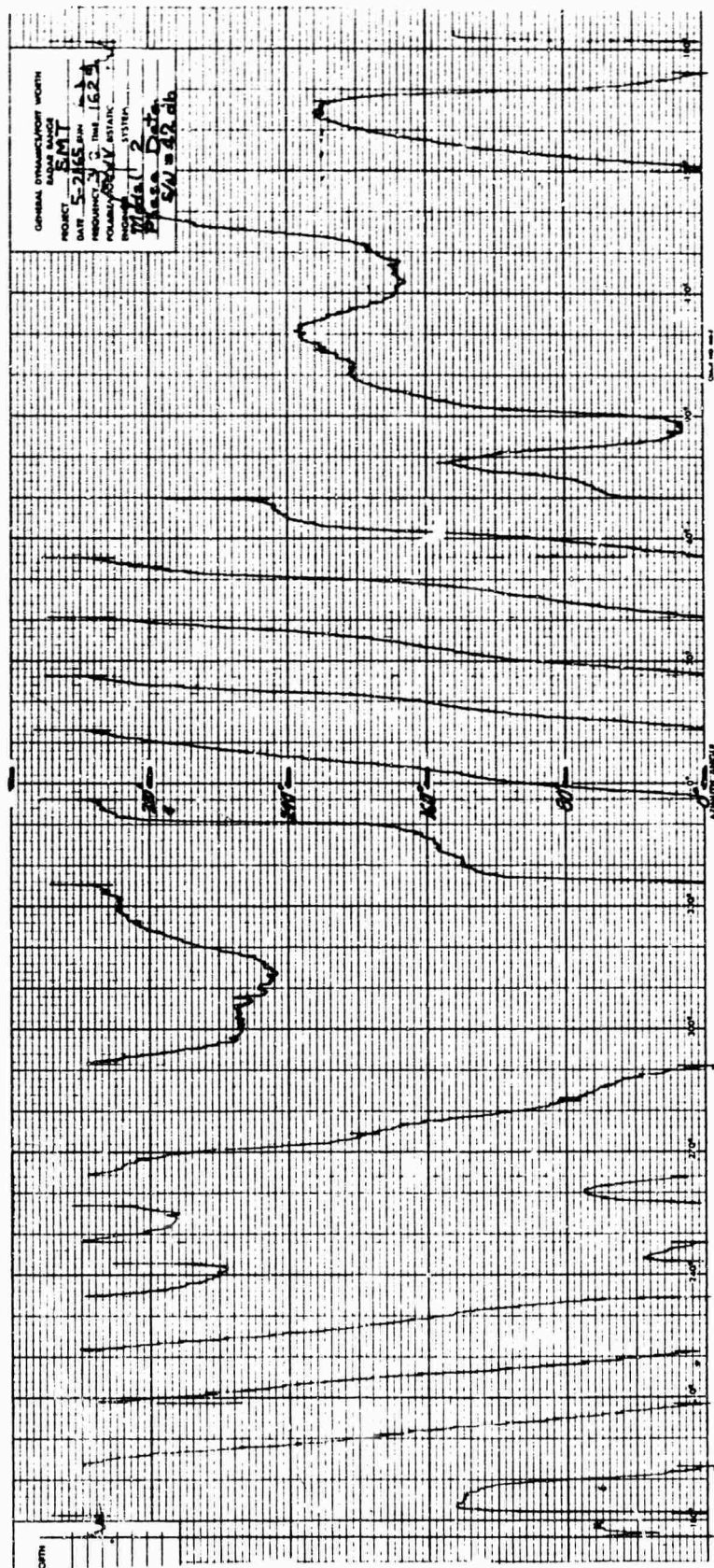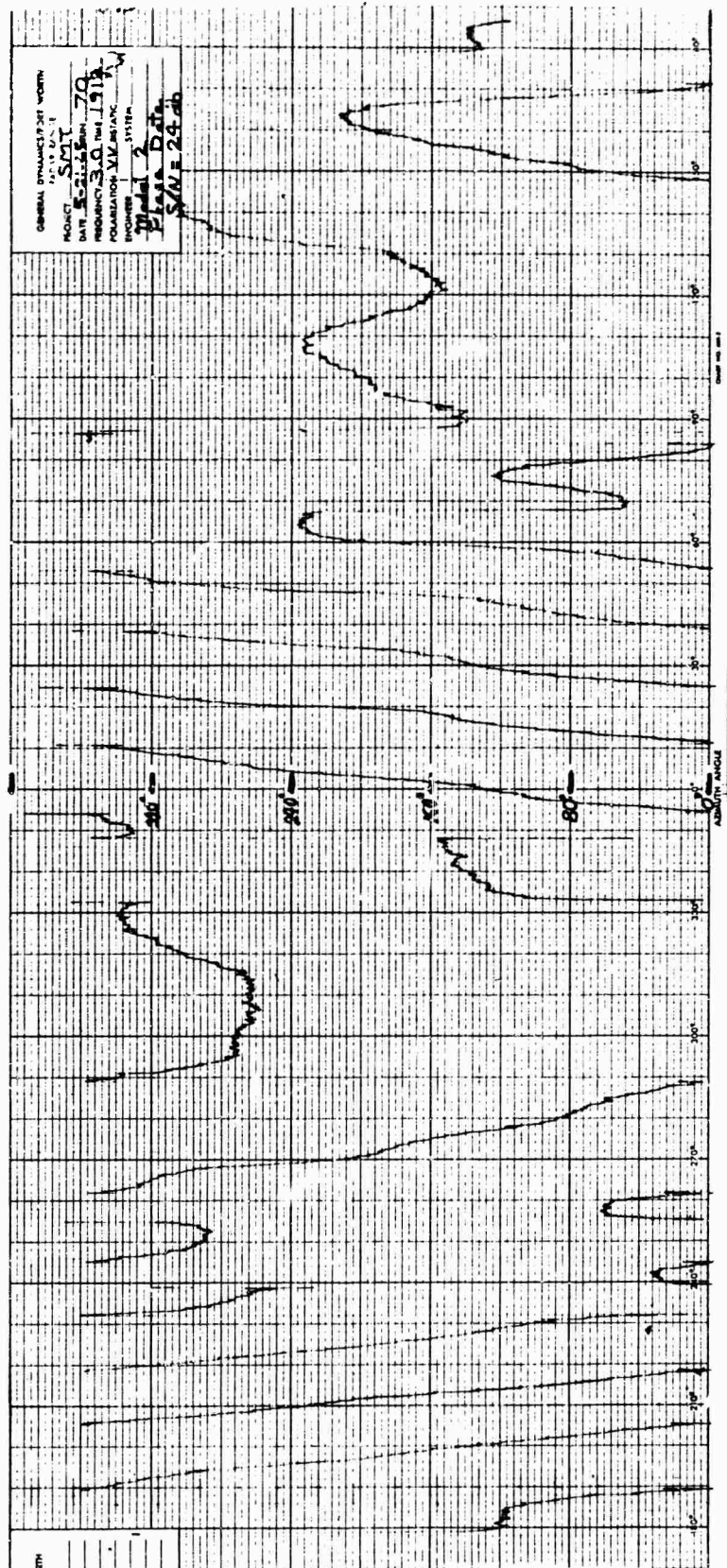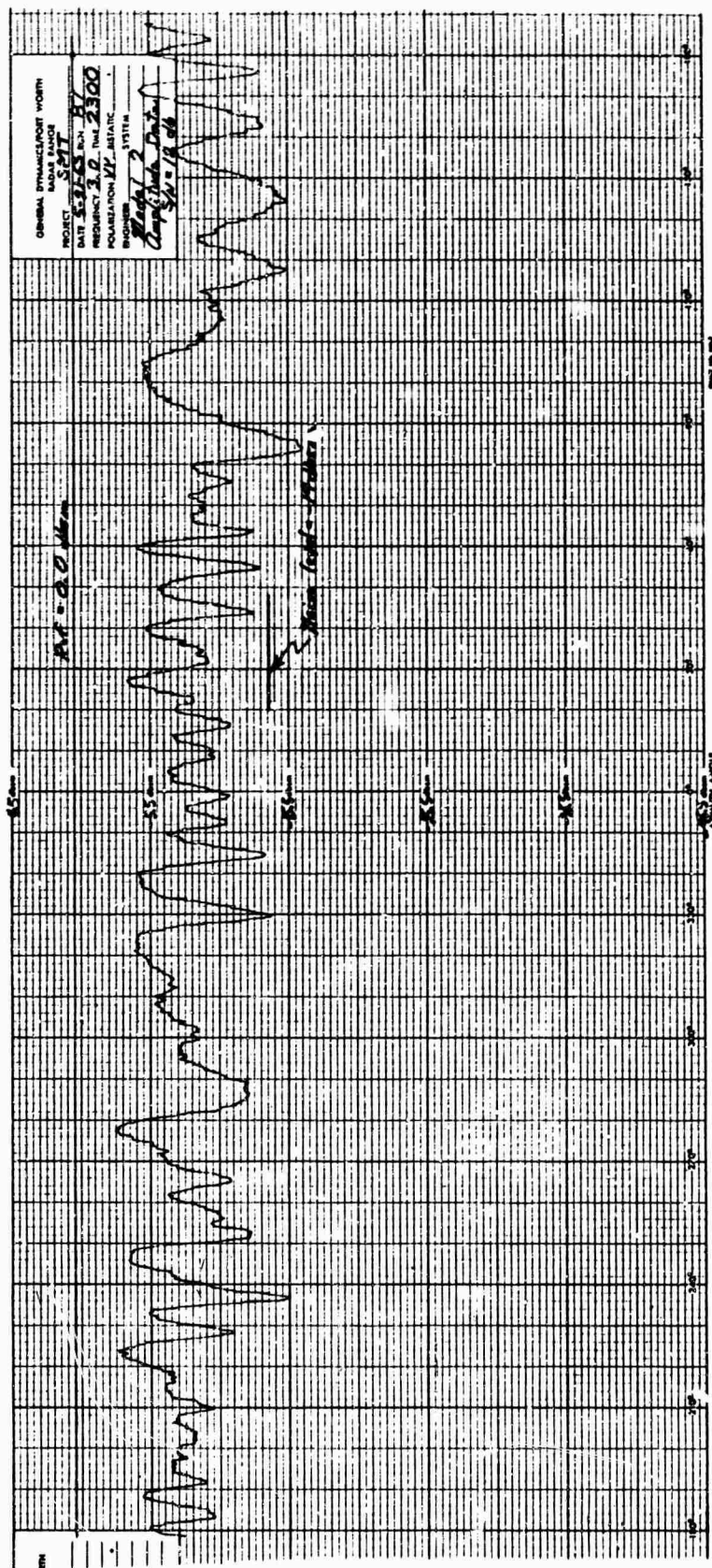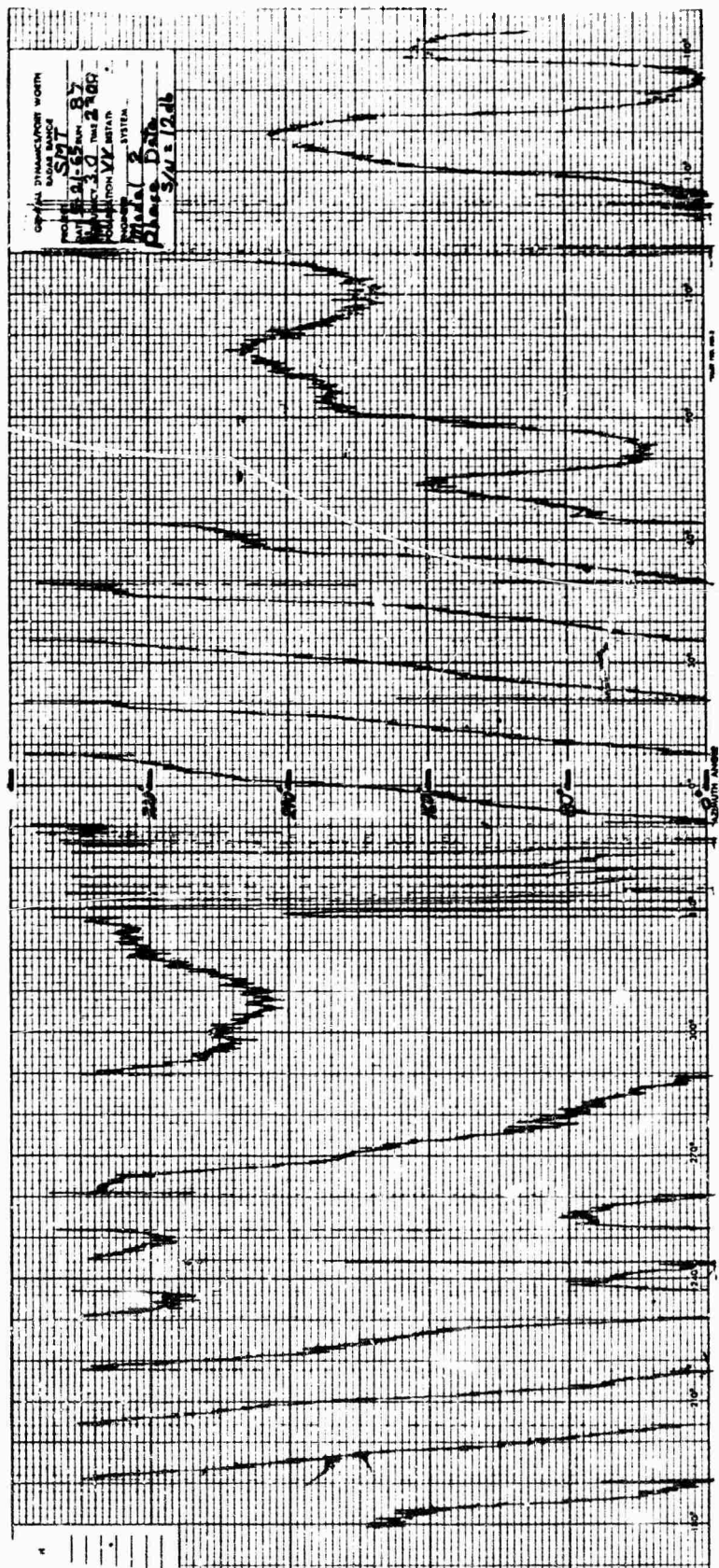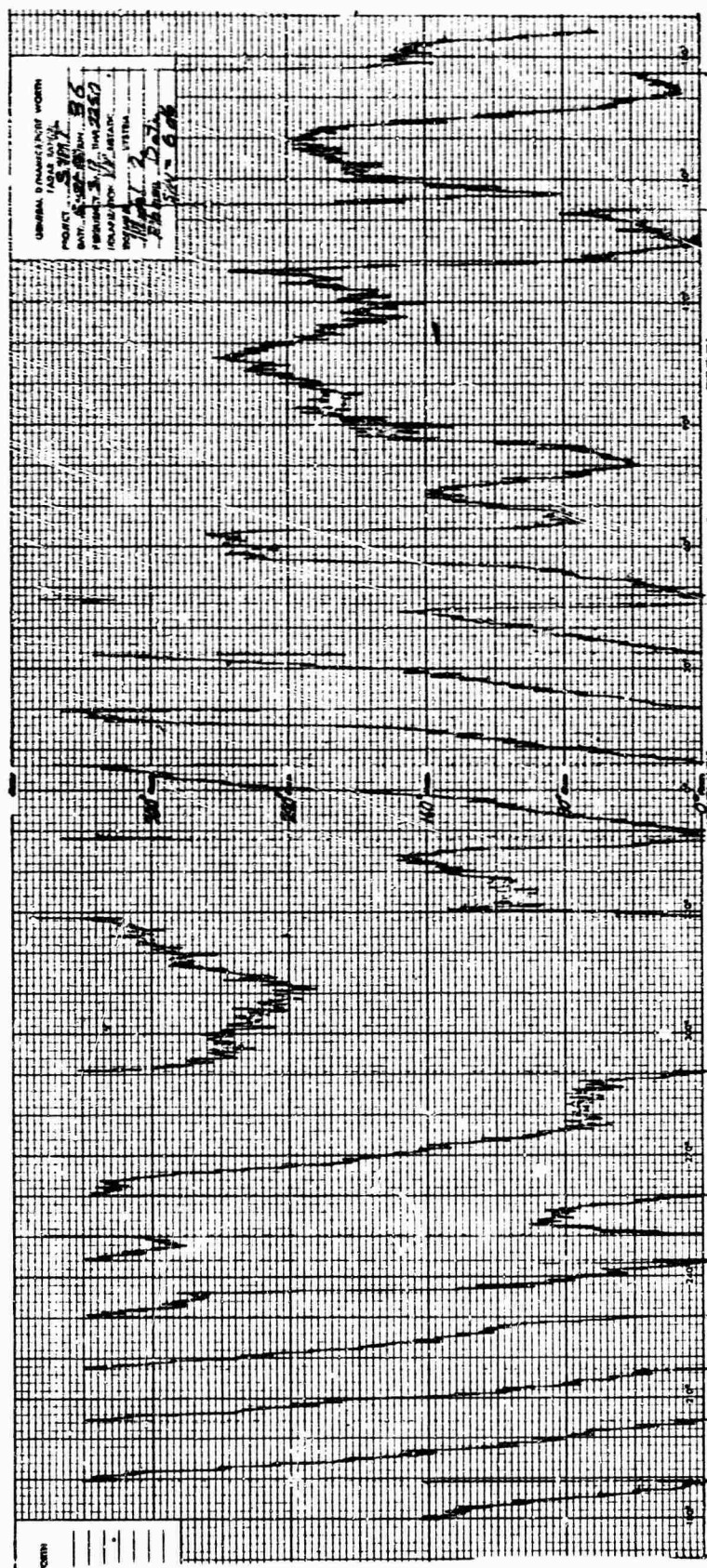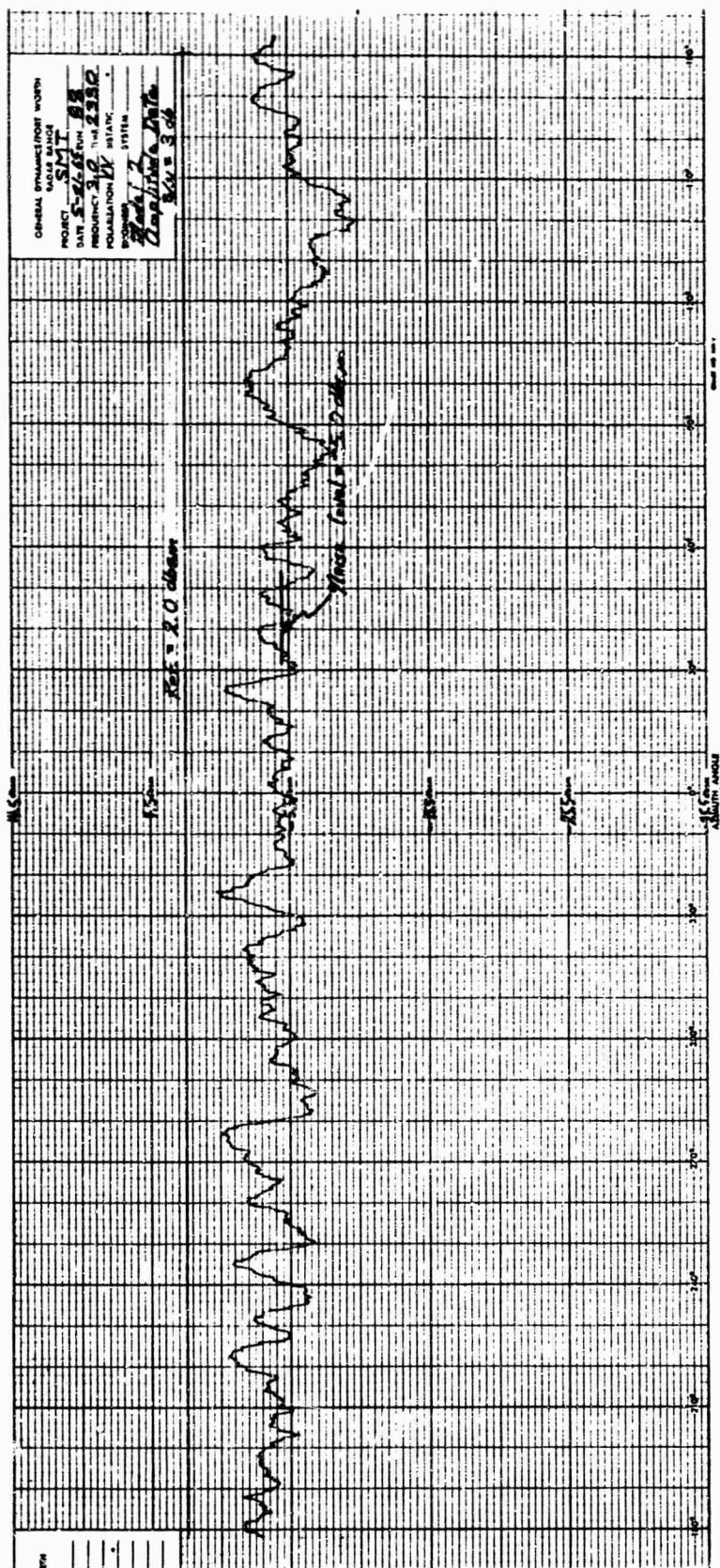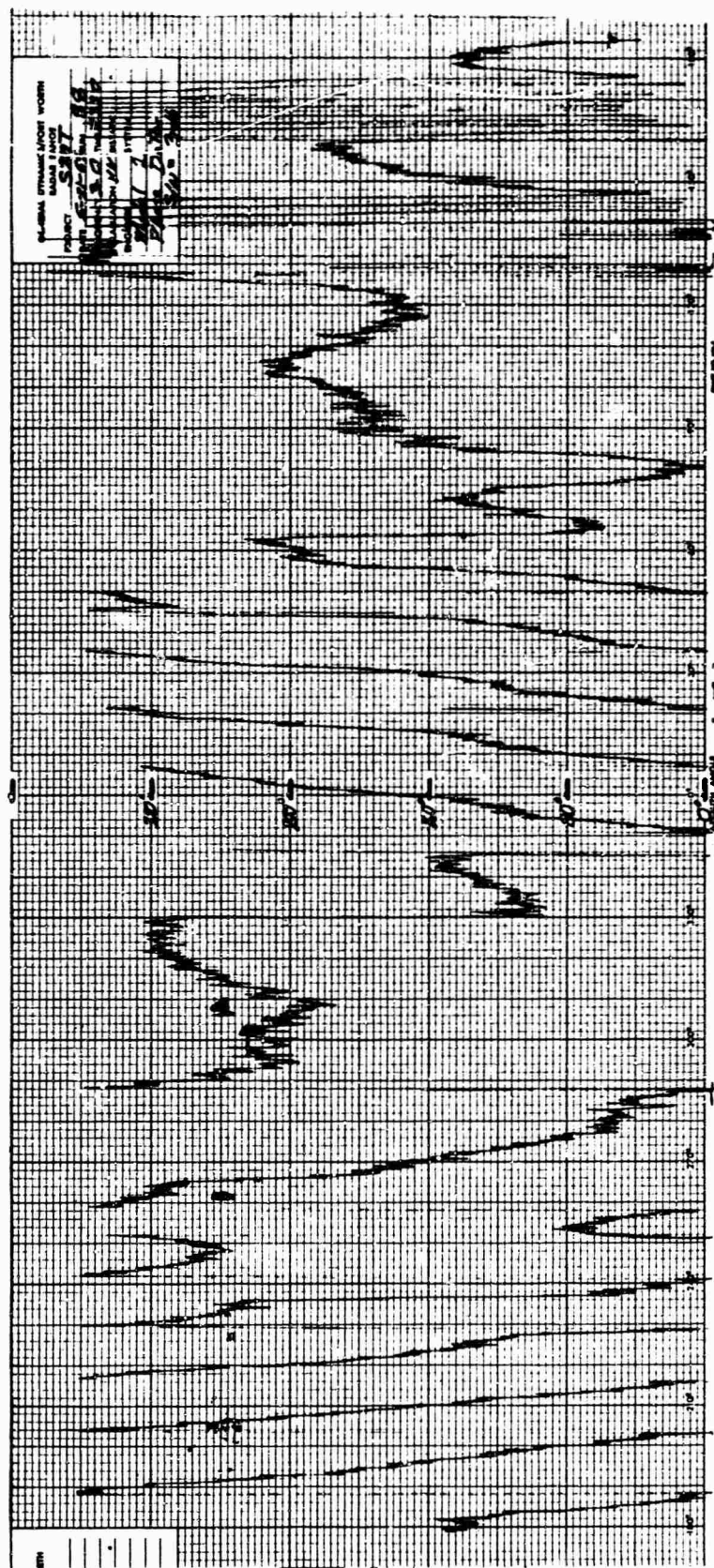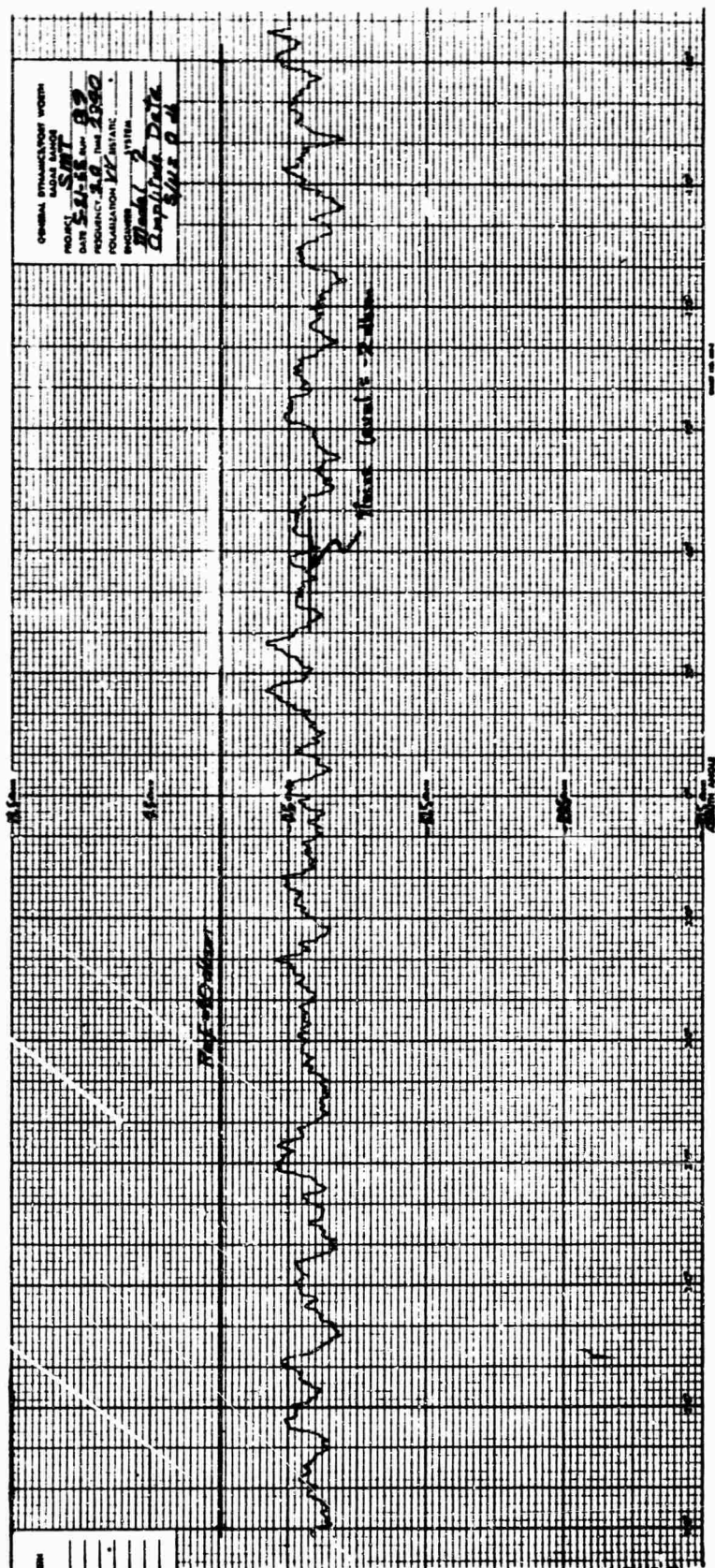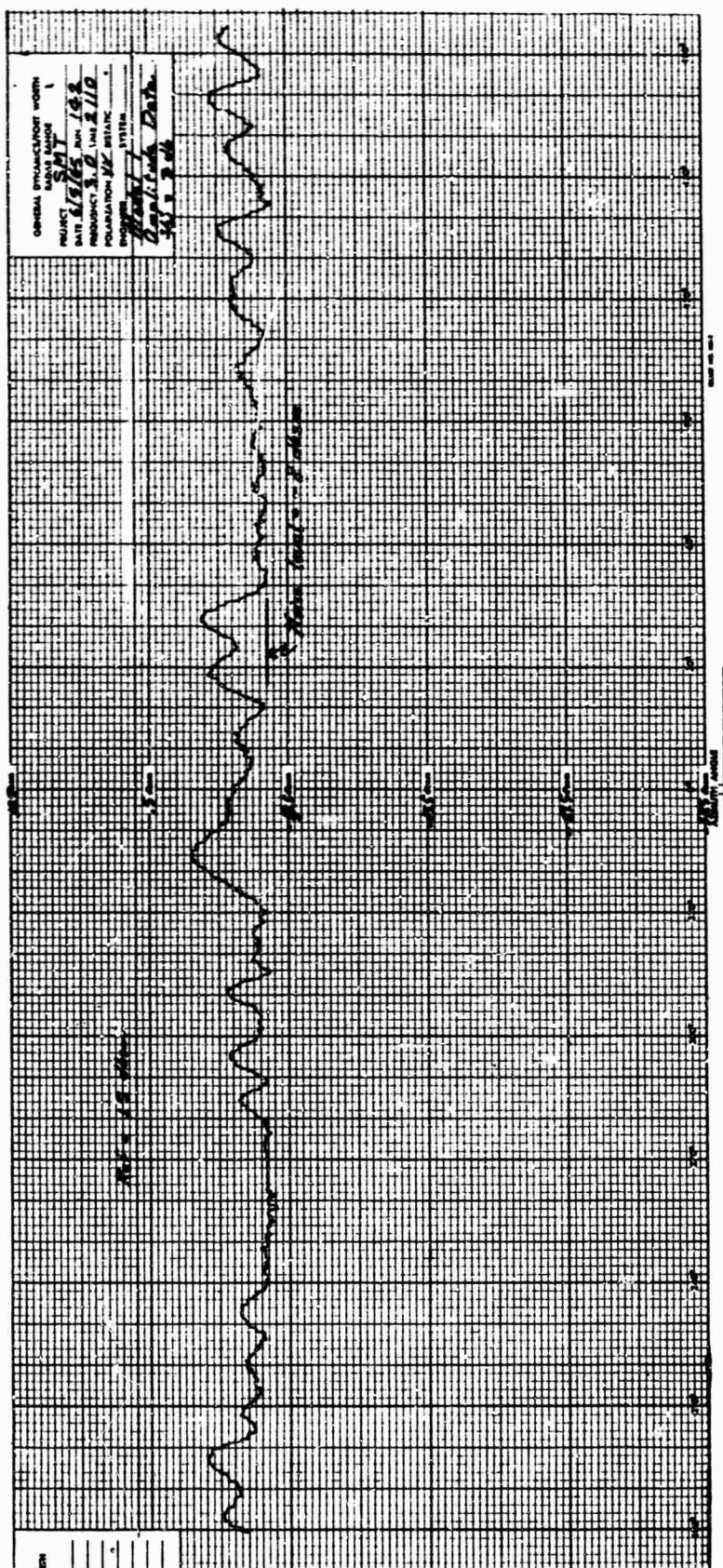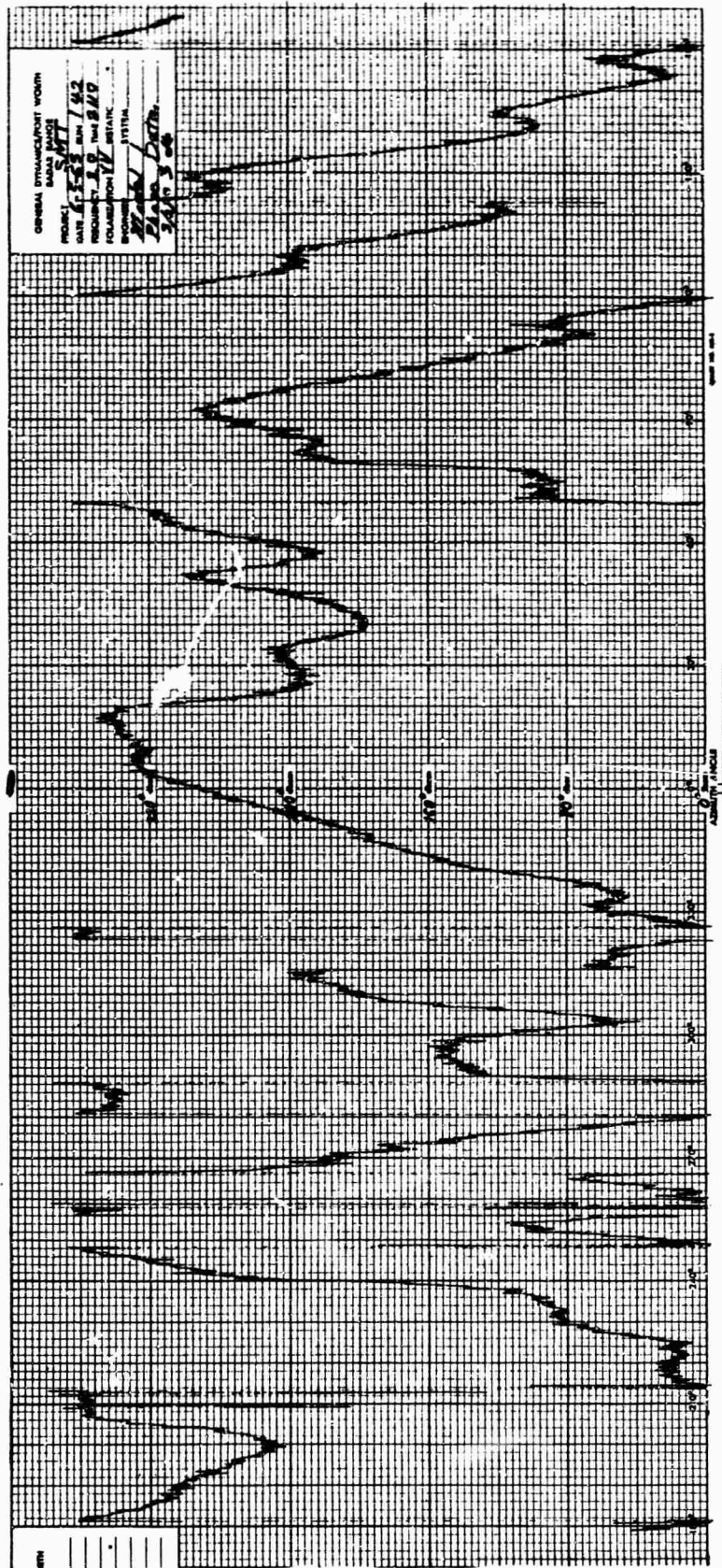
Fig. 65 MODEL 1 PHASE FOR S/N = 3 db

Fig. 66 MODEL 1 CROSS SECTION FOR S/N = 0 db

Fig. 67 MODEL 1 PHASE FOR S/N = 0 db

87

Table 3 COMPUTED RESULTS FOR MODEL 1 REFERENCE DATA (TR,RL)

GENERAL DYNAMICS/FORT WORTH F72 PROB 035473-002 DATE 06/16/65 PAGE 055

GAMMA R	GAMMA T	DELTA R	DELTA T
0.7853981	0.7853981	1.5707963	-1.5707963

AZIMUTH IN DEGREES	SIGMA IN SQUARE METERS	PHASE IN DEGREES	SIGMA IN DBSM	AMPLITUDE ERROR IN DBSM	PHASE ERROR IN DEGREES
180.1	0.16962-01	-36.31	-17.7052		
180.0	0.16612-01	-36.50	-17.7958		
179.9	0.14063-01	-38.48	-18.5192		
179.8	0.11716-01	-40.37	-19.3120		
179.7	0.11516-01	-40.69	-19.3870		
179.6	0.10247-01	-42.15	-19.8939		
179.5	0.88889-02	-44.17	-20.5115		
179.3	0.77196-02	-46.16	-21.1241		
179.2	0.67906-02	-47.06	-21.6809		
179.0	0.44400-02	-50.77	-23.5262		
178.9	0.40039-02	-53.16	-23.9752		
178.7	0.27964-02	-55.29	-25.5340		
178.6	0.26763-02	-55.25	-25.7247		
178.4	0.21110-02	-59.27	-26.7552		
178.3	0.17484-02	-64.88	-27.5736		
178.1	0.17224-02	-67.95	-27.6388		
178.0	0.14475-02	-70.94	-28.3939		
177.9	0.15555-02	-72.39	-28.0814		
177.8	0.11815-02	-76.78	-29.2757		
177.7	0.12794-02	-79.25	-28.9299		
177.6	0.93449-03	-81.98	-30.2942		
177.4	0.82928-03	-82.69	-30.8130		
177.3	0.85927-03	-86.02	-30.6587		
177.1	0.93416-03	-86.82	-30.2958		
177.0	0.93226-03	-84.75	-30.3046		
176.8	0.96276-03	-86.21	-30.1648		
176.7	0.15849-02	-83.31	-28.0000		
176.5	0.15192-02	-82.46	-28.1838		
176.4	0.17019-02	-79.24	-27.6908		
176.3	0.17019-02	-79.24	-27.6908		
176.2	0.19371-02	-76.23	-27.1286		
176.1	0.24415-02	-71.39	-26.1234		
175.9	0.27740-02	-67.55	-25.5689		
175.8	0.31454-02	-63.97	-25.0233		
175.6	0.35765-02	-61.71	-24.4654		
175.5	0.40063-02	-57.96	-23.8878		
175.3	0.54197-02	-52.19	-22.6603		
175.2	0.56073-02	-52.18	-22.5124		
175.1	0.67148-02	-48.64	-21.7297		
174.9	0.74610-02	-46.48	-21.2720		
174.7	0.93306-02	-42.22	-20.3009		
174.6	0.96895-02	-41.84	-20.1370		
174.5	0.10778-01	-40.33	-19.6748		
174.3	0.12250-01	-38.54	-19.1187		

88

Table 4 COMPUTED RESULTS FOR MODEL 1 S/N = 35 db (TR, RL)

GENERAL DYNAMICS/FORT WORTH F72 PROB 035473-002 DATE 06/16/65 PAGE 322

GAMMA R	GAMMA T	DELTA R	DELTA T
0.7853981	0.7853981	1.5707963	-1.5707963

AZIMUTH IN DEGREES	SIGMA IN SQUARE METERS	PHASE IN DEGREES	SIGMA IN DBSM	AMPLITUDE ERROR IN DBSM	PHASE ERROR IN DEGREES
180.0	0.14212-01	-41.33	-18.4733	0.67754+00	4.83
179.9	0.14876-01	-40.60	-18.2750	0.24412-00	2.12
179.8	0.13819-01	-42.14	-18.5953	0.71671+00	1.77
179.7	0.12578-01	-42.93	-19.0038	0.38316-00	2.23
179.6	0.12157-01	-43.85	-19.1518	0.74208+00	1.70
179.5	0.10368-01	-45.87	-19.8430	0.66850+00	1.70
179.3	0.86674-02	-49.05	-20.6211	0.50297+00	2.88
179.2	0.75906-02	-51.31	-21.1972	0.48367-00	4.26
179.1	0.62015-02	-53.34	-22.0759	***	***
179.0	0.66958-02	-52.49	-21.7420	0.17842+01	1.73
178.9	0.53985-02	-56.95	-22.6772	0.12779+01	3.79
178.7	0.41054-02	-61.58	-23.6665	0.16676+01	6.29
178.6	0.39379-02	-63.90	-24.0474	0.16773+01	8.65
178.4	0.29421-02	-69.50	-25.3135	0.14417+01	10.23
178.3	0.25302-02	-73.29	-25.9685	0.16051+01	8.41
178.1	0.20671-02	-78.07	-26.8464	0.79236+00	10.11
177.9	0.21437-02	-79.55	-26.6885	0.13929+01	7.16
177.8	0.11322-02	-93.78	-29.4607	0.18501-00	17.01
177.7	0.18494-02	-87.78	-27.3297	0.16002+01	8.54
177.6	0.18467-02	-89.63	-27.3360	0.29582+01	7.65
177.3	0.15658-02	-93.55	-28.0527	0.26061+01	7.53
177.1	0.14987-02	-94.48	-28.2428	0.20530+01	7.66
177.0	0.14582-02	-100.14	-28.3618	0.19428+01	15.39
176.9	0.13068-02	-103.57	-28.8378	***	***
176.8	0.13882-02	-103.98	-28.5753	0.15895+01	17.76
176.7	0.17478-02	-96.66	-27.5750	0.42500-00	13.34
176.5	0.18794-02	-94.08	-27.2597	0.92407+00	11.62
176.4	0.22737-02	-87.97	-26.4326	0.12582+01	8.73
176.3	0.20021-02	-90.26	-26.9851	0.70569+00	11.03
176.2	0.25433-02	-83.02	-25.9460	0.11826+01	6.79
176.1	0.29007-02	-78.43	-25.3749	0.74843+00	7.04
175.9	0.28493-02	-77.49	-25.4526	0.11630-00	9.93
175.8	0.35483-02	-71.04	-24.4998	0.52345+00	7.07
175.7	0.39812-02	-67.70	-23.9999	***	***
175.6	0.39630-02	-66.87	-24.0197	0.44571-00	5.16
175.5	0.42762-02	-65.54	-23.6894	0.19837-00	7.58
175.3	0.54792-02	-57.80	-22.6129	0.47399-01	5.61
175.1	0.64401-02	-53.16	-21.9111	0.18138-00	4.52
174.9	0.69971-02	-50.81	-21.5508	0.27879-00	4.33
174.8	0.78545-02	-48.60	-21.0488	***	***
174.7	0.87892-02	-46.47	-20.5605	0.25959-00	4.25
174.6	0.91648-02	-45.72	-20.3788	0.24181-00	3.88
174.5	0.10208-01	-44.14	-19.9108	0.23598-00	3.81
174.3	0.11555-01	-41.46	-19.3724	0.25365-00	2.92

Table 5 COMPUTED RESULTS FOR MODEL 3 REFERENCE DATA
(T $\pi/4$, R $\pi/4$)

GAMMA R	GAMMA T	OELTA R	OELTA T
0.7853981	0.7853981	0.	0.

AZIMUTH IN DEGREES	SIGMA IN SQUARE METERS	PHASE IN OEGREES	SIGMA IN DBSM	AMPLITUOE ERROR IN DBSM	PHASE ERROR IN OFGREES
180.0	0.13076-00	9.21	-8.8352		
179.9	0.12694-00	9.91	-8.9640		
179.7	0.12799-00	9.42	-8.9281		
179.6	0.12369-00	10.06	-9.0767		
179.5	0.12002-00	10.42	-9.2074		
179.4	0.12064-00	8.77	-9.1950		
179.3	0.11912-00	9.32	-9.2402		
179.2	0.12029-00	10.53	-9.1976		
179.1	0.11394-00	9.70	-9.4332		
179.0	0.11382-00	9.47	-9.4379		
179.9	0.11072-00	8.33	-9.5576		
178.8	0.11072-00	8.33	-9.5576		
178.7	0.11126-00	9.13	-9.5366		
178.6	0.11320-00	9.15	-9.4614		
178.5	0.10756-00	10.01	-9.6836		
178.4	0.10635-00	8.69	-9.7326		
178.3	0.10387-00	9.92	-9.8351		
178.1	0.10635-00	10.10	-9.7327		
178.0	0.10562-00	9.66	-9.7624		
177.9	0.10261-00	9.52	-9.8881		
177.8	0.99327-01	10.03	-10.0293		
177.7	0.98432-01	10.91	-10.0686		
177.6	0.92877-01	9.74	-10.3209		
177.5	0.97084-01	9.37	-10.1285		
177.3	0.85672-01	10.80	-10.6716		
177.2	0.85257-01	10.12	-10.6927		
177.1	0.84386-01	9.88	-10.7373		
176.9	0.86692-01	9.56	-10.6202		
176.7	0.83171-01	10.88	-10.8003		
176.6	0.86068-01	11.70	-10.6516		
176.5	0.75338-01	11.36	-11.2299		
176.4	0.78699-01	12.54	-11.0403		
176.3	0.76869-01	11.39	-11.1425		
176.2	0.71955-01	11.84	-11.4294		
176.1	0.73652-01	10.26	-11.3282		
175.9	0.71763-01	11.85	-11.4410		
175.8	0.70367-01	13.31	-11.5263		
175.6	0.71895-01	13.93	-11.4330		
175.5	0.67897-01	12.26	-11.6015		
175.3	0.65378-01	12.76	-11.8457		
175.2	0.65068-01	16.07	-11.8663		
175.1	0.63637-01	14.40	-11.9629		
175.0	0.60195-01	13.12	-12.2044		
174.9	0.59662-01	16.43	-12.2430		

Table 6 COMPUTED RESULTS FOR MODEL 3 S/N = 24 db
(T $\pi/4$, R $\pi/4$)

GENERAL DYNAMICS/FORT WORTH F72 PROB 035436-002 DATE 06/15/65 PAGE   788

GAMMA R	GAMMA T	DELTA R	DELTA T
0.7853981	0.7853981	0.	0.

AZIMUTH IN DEGREES	SIGMA IN SQUARE METERS	PHASE IN DEGREES	SIGMA IN DBSM	AMPLITUDE ERROR IN DBSM	PHASE ERROR IN DEGREES
180.4	0.18174-00	7.99	-7.4055	***	***
180.2	0.17799-00	8.17	-7.4959	***	***
180.1	0.18424-00	9.32	-7.3462	***	***
180.0	0.16777-00	7.00	-7.7528	0.10825+01	2.21
179.9	0.17758-00	10.39	-7.5060	0.14579+01	0.48
179.8	0.16299-00	9.60	-7.8785	***	***
179.7	0.15383-00	9.77	-8.1295	0.79858+00	0.35
179.6	0.14577-00	8.09	-8.3633	0.71346+00	1.97
179.5	0.14577-00	8.09	-8.3633	0.84409+00	2.33
179.4	0.14389-00	7.37	-8.4198	0.75514+00	1.40
179.2	0.14721-00	7.53	-8.3206	0.87695+00	2.99
179.1	0.15239-00	8.15	-8.1703	0.12629+01	1.55
179.0	0.15878-00	12.08	-7.9920	0.14459+01	2.65
178.9	0.14867-00	11.49	-8.2779	0.12797+01	3.15
178.8	0.14369-00	11.43	-8.4256	0.11320+01	3.10
178.6	0.14842-00	10.57	-8.2850	0.11764+01	1.42
178.5	0.15049-00	10.74	-8.2250	0.14585+01	0.72
178.4	0.15322-00	11.00	-8.1467	0.15859+01	2.30
178.3	0.14870-00	9.06	-8.2768	0.15583+01	0.86
178.2	0.13361-00	11.07	-8.7418	***	***
178.0	0.13618-00	10.58	-8.6587	0.11037+01	0.92
177.9	0.13480-00	10.27	-8.7031	0.11850+01	0.75
177.8	0.13494-00	11.09	-8.6987	0.13306+01	1.06
177.7	0.14209-00	11.33	-8.4745	0.15942+01	0.42
177.6	0.14376-00	11.10	-8.4237	0.18972+01	1.37
177.4	0.13312-00	11.85	-8.7575	***	***
177.3	0.12140-00	11.57	-9.1577	0.15139+01	0.77
177.2	0.11965-00	13.75	-9.2209	0.14718+01	3.63
177.1	0.12510-00	13.58	-9.0274	0.17098+01	3.69
177.0	0.12647-00	14.04	-8.9802	***	***
176.9	0.12522-00	13.32	-9.0234	0.15968+01	3.77
176.8	0.10471-00	12.55	-9.8002	***	***
176.6	0.96859-01	14.02	-10.1386	0.51294+00	2.31
176.5	0.10219-00	14.63	-9.9060	0.13239+01	3.27
176.4	0.10030-00	14.95	-9.9868	0.10535+01	2.41
176.3	0.10484-00	15.44	-9.7949	0.13475+01	4.05
176.2	0.10403-00	16.17	-9.8285	0.16009+01	4.33
176.0	0.10351-00	16.73	-9.8502	***	***
175.8	0.10258-00	16.64	-9.8893	0.16370+01	3.33
175.7	0.10391-00	20.80	-9.8333	***	***
175.6	0.91863-01	19.00	-10.3686	0.10644+01	5.07
175.5	0.98945-01	18.51	-10.0461	0.16354+01	6.25
175.4	0.93850-01	18.13	-10.2756	***	***
175.2	0.91128-01	18.28	-10.4035	0.14629+01	2.21

The cumulative error curves for each of the models are presented in Figures 68 through 79. In Figures 68 through 73, the degradation curves are labeled by use of the maximum cross section reference whereas in Figures 74 through 79, the curves are labeled by use of the average dbsm reference of the largest element of the model matrix. Inspection of the scattering patterns of the three models indicates why the curves based on the use of the maximum as reference indicates that Models 1 and 2 are degraded much less than Model 3, but when the average is used as a reference, this situation is slightly reversed. That is, the average levels of Models 1 and 2 are much closer to their maximum references than in the case of Model 3. Hence the degradation references used in the case of Models 1 and 2 are shifted much less than the references used for Model 3. When the average reference level is used, the degradation data tends to become normalized in that the amount of degradation as a function of S/N tends to become independent of the model. This trend is of course a consequence of averaging and supports the selection of an average reference level as the more practical criterion for use in discussing the results of the study.

The polarizations which were used in the study were selected to give transformations considered typical of the type most likely to be used. In all but one case, (TR, RR), the polarizations were basically nonorthogonal type polarizations. That is, the absolute value of the transmitter vector times the receiver vector (dot product) was maintained near the maximum value in four of the five polarizations used. However, one orthogonal polarization was used (TR, RR) since this operation must be performed in cases where the linear scattering matrix is transformed to the circular scattering matrix (see Section II). However, the accuracy of this computation depends on the difference of two cross sections (σ_{VV}, σ_{HH}) which are often approximately equal in magnitude and phase (refer to Equation 6). Hence small errors in the measured data tend to produce large errors in computed cross section for this and other conditions of orthogonal polarization. In the case of Models 1 and 2, this tendency was suppressed by the design of the models. However, in the case of Model 3, there were several regions where the above "error amplification tendency" was quite noticeable.

In the case of each model, the largest S/N degradation curve is indicative of the bound on errors generated as a result of errors in the measured data. In each of these cases, only a small percent of the measured data was degraded by noise. Hence a significant portion of the errors used to obtain these particular curves was due to measurement errors, such as angular misalignment between reference data tapes and lower S/N data tapes; phase errors caused by calibration, drift, and target motion; amplitude errors caused by calibration and system drift; and bad data points caused by the digital encoder. However, this latter type of error was not observed in any of the data checked. These inherent system errors could be completely eliminated if S/N levels were artificially induced into the data obtained at maximum S/N. If this technique were used, all of the error dat would be caused by noise degradation. However, it was anticipated that the measurement errors would induce only a small amount of additional error into the results, and it was desirable to obtain data which would allow an estimate of the effect of errors from an actual system on computations depending upon the scattering matrix.

An estimate of these types of errors was investigated by comparing measured data with data computed by use of the scattering matrix. Although the error sources are more numerous in this latter experiment than the error sources mentioned earlier, the results in most cases show differences commensurate with (see section 4) those indicated by cumulative error curves for the best S/N condition shown in Figures 68 through 79.
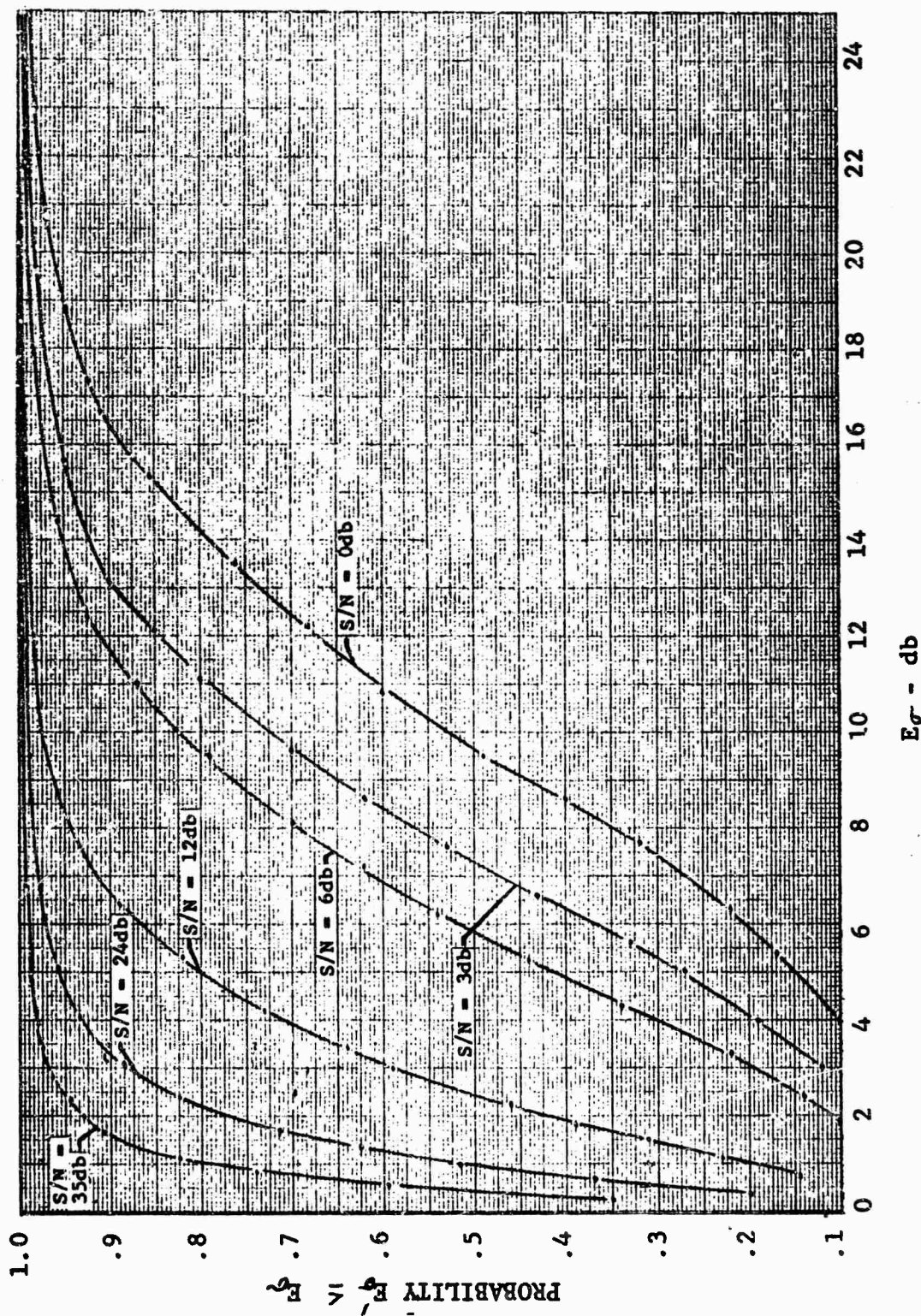
92

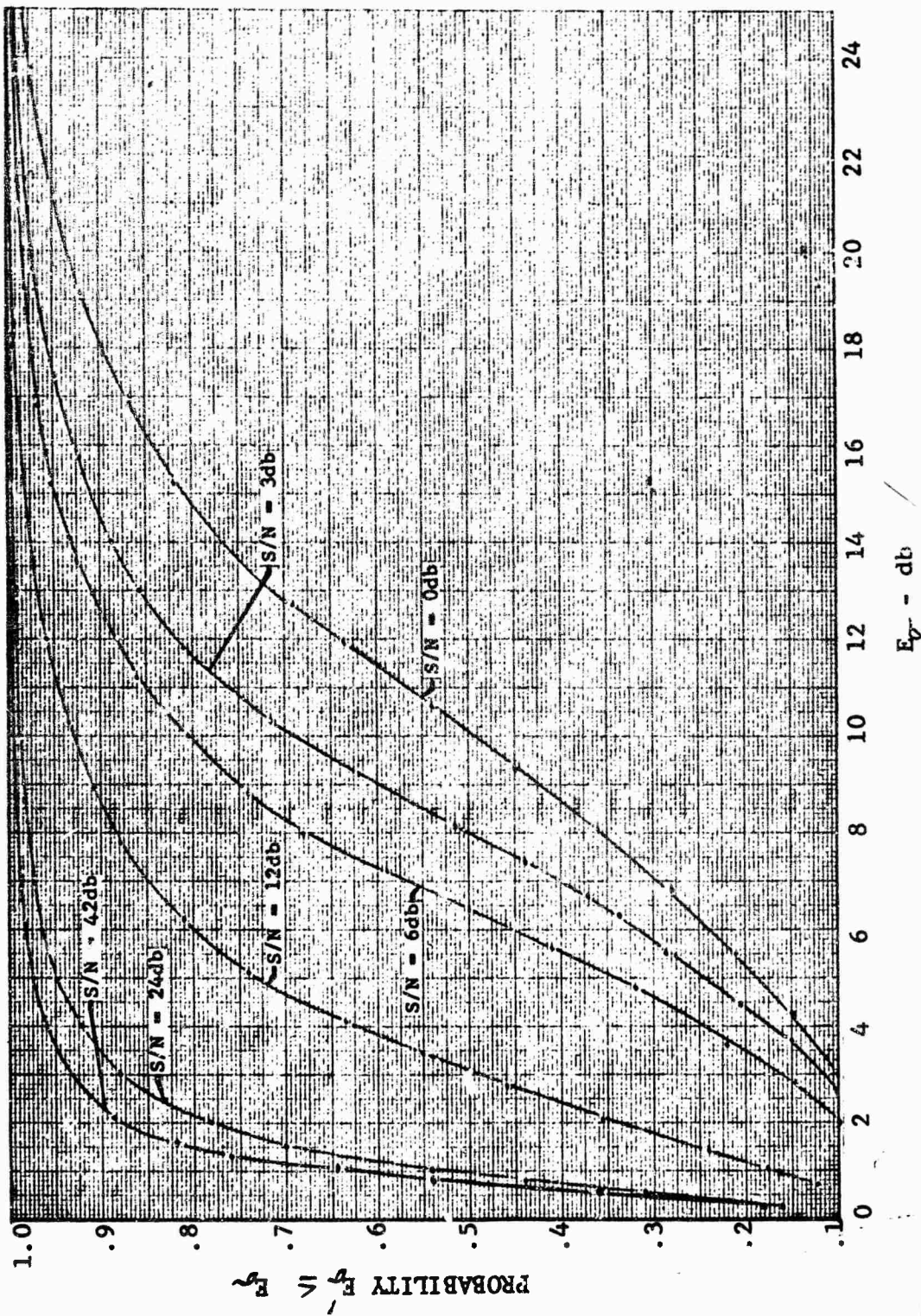Fig. 68   CROSS SECTION DEGRADATION OF MODEL 1 BASED ON
MAXIMUM REFERENCE

Fig. 69 CROSS SECTION DEGRADATION OF MODEL 2 BASED ON
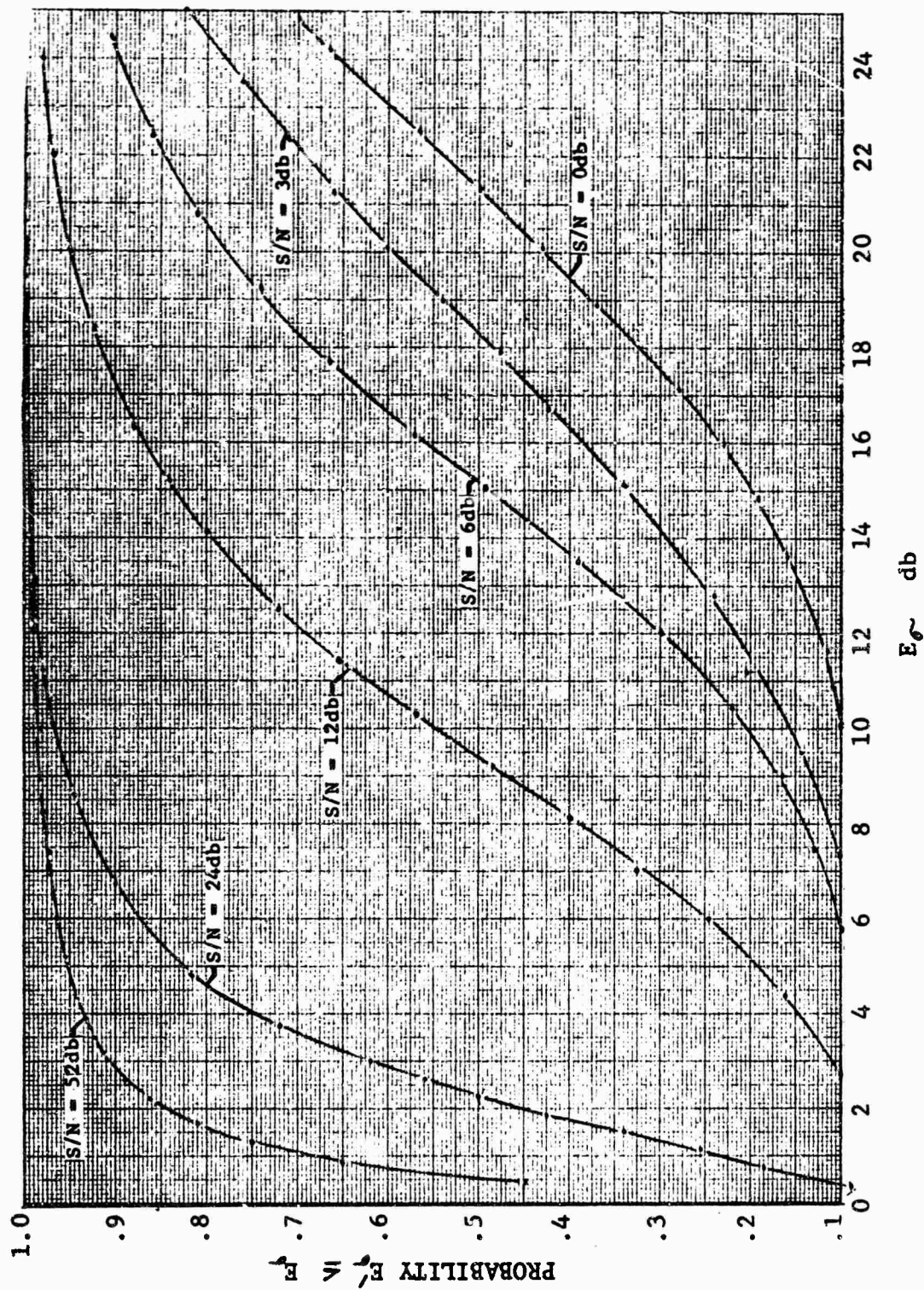MAXIMUM REFERENCE

94

Fig. 70 CROSS SECTION DEGRADATION OF MODEL 3 BASED ON
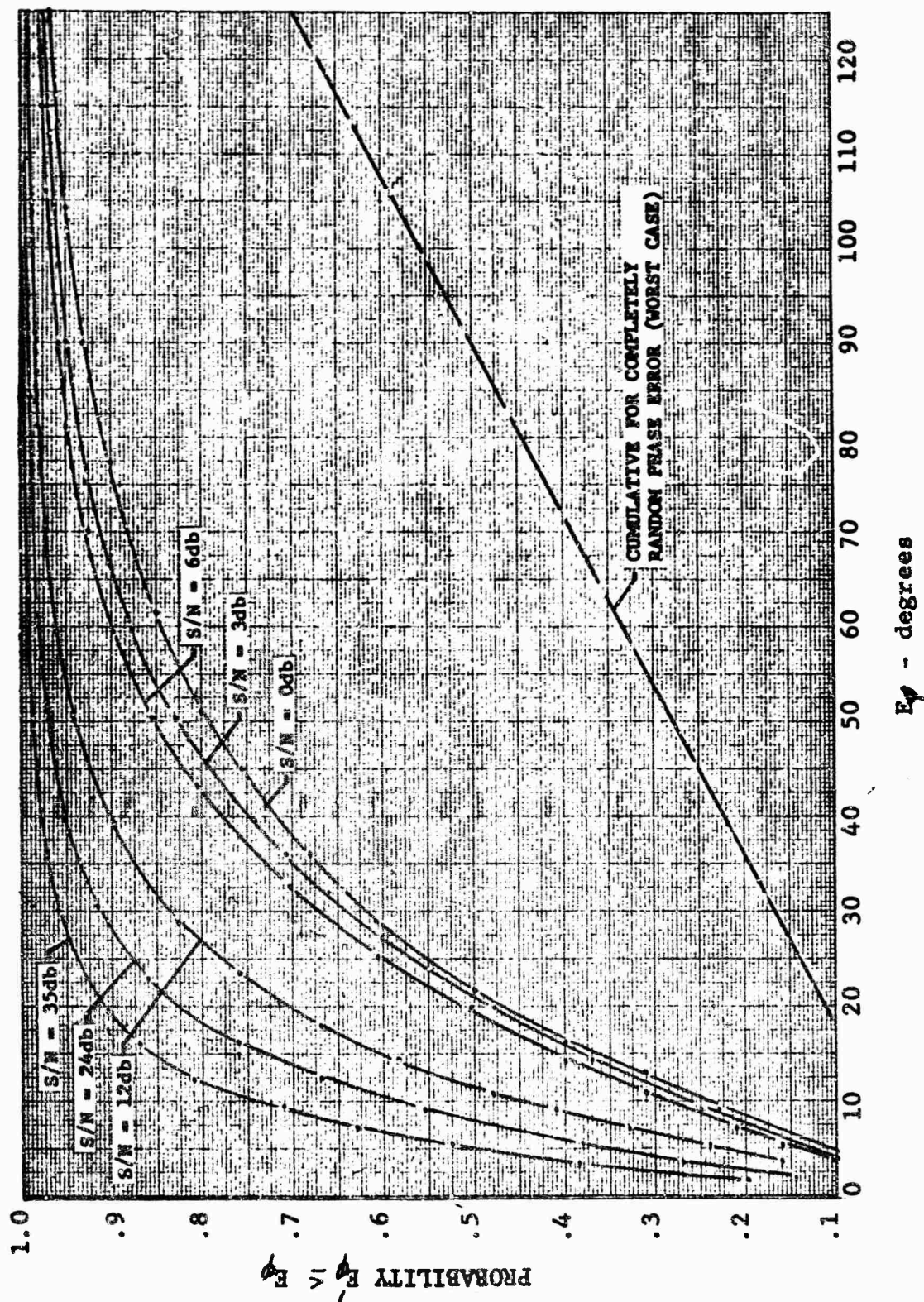MAXIMUM REFERENCE

95

Fig. 71 PHASE DEGRADATION OF MODEL 1 BASED ON MAXIMUM REFERENCE

Fig. 72 PHASE DEGRADATION OF MODEL 2 BASED ON
MAXIMUM REFERENCE

97
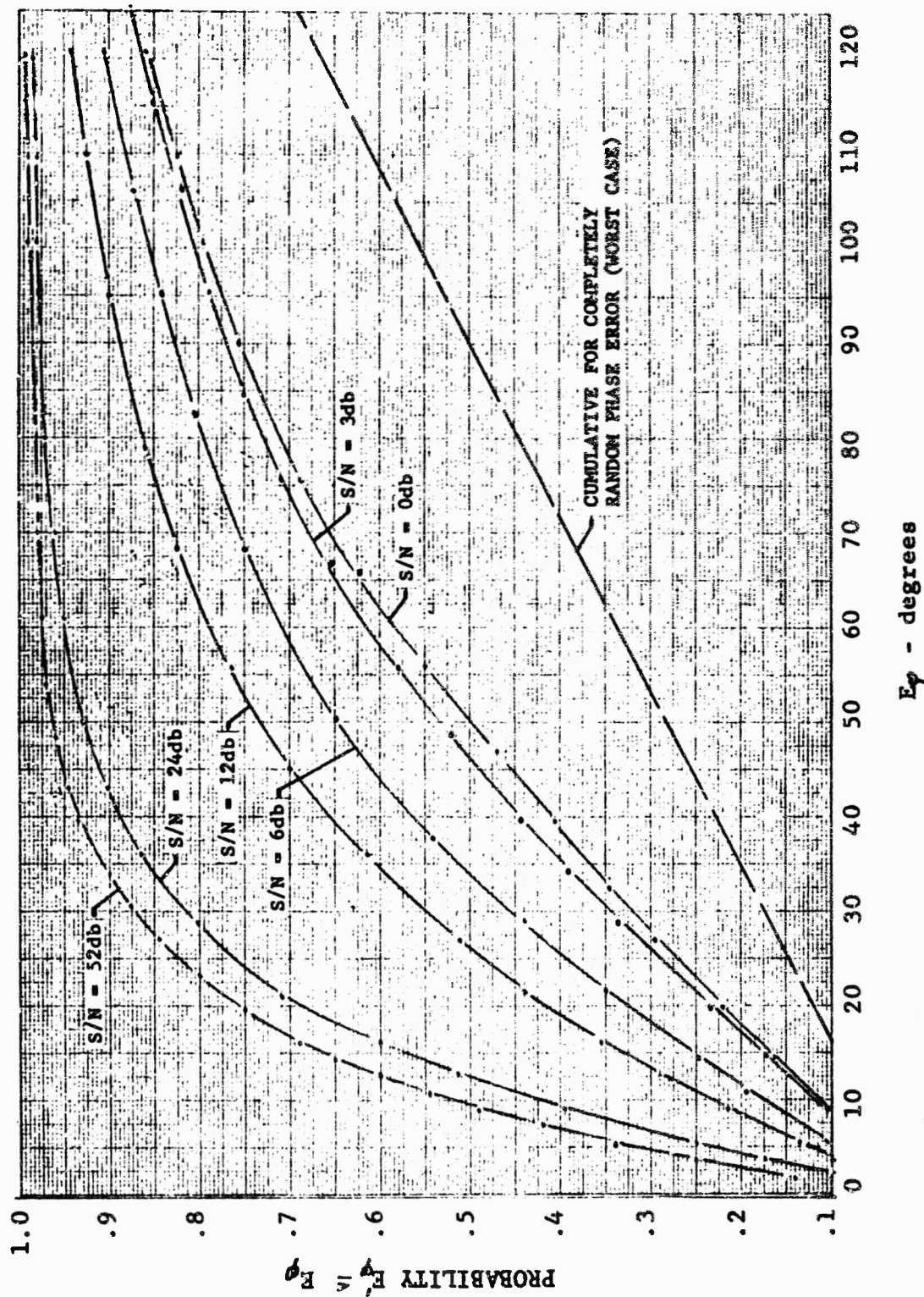
Fig. 73 PHASE DEGRADATION OF MODEL 3 BASED ON
MAXIMUM REFERENCE

98

Fig. 74 CROSS SECTION DEGRADATION OF MODEL 1 BASED ON
AVERAGE REFERENCE

99

Fig. 75 CROSS SECTION DEGRADATION OF MODEL 2 BASED ON AVERAGE REFERENCE

100

Fig. 76 CROSS SECTION DEGRADATION OF MODEL 3 BASED
ON AVERAGE REFERENCE

101

Fig. 77 PHASE DEGRADATION OF MODEL 1 BASED ON
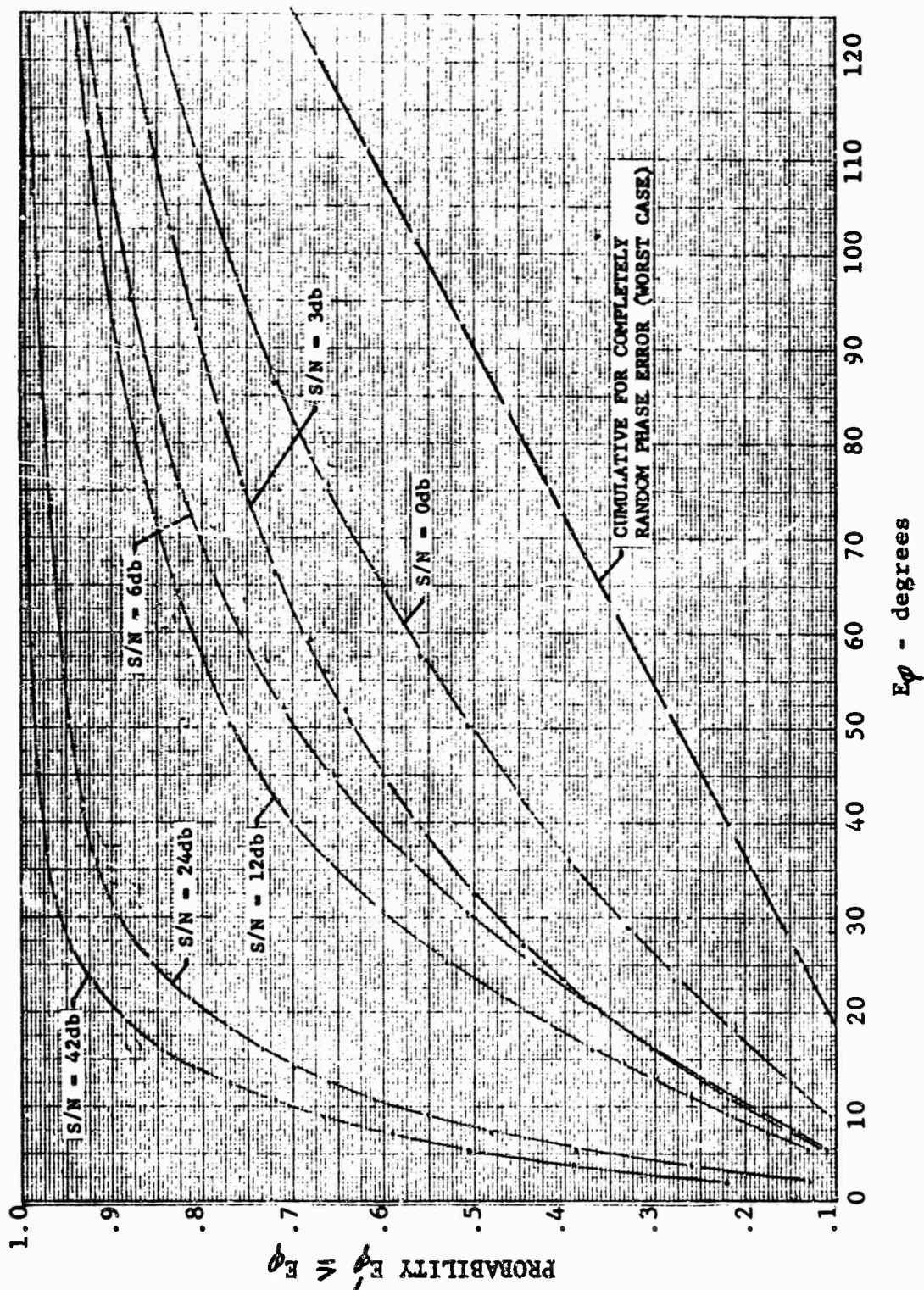AVERAGE REFERENCE

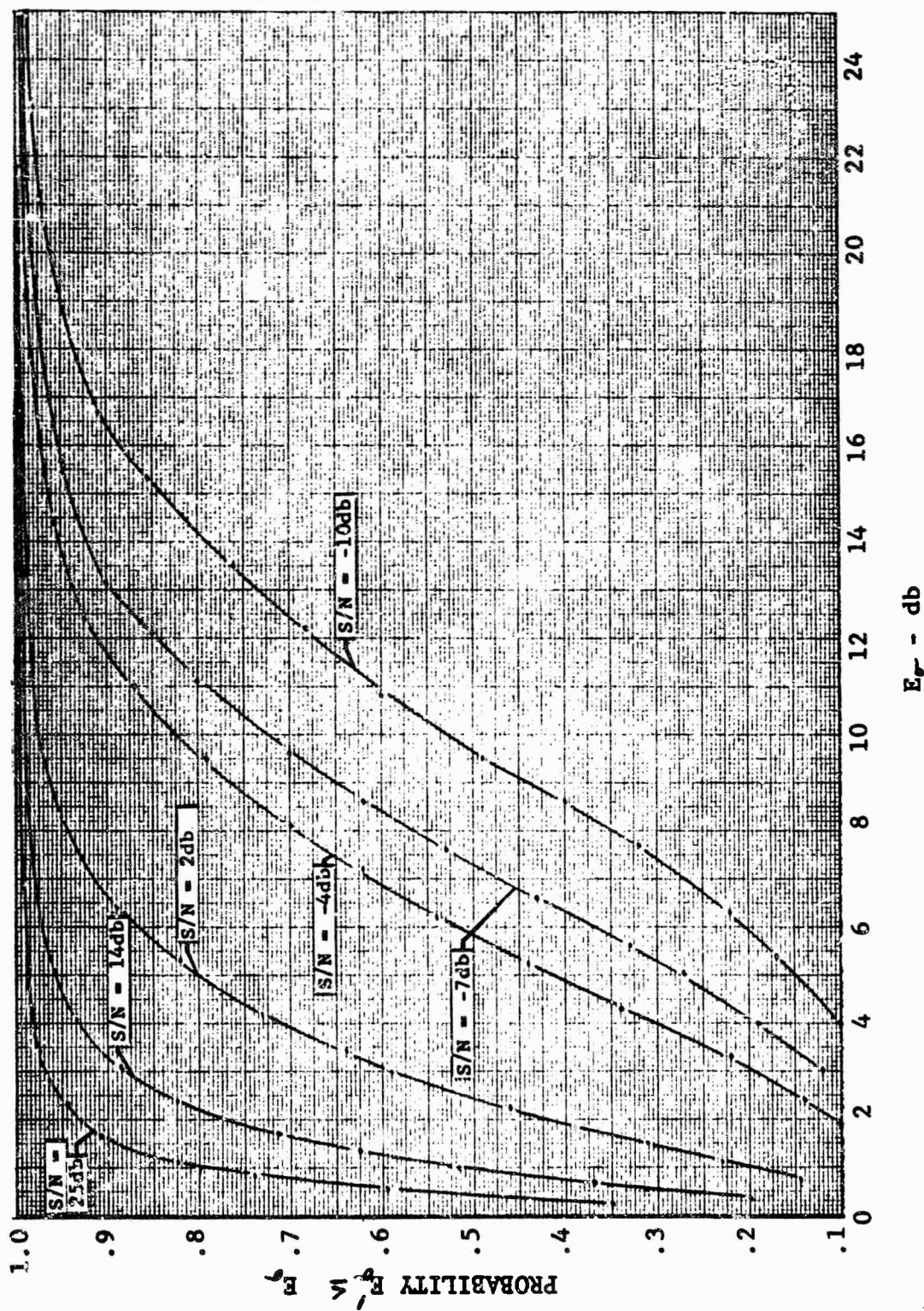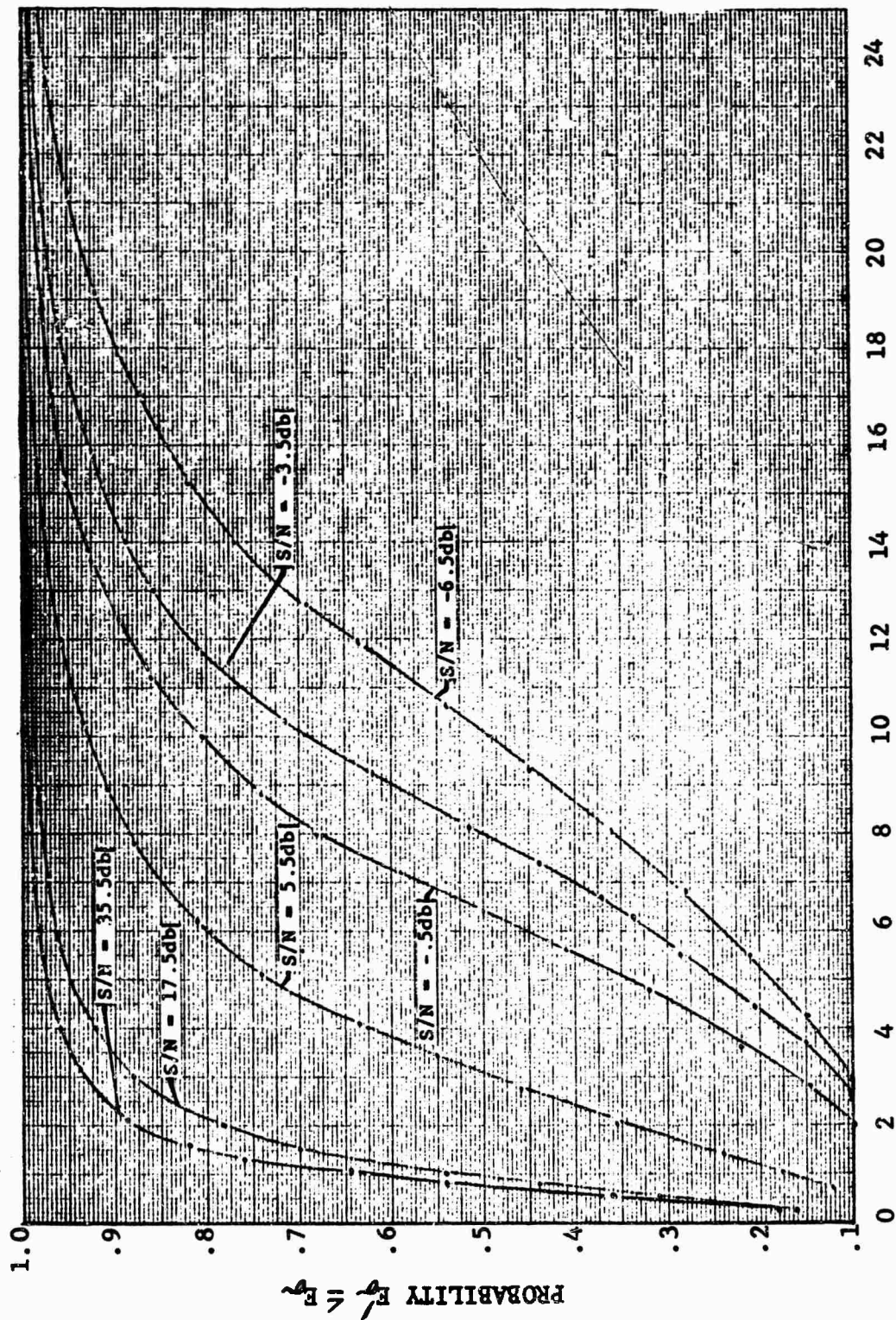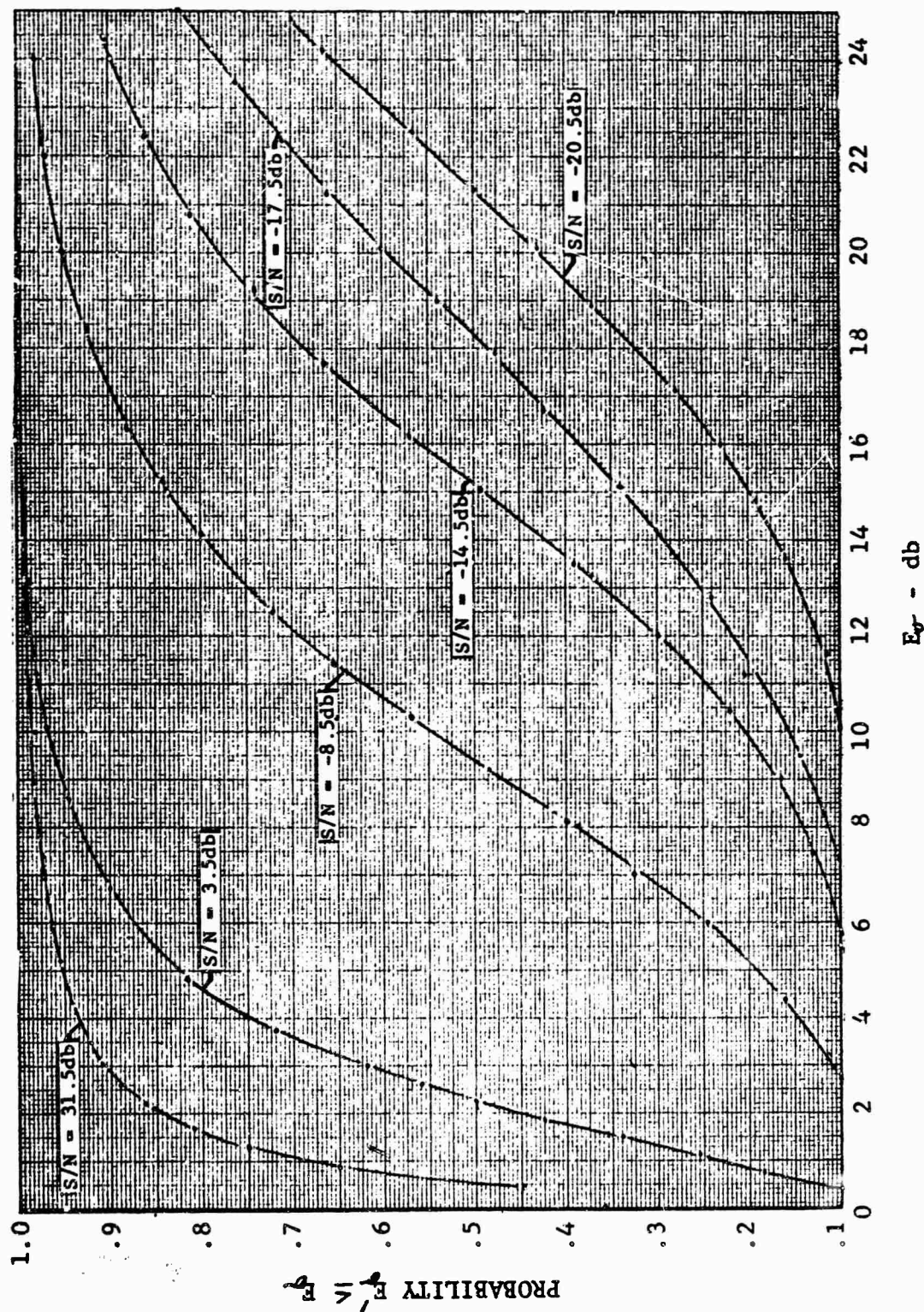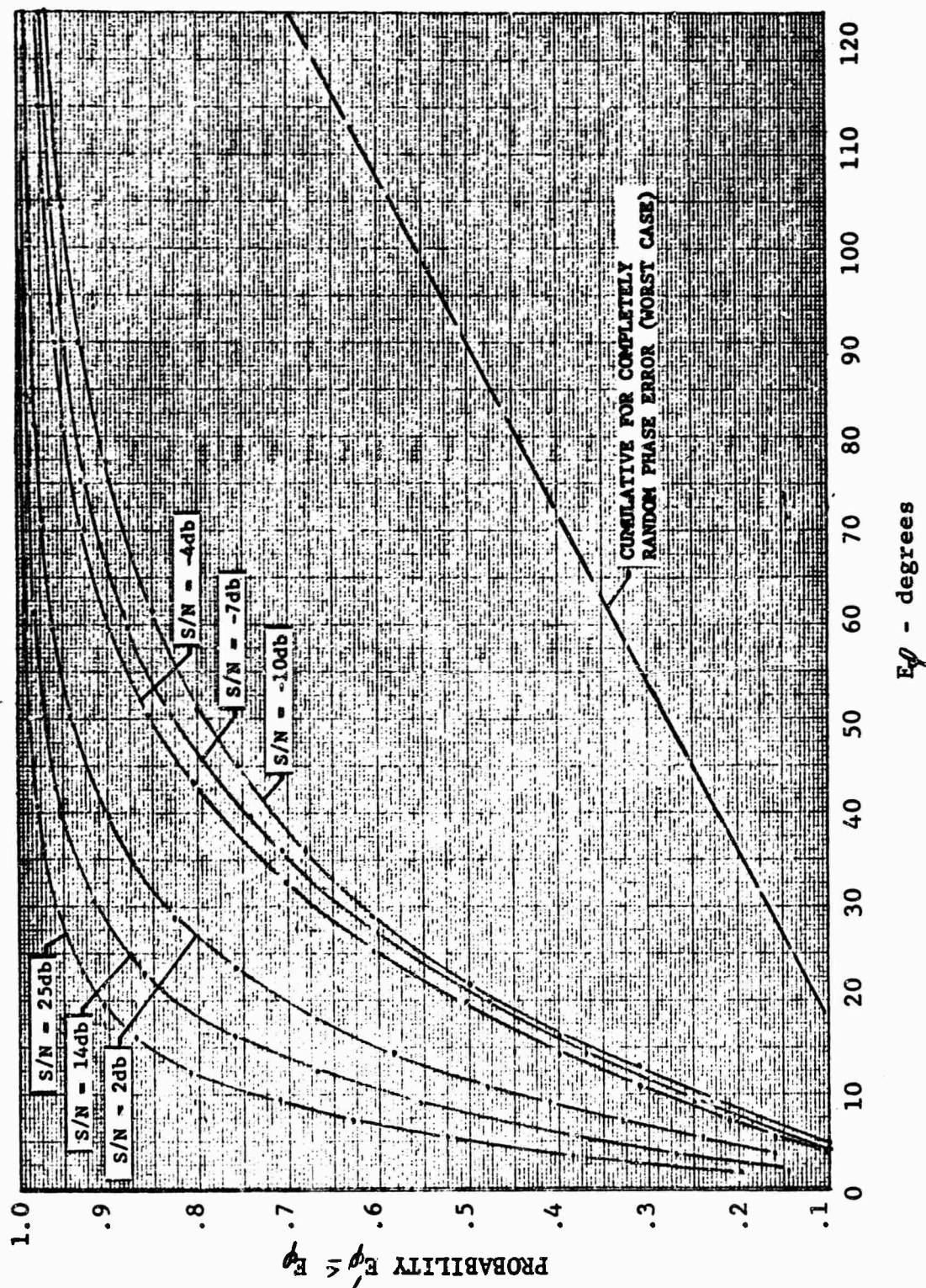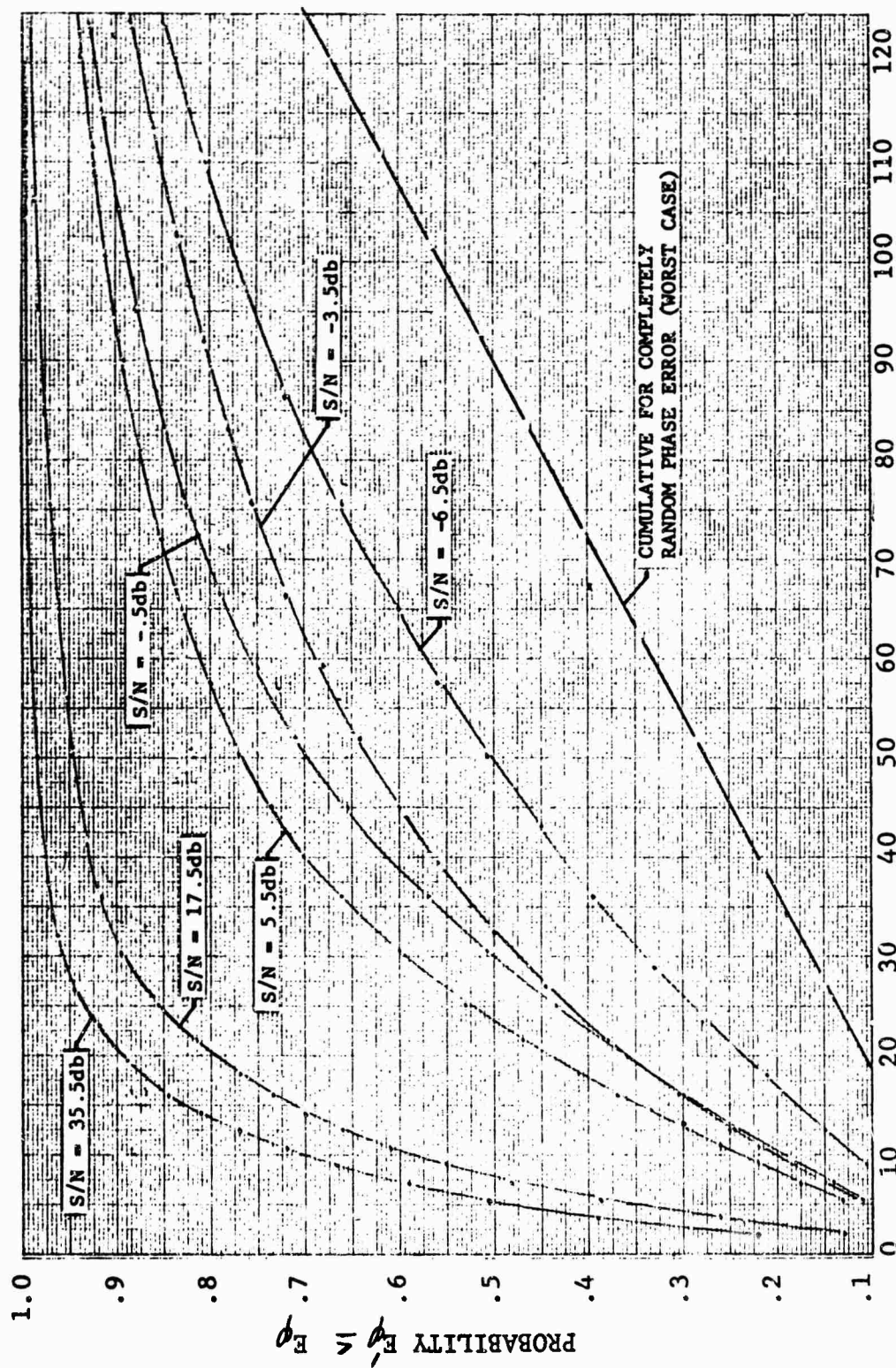Fig. 78 PHASE DEGRADATION OF MODEL 2 BASED ON
AVERAGE REFERENCE

103
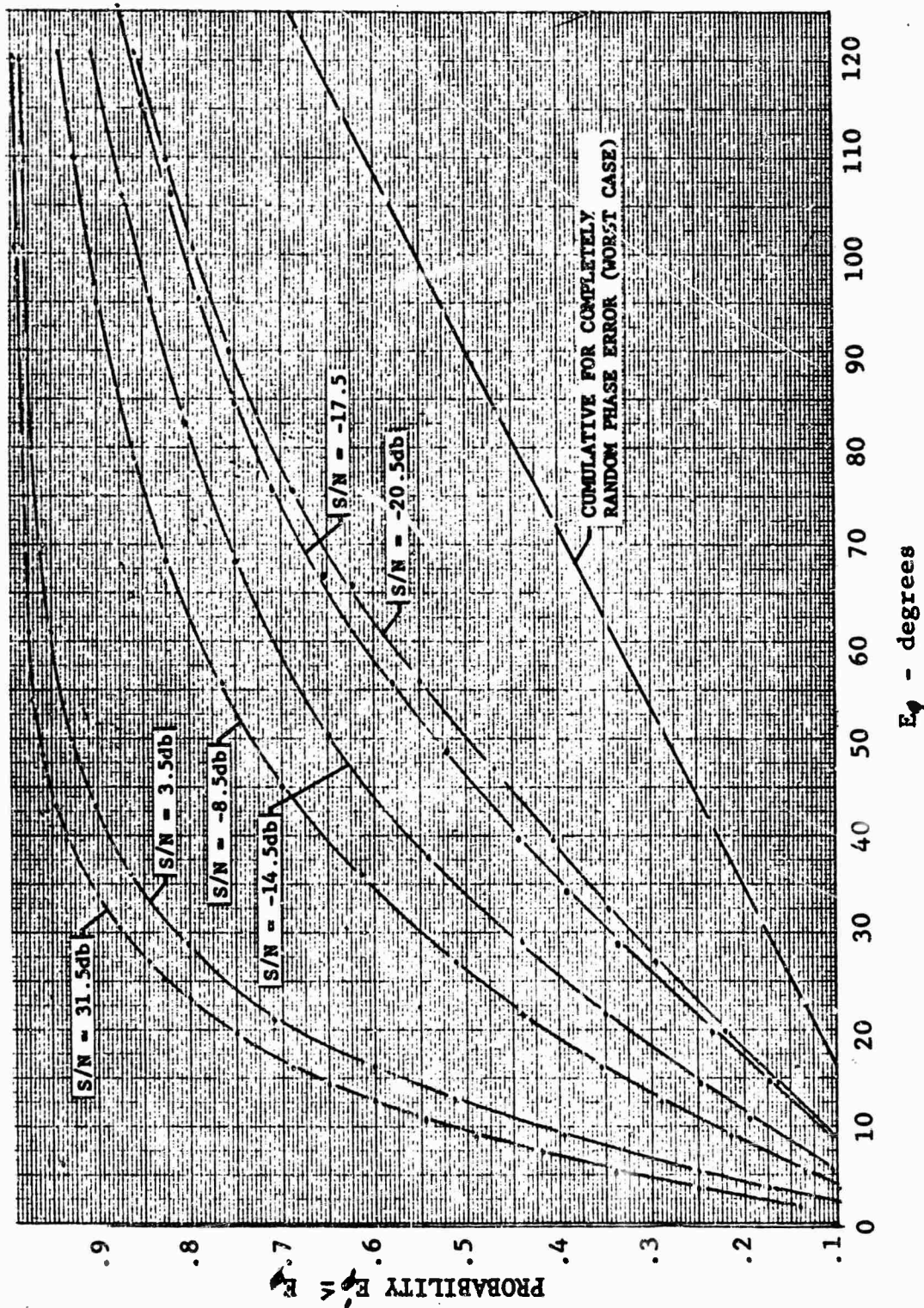
Fig. 79 PHASE DEGRADATION OF MODEL 3 BASED ON AVERAGE
REFERENCE

104

The measured and computed results obtained for the case of (T $\pi/4$, R $\pi/4$) are presented in Figures 80 through 91. The matrix data used in the computations was that obtained under the best S/N conditions. Inspection of the data indicates that remarkable cross section and phase fidelity is maintained by use of the scattering matrix. This is most noticeable in a comparison of the computed and measured results obtained in the case of Model 3 which exhibits the finest lobe structure of the three models measured. The results of this experiment indicate the practicality of using the scattering matrix to obtain cross section and phase for polarization conditions other than the principal polarizations used in the scattering matrix. Use of this approach could result in a substantial reduction in the cost of obtaining data since the computation time required for a given polarization condition is less than a minute when a 7090-type computer is used and data is computed at every 0.1 degree through 360 degrees. Hence the time involved in obtaining cross section information by using the scattering matrix versus that using a measurement system is several orders of magnitude smaller.

Fig. 80 MEASURED CROSS SECTION FOR (T π/4, R π/4) MODEL 1

Fig. 81 COMPUTED CROSS SECTION FOR $(T \pi/4, R \pi/4)$ MODEL 1

Fig. 82 MEASURED PHASE FOR (T π/4, R π/4) MODEL 1

108

Fig. 83 COMPUTED PHASE FOR (T π/4, R π/4) MODEL 1

109

Fig. 84 MEASURED CROSS SECTION FOR (T π/4, R π/4) MODEL 2

110

Fig. 85 COMPUTED CROSS SECTION FOR (T π/4, R π/4) MODEL 2

111
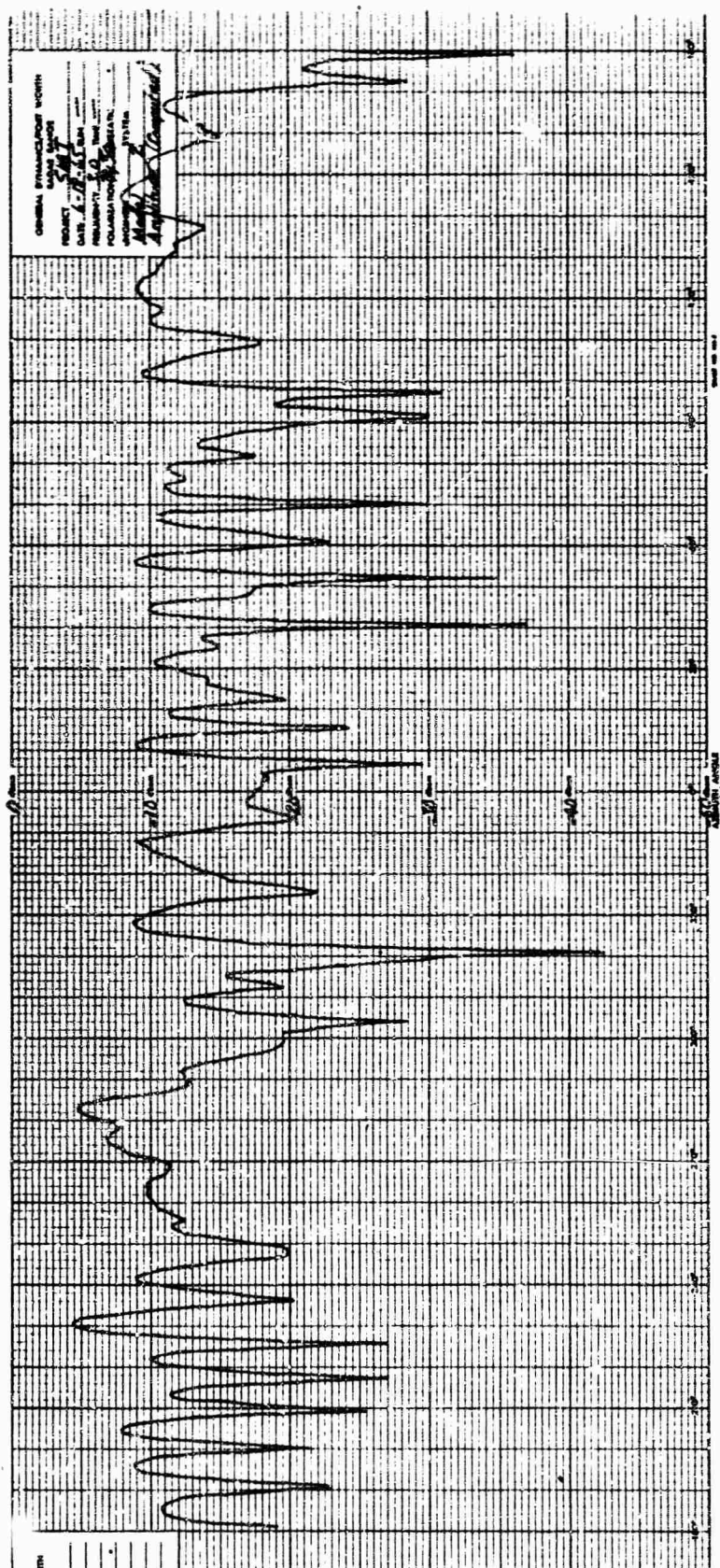
Fig. 86 MEASURED PHASE FOR (T π/4, R π/4) MODEL 2
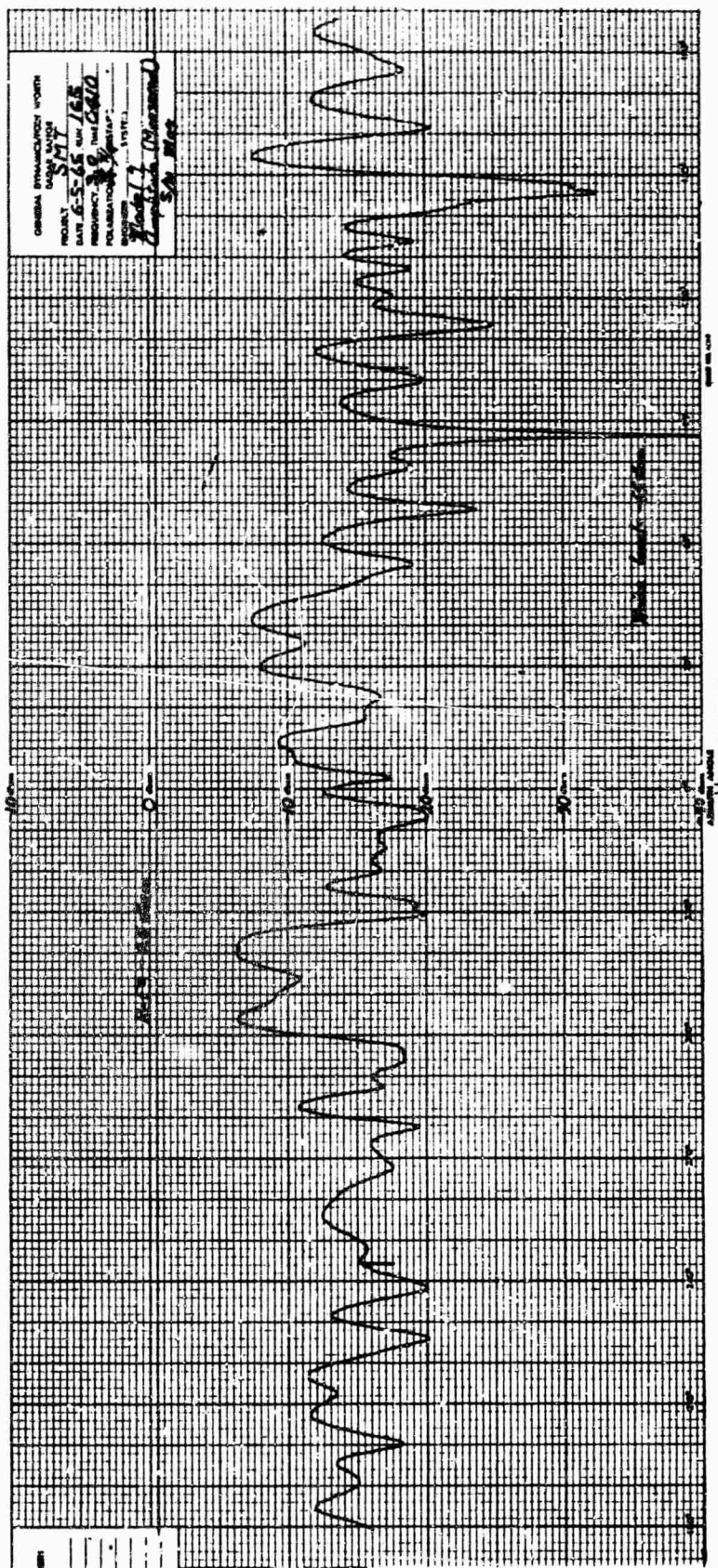
Fig. 87 COMPUTED PHASE FOR (T π/4, R π/4) MODEL 2

113

Fig. 88 MEASURED CROSS SECTION FOR (T π/4, R π/4) MODEL 3

114
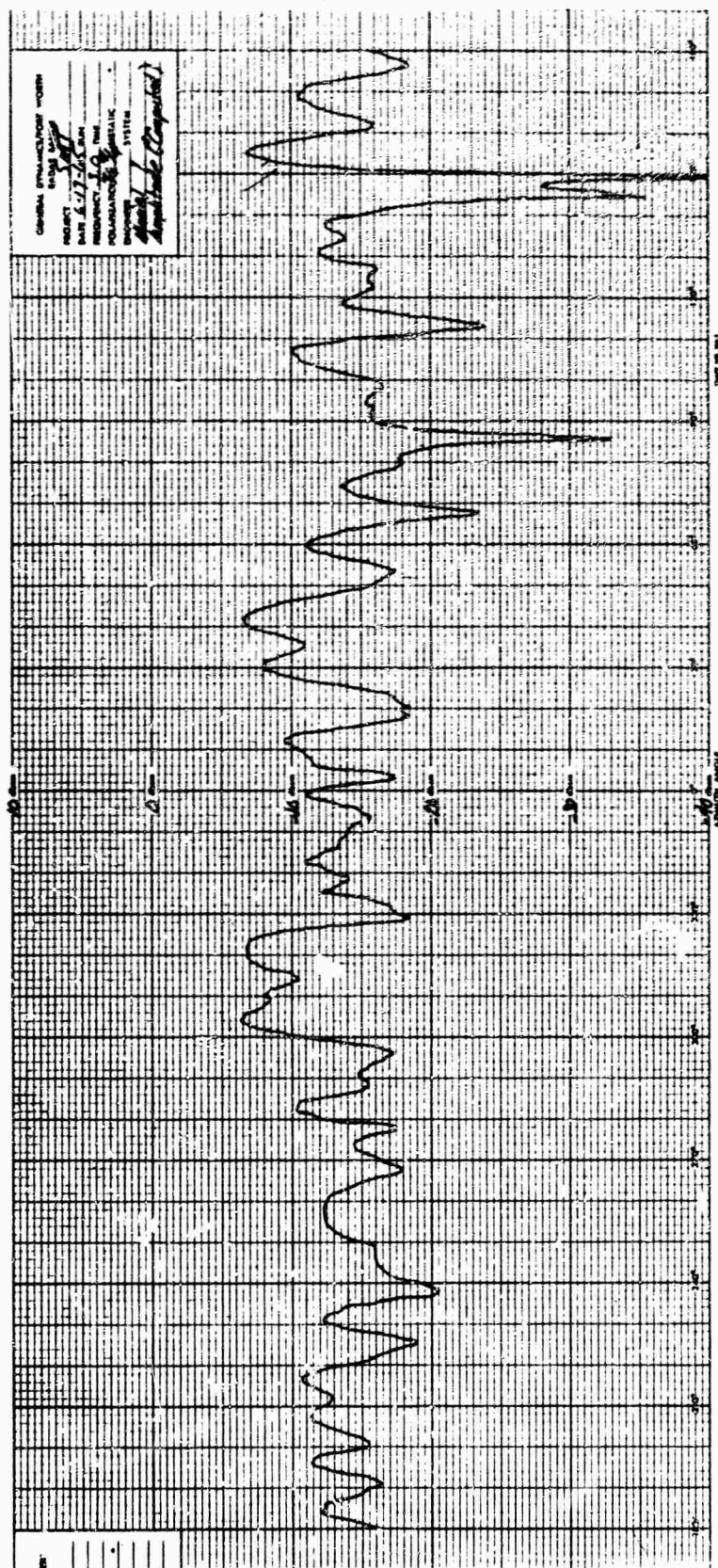
Fig. 89 COMPUTED CROSS SECTION FOR (T π/4, R π/4) MODEL 3
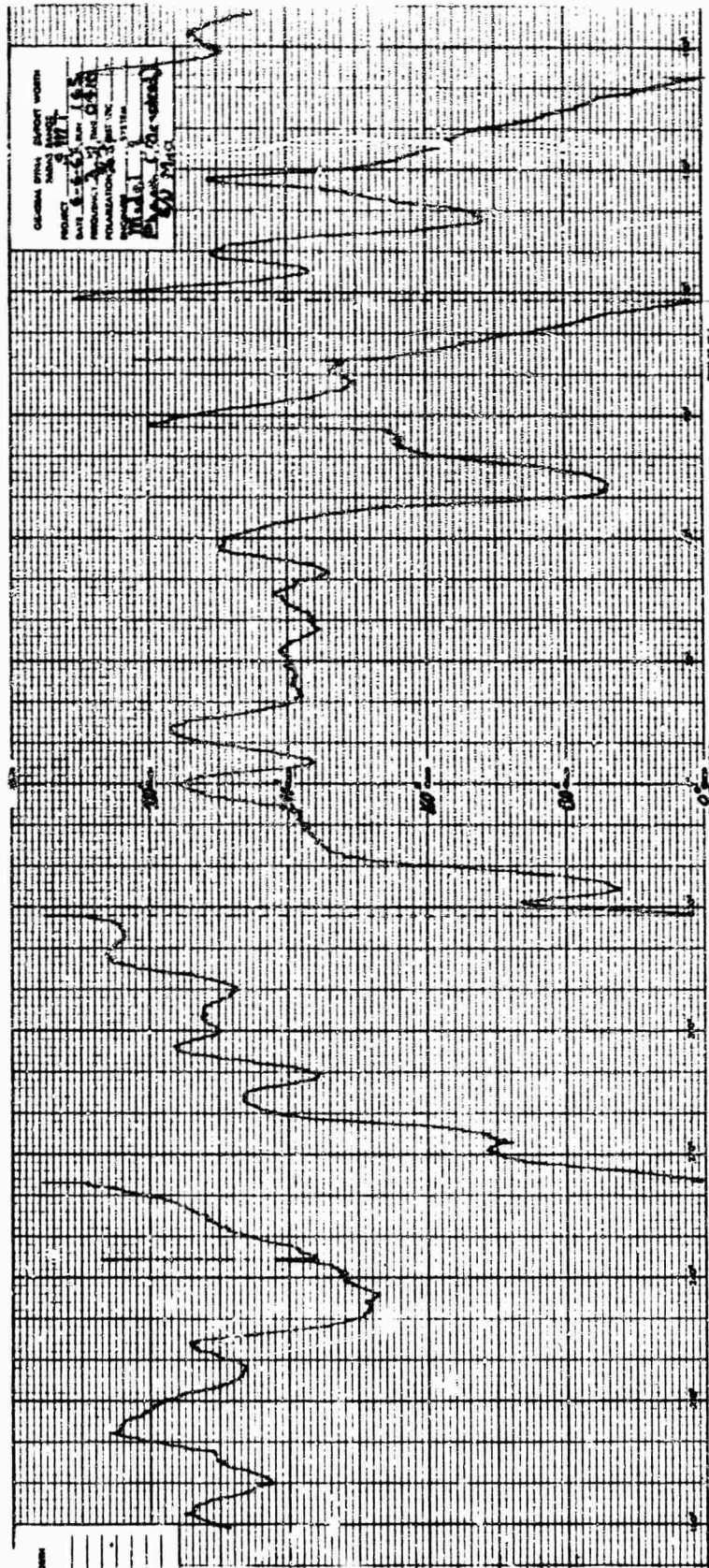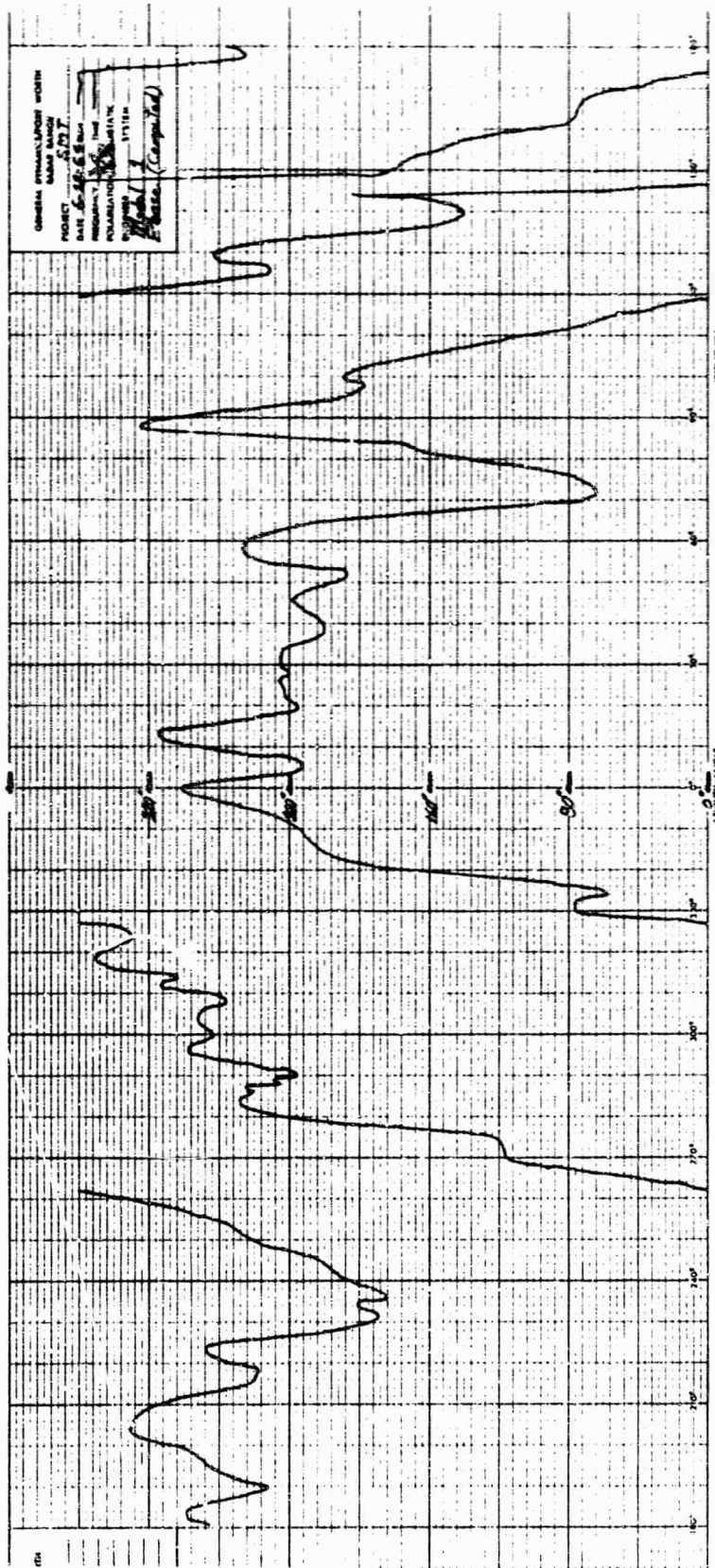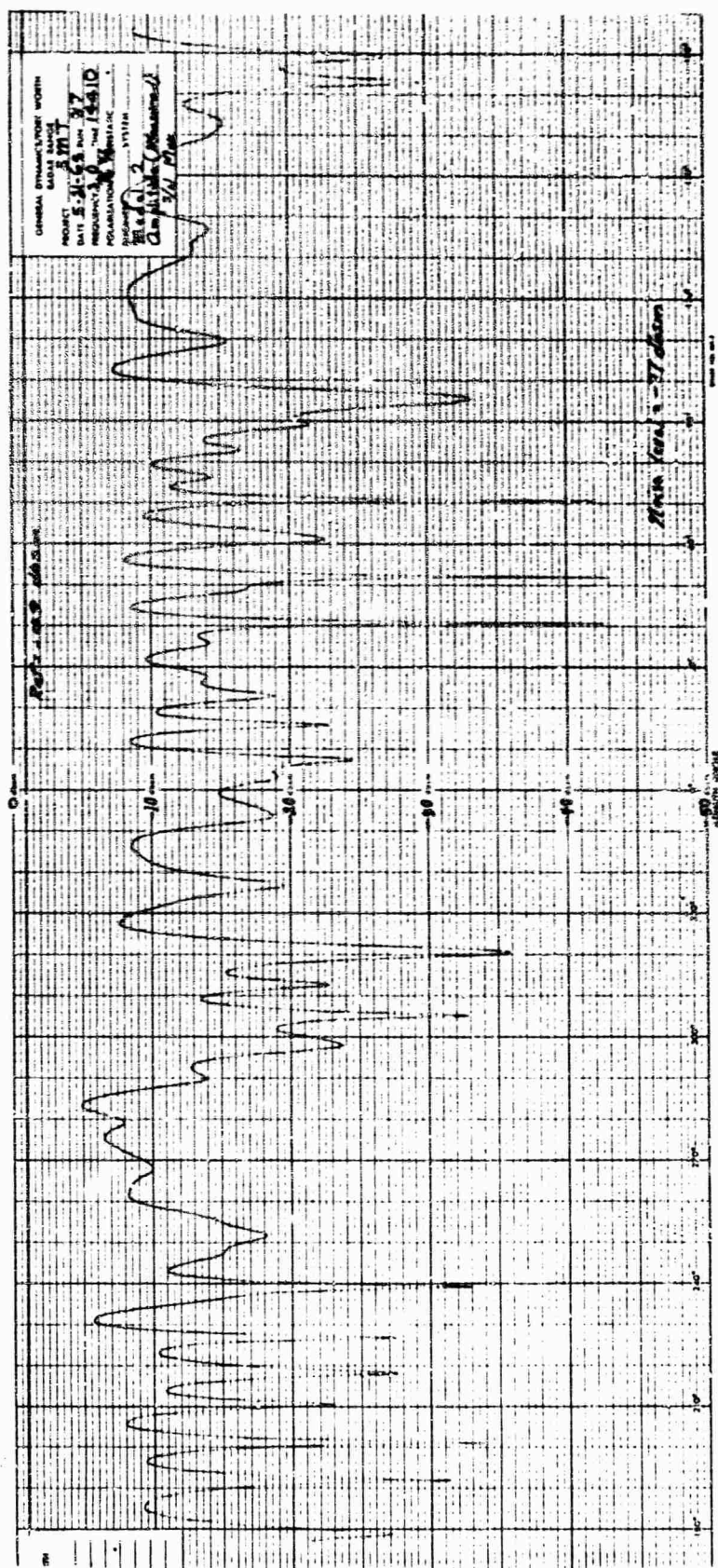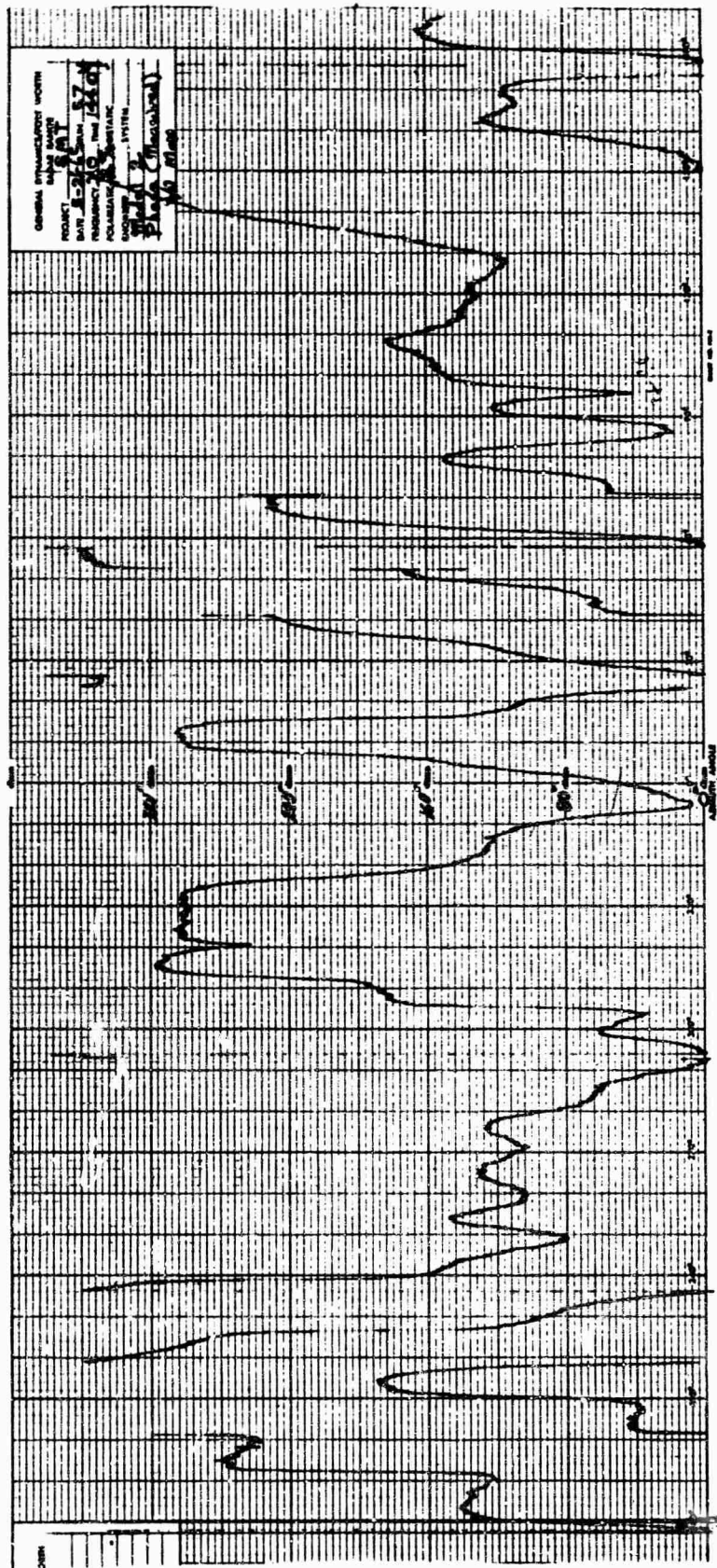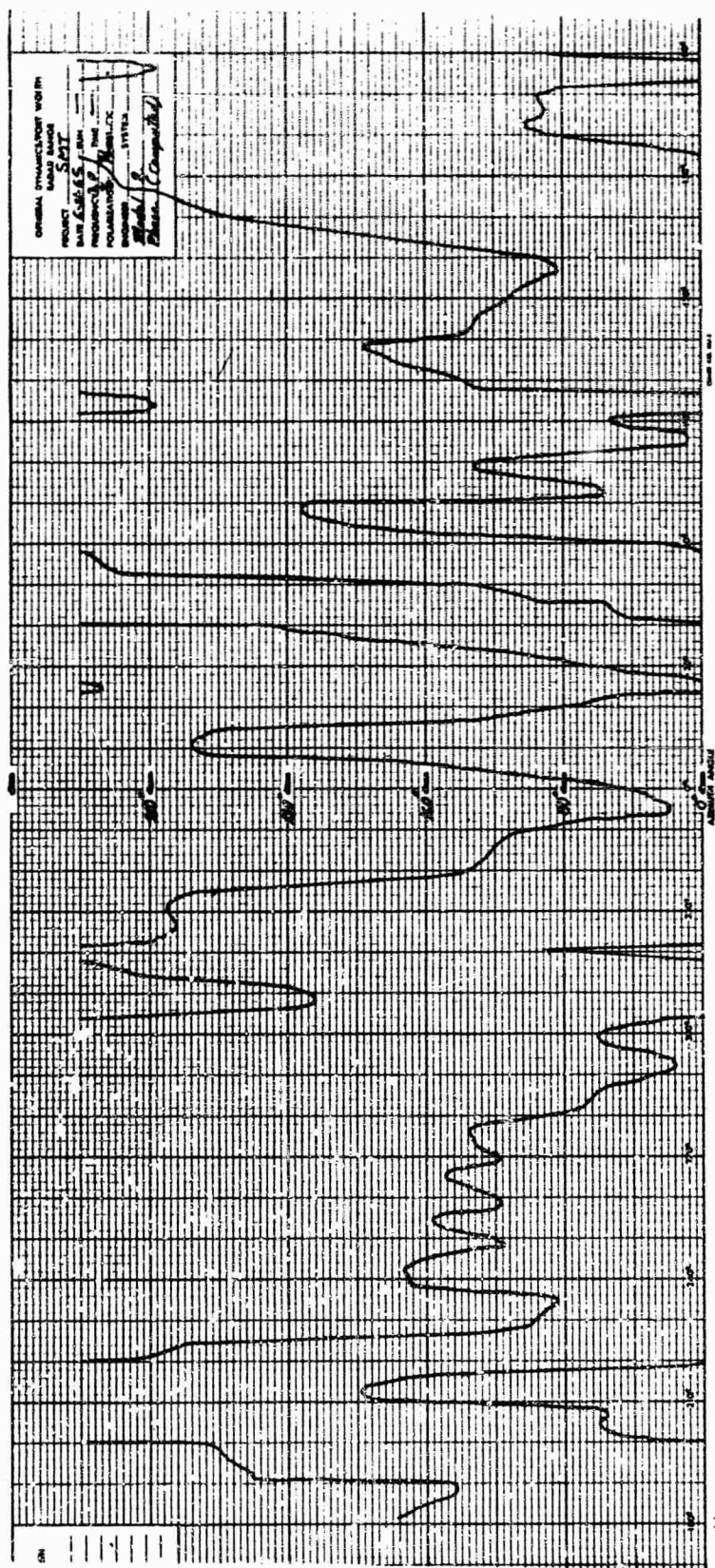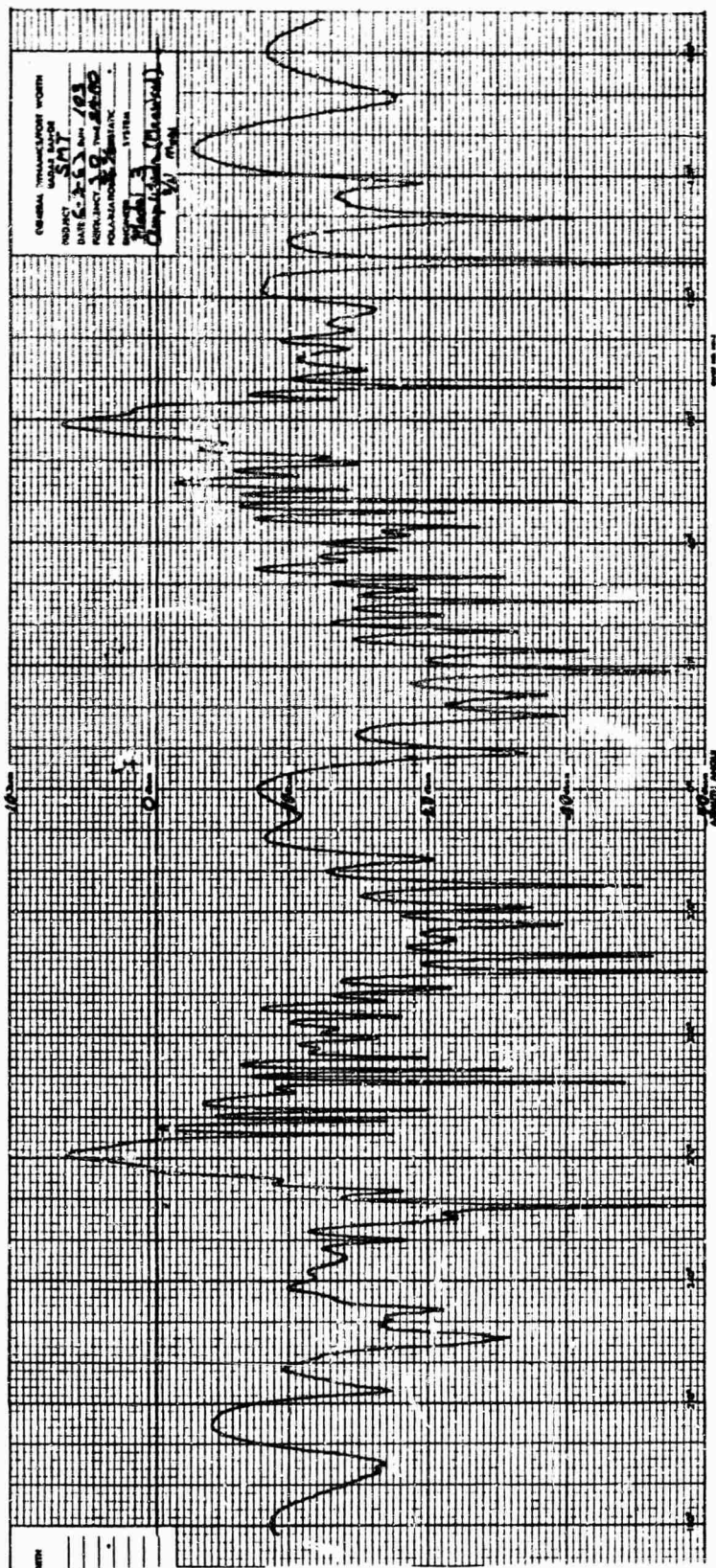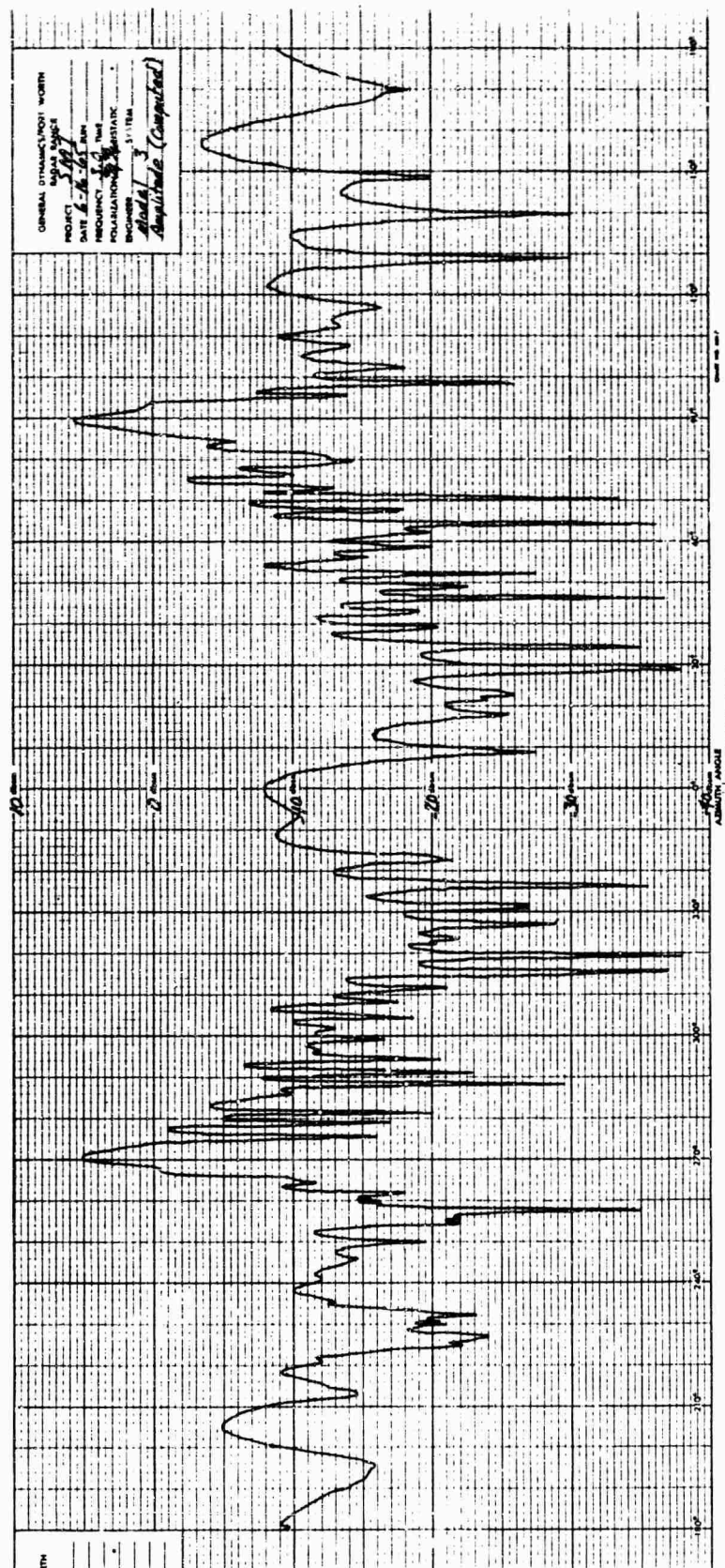
Fig. 90 MEASURED PHASE FOR (T π/4, R π/4) MODEL 3

Fig. 91 COMPUTED PHASE FOR (T π/4, R π/4) MODEL 3

117
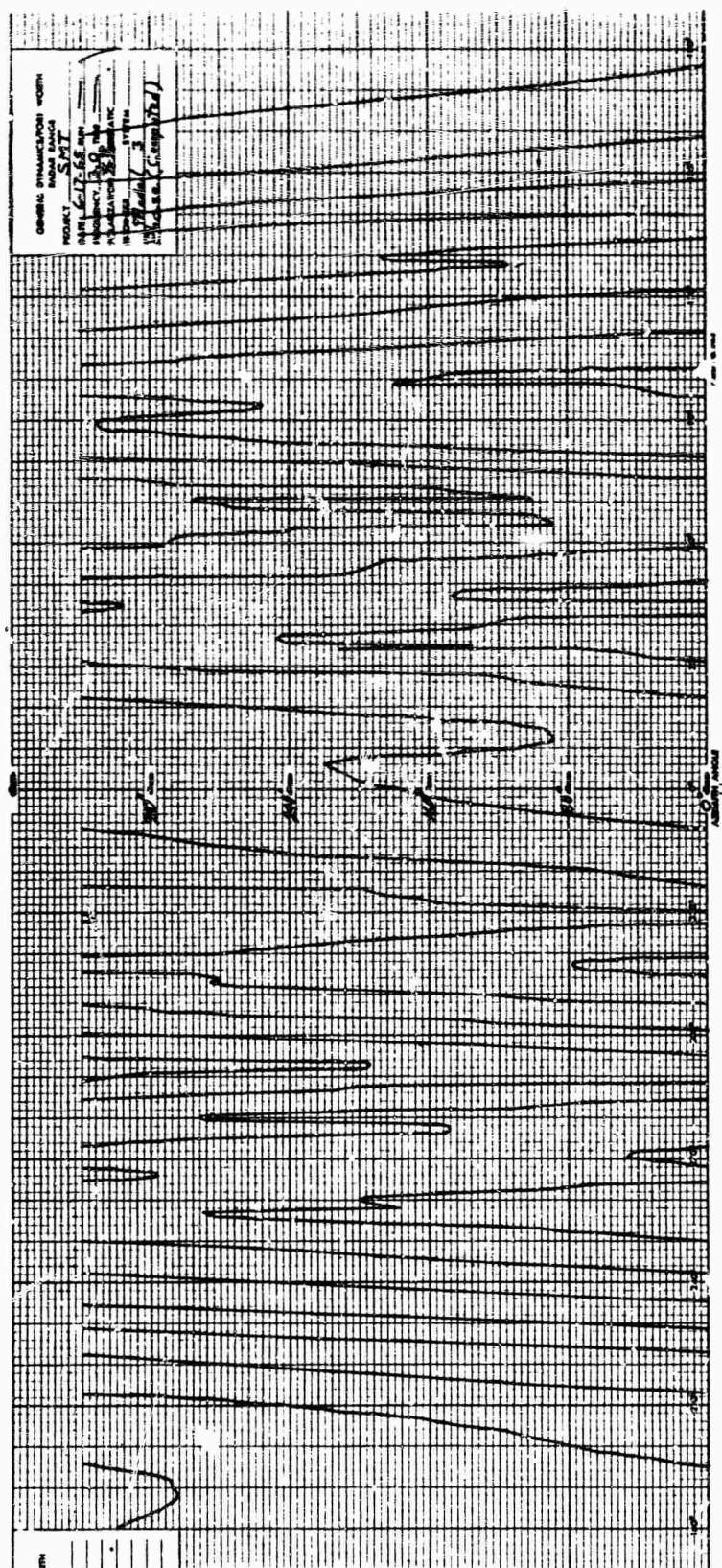
SECTION IV

SUMMARY

The data presented in Section III, along with the other data obtained during the program provide a substantial amount of information for use in studying phenomena associated with target scattering matrices. The data were obtained by using models which produced distinctly different types of matrices; hence the resultant information can be applied to the study of a large class of scatterers. The conditions under which the data were obtained, along with the quality of the data, provide information related to the feasibility of using the scattering matrix to obtain cross section at arbitrary polarizations rather than using a measurement capability to perform this task.

Although there are many investigations which could be conducted by using the data obtained, the primary purpose set for this initial investigation was to examine the influence of using noisy matrix element data to perform cross section calculations at other polarizations. The results of this study directly apply to the design of a radar to be used in obtaining scattering matrix data on a particular class of targets. Conversely, the results of the program indicated the error to be expected by using a scattering matrix of use elements were obtained with an X-db (peak or average) S/N ratio. The program results are discussed in terms of the degradation curves and the computed versus measured data; other investigations are then described in terms of those which could be performed by using the data available from this program; finally, other investigations are suggested in terms of those which would yield useful information concerning the use of target scattering matrices.

Degradation Results

Although other parameters, such as aspect alignment and calibration errors (phase and/or amplitude) between elements of the matrix, would also degrade the data obtained from the scattering matrix, noise degradation is a common problem associated with radar design. This is especially true if the radar is to be designed to obtain scattering matrix information for use in vehicle signature studies. Section III contains an outline of the approach selected to study data degradation that results from using a scattering matrix whose elements are degraded by noise.

In order to obtain results applicable to a number of practical situations, the models were selected to produce matrices of the types which would often be observed during use of the vehicles and frequencies of interest. For each model, thirty six hundred azimuth points and five polarizations were used in order to generate an ensemble of errors which were considered representative of those to be encountered in general via computations based on the use of a scattering matrix transformation. In the case of each model, the S/N was varied over a dynamic range to obtain data substantially without error and such that each element of the matrix had noise error 100 percent of the time. However, because of the possible uses of scattering matrix data, the results, Figures 68 through 79, are difficult to interpret relative to some single criterion of goodness (i.e., it is difficult to draw a set of conclusions, which are quite general and yet directly applicable to most situations). However, the degradation data has been put in such a form that a sufficient value of S/N can be determined if the amount of error E_σ and E_ϕ which can be tolerated and certain target scattering characteristics can be determined. The target scattering characteristics which need be determined are the type matrix properties as classified for Models 1, 2, and 3, and either the average of maximum cross section to be expected.

118

If the average cross section level (dbsm average) is used, comparison of Figures 74 through 79 versus Figures 68 through 73 shows that the need for classifying the target scattering matrix becomes relatively unimportant. That is, inspection of the average reference curve data indicates that for a selected error and a selected percent of the time, the S/N is approximately the same for all three types of targets. However, there is enough of a difference between the curves as a function of model matrix to indicate a trend. The trend indicates that required S/N levels for complex targets such as Models 1 and 2, which have a significant amount of depolarization, are as high or higher than for Model 3 type targets. Although this may seem surprising because of the dynamic range and rapid variations associated with Model 3, in comparison to those for the other models, Model 3 also exhibits considerably less depolarization than the other two models. Hence, in the case of Models 1 and 2, matrix transformation data depends primarily upon three amplitudes and two phases; whereas in the case of Model 3, it depends primarily on only two amplitudes and one phase. When a comparison is made of the degradation data of Model 1, in which the relative phase terms are slowly varying, and that of Model 2, in which phase and amplitude variations are rapid, it appears that the errors in data obtained using the three elements with slowly varying relative phase are the same as the errors in that obtained using two elements whose relative phase varied rapidly with azimuth. However, in the case of Model 2, the transformations involved a three element, rapidly varying phase matrix, and the errors were noticeably larger than those obtained in the other two cases.

In the case of a particular polarization, such as (TR, RR), the above conclusions would probably be reversed since, in the case of these conditions, specular and symmetrical type targets would tend to exhibit zero cross section; whereas Models 1 and 2 type target would not. However, as discussed earlier, in order to generate error curves of practical interest, only one orthogonal type polarization was used of the five studied.

Although the particular values of E_σ and E_ϕ will depend upon the intended use of data generated from the scattering matrix, it is noted that, when a goodness criterion of 3 db at the 1σ point ($E_\sigma \leq 3$ db 65 percent of the time) is used, the S/N (average reference) must be greater than 5 to 14 db depending on the type of target. Signal-to-noise ratios of this type are presently used in radar design based on detection criterion using acceptable false alarm rates (Reference 5). However, if the 3 db criterion is shifted to 2σ points ($E_\sigma \leq 3$ db 95 percent of the time) the required S/N is greater than 20 to 30 db, or practically speaking, large enough to include the dynamic range of the scattering matrices of the type being considered. Another interpretation would be that 5 percent of the time errors greater than 3 db would most likely be present due to error sources in the measured data. Although this might seem unrealistic at first glance, inspection of Equation 19 shows that for any target which has a significant dynamic signature, the number of times that a σ_{tr} computation will depend upon the difference of two numbers approximately equal will be significant. Hence, seemingly insignificant errors in the measured data can yield significant errors in computed results. (This problem is not eliminated by a measurement system capable of measuring $\sqrt{\sigma_{tr}}$ since minor discrepancies in adjusting γ_t, γ_r, δ_t and δ_r produce the same magnitude errors.) That is, when a vector summation involving three vectors (analytically or mechanically) each which cover a significant amplitude and phase dynamic range is performed, unless the vectors are unrealistically error free, there is a large likelihood that large errors will be present a few percent of the time. The data obtained in this study indicate that the magnitude of this few percent is around 5 in the case of the class of targets considered. This percentage would of course be reduced if matrices of the static scalar type (e.g., a sphere type) had been considered.

119

Before the computed versus measured results are discussed, it is interesting to compare the required S/N ratios indicated by the matrix degradation study with those based on a different type of scattering characteristic degradation. The scattering characteristic chosen for comparison was one associated with lobe widths as a function of azimuth. Although other characteristics, such as the maximum value of the major lobes, could be used, the lobe width parameter L/λ which commonly appears in functional forms such as $(\sin X/\chi)^2$ and $(J_1(X)/\chi)^2$ was selected for use as a degradation measure. There is a difficulty in applying a degradation measure of this type in that it is difficult to select the lobes and/or number of lobes to be used in arriving at an acceptable S/N level. This problem is associated with the decision as to the functional form which best relates the lobe structure to some characteristic dimension. However, an indication as to the amount of error in the parameter L/λ as a function of S/N can be obtained using either of the functional forms indicated above; the differences in results being second order.

Shown in Figure 92 is a plot of percent error in the parameter L as a function of S/N. The curve was generated using the functional form $\sin X/\chi$ where $X = KL$ $\sin \Delta\theta$, L represents the characteristic dimension, $\Delta\theta$ the angular distance from the lobe maximum, and K a constant proportional to frequency. The expression for error in percent is given by

$$\% \text{ error} = \left(\frac{X^1}{X} - 1\right) 100 \qquad (20)$$

where

$X^1 = KL^1 \sin \Delta\theta$ = value of X determined using lobe plus noise

$X = KL \sin \Delta\theta$ = value of X determined using lobe.

The value of X used as a reference was that determined by the 6 db value of $(\sin X/\chi)^2$. Also, the S/N axis plotted in Figure 92 was referenced to this point. The percent error curve is relatively insensitive to the value of X chosen as a reference as long as the S/N axis remains fixed relative to some criterion such as the one used (i.e., relative to the 6 db point). If the curve of Figure 92 is applied to the data obtained for each of the models in the (TV, RV) case, it is seen that using a 10 percent error criterion the required noise should be approximately 3 db below the 6 db point of the major lobes of interest. Using this criterion and selecting the two largest lobes on each of the model plots indicates that in the case of Model 1 a noise level equal to 1 db above the average cross section is acceptable. In the case of Model 2 a noise level approximately 2 db below the average is acceptable. In the case of Model 3 a noise level approximately 11 db above the average is acceptable. If the characteristic dimension error requirement is changed to 5 percent the above noise levels are decreased by 3 db.

Comparing these requirements with those discussed earlier, it is seen that the requirements are substantially relaxed, over those determined using the 3 db at 1σ point criterion. Hence, it is apparent that S/N ratios for systems designed to obtain the scattering matrix will normally be greater than for those designed to preserve simple characteristics of the major lobes of the target cross section.
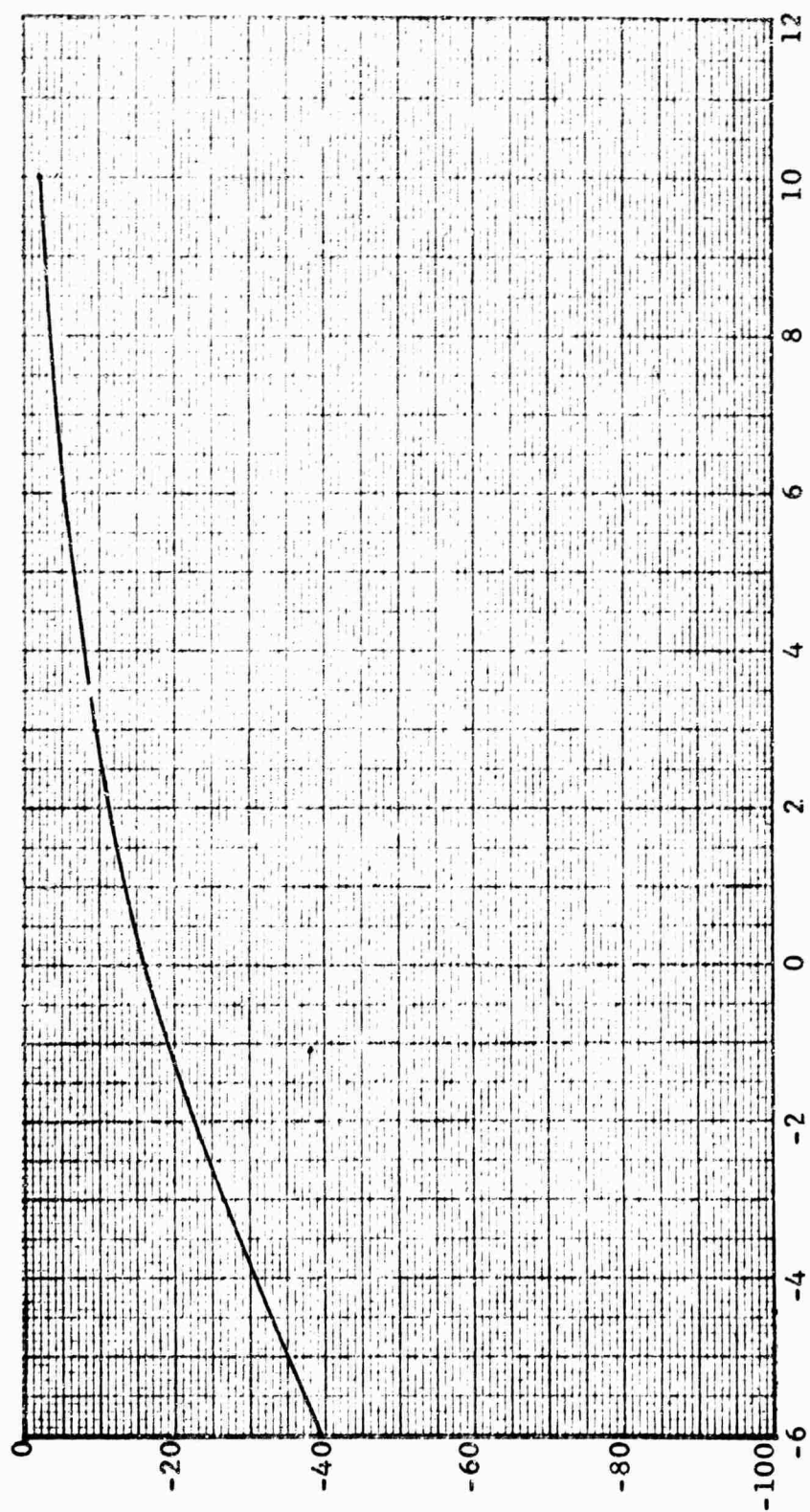
S/N RATIO AT THE LOBE 6 db POINT - db

Fig. 92   DIMENSION ERROR VERSUS S/N

121

In connection with the preservation of simple lobe characteristics, the data presented in Figure 93 shows the "false" lobe structure generated by computing cross section via the scattering matrix using data which is degraded with noise. The data in Figure 93 was computed using the matrix data obtained with a S/N ratio of -8.6 db referenced to average (12 db referenced to maximum). The data used in the computations is illustrated in Figures 36 and 37. The results of the computation indicate that a substantial amount of lobe structure was generated which could not be observed in a measurement system. Also, a comparison of Figure 93 with the data in Figure 88 indicates that a considerable amount of the "false" lobes in Figure 93 are of the same width as in the correct data of Figure 88.

Computed Versus Measured Data

A secondary but important part of the investigation was to compare cross section calculated via a scattering matrix transformation with measured data. The results of these experiments would provide information on the feasibility of using the scattering matrix to obtain cross section data for polarizations other than those needed for the matrix rather than measuring cross section under these other conditions. The data obtained in the investigation (Figures 80 through 91) indicate the results which can be achieved by using an absolute phase measuring system. Error cumulatives for these data are presented in Figures 94 and 95. The cumulatives in Figures 94 and 95 indicate errors similar to those produced in the degradation analysis using the next largest S/N ratio. Only in the case of Model 2 was there a significant azimuth range over which the amplitude and phase differences exceeded that which would probably suffice for most programs.

Although no attempt was made to estimate phase accuracy improvements which would be achieved by using a relative phase measuring system rather than an absolute type, the relative phase data presented in Figures 96 through 98 give an indication of the reduced requirements for the measuring system when these data are compared with the absolute phase data of Figures 82, 86, and 90. Although the relative phase patterns are shown for the case of $(T \pi/4, R \pi/4)$ relative to (TV, RV), the data is representative of the range independent θ and ψ parameters of Equation 19 which would be measured directly in a relative phase measuring system. In addition to the relaxed requirements for the recording system, the need for an extremely stable coherent oscillator is eliminated, and errors generated by target motions become insignificant.

On the basis of the results attained by using matrix data obtained in this study, it is considered quite feasible that an operational relative phase measuring system would provide matrix data sufficiently accurate to produce reliable cross section data at arbitrary polarizations if relative phase measuring equipment were used. Also, the program results indicate that in the case of static measurements, an absolute phase measuring system can be used at S band and below. However, when an absolute phase system is used on an outdoor range, target motion is a constant problem which degrades the phase data.

Additional Studies

In addition to the investigation of the noise degradation discussed, the data obtained during the program can be used in a number of studies, some of which are similar to that performed while others are associated with various uses of the scattering matrix.

122
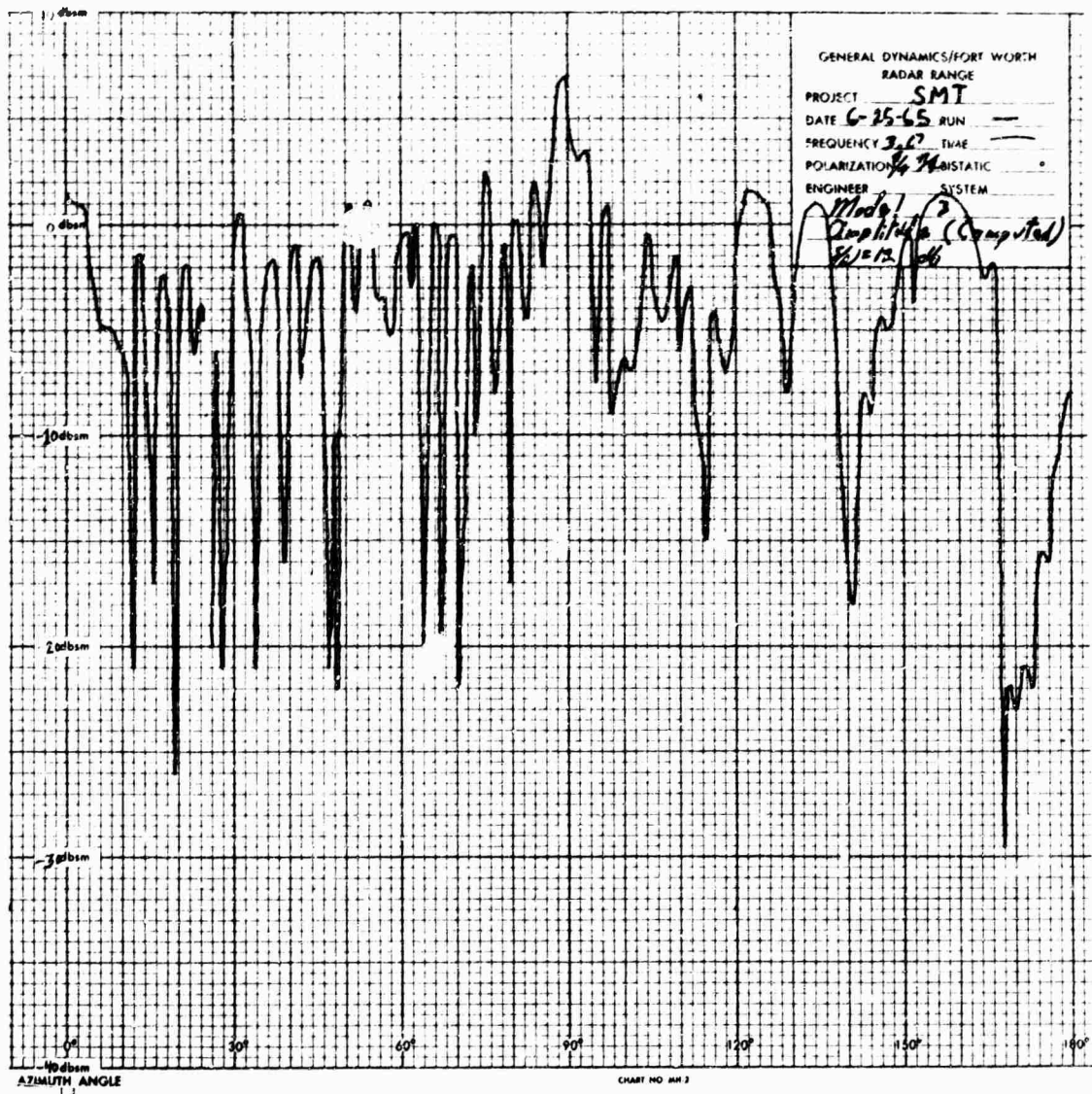
Fig. 93 COMPUTED CROSS SECTION OF MODEL 3 BASED ON DATA
OBTAINED AT S/N = -8.5
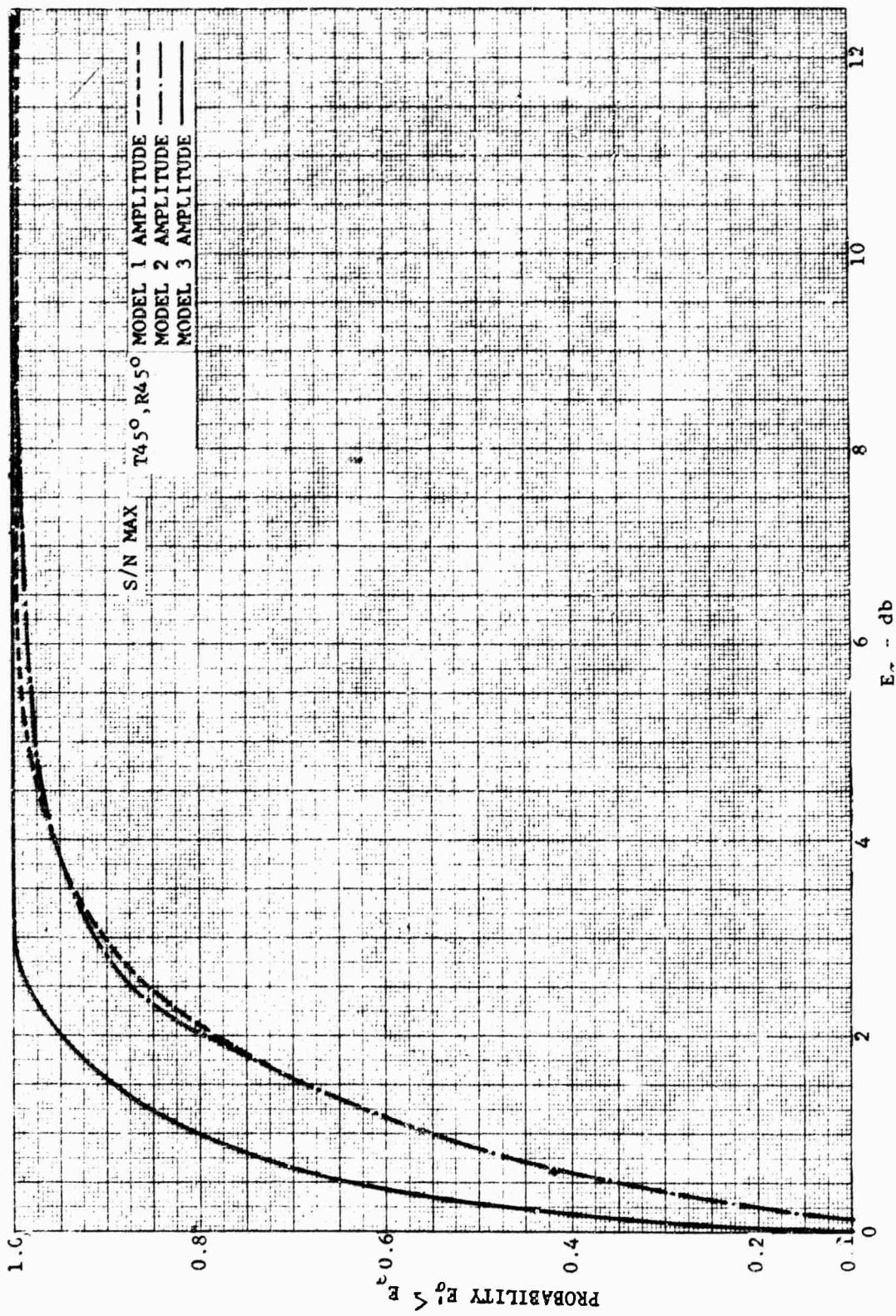
Fig. 94 CROSS SECTION ERROR BASED ON COMPUTED VERSUS MEASURED DATA

124
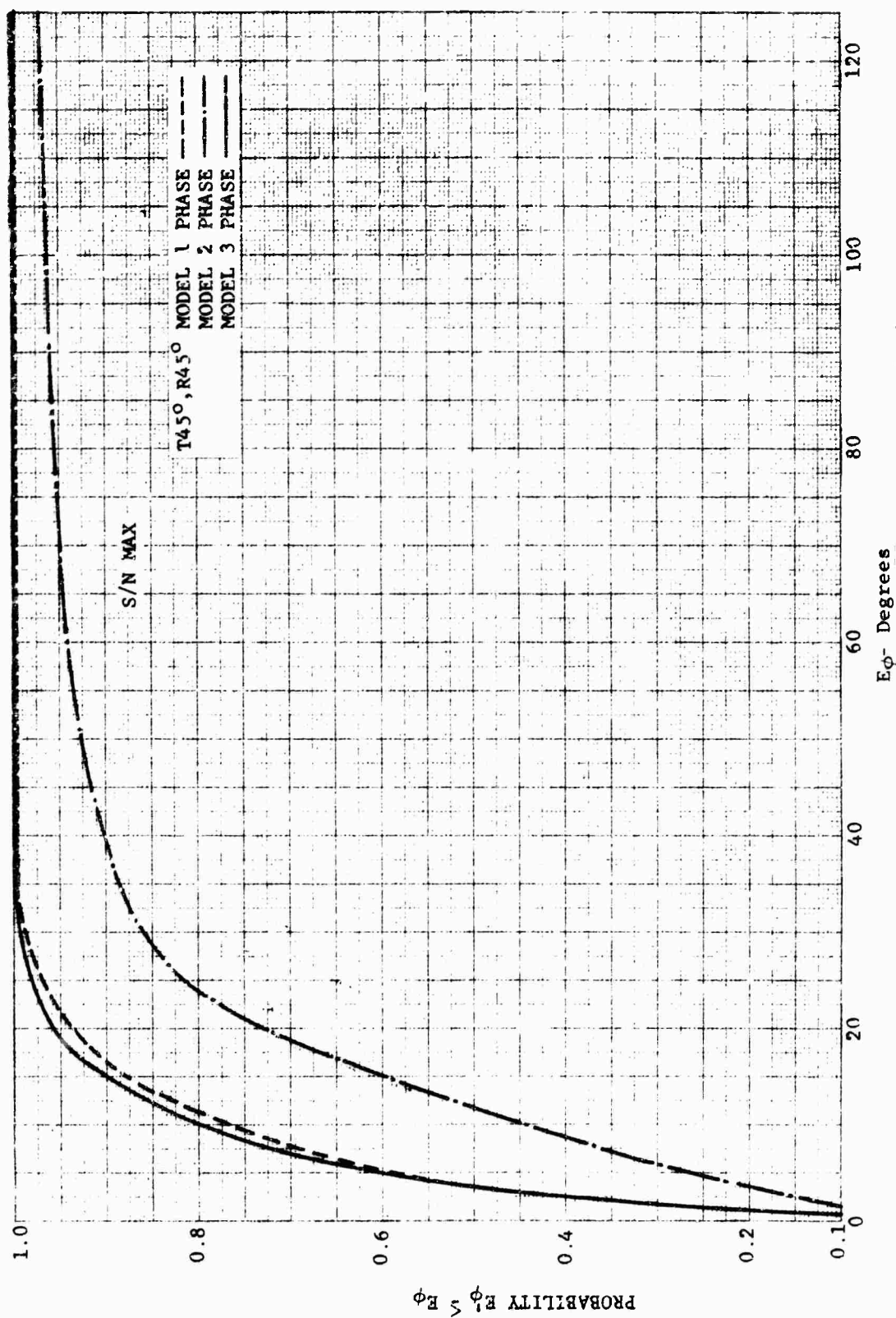
Fig. 95   PHASE ERROR BASED ON COMPUTED VERSUS MEASURED DATA
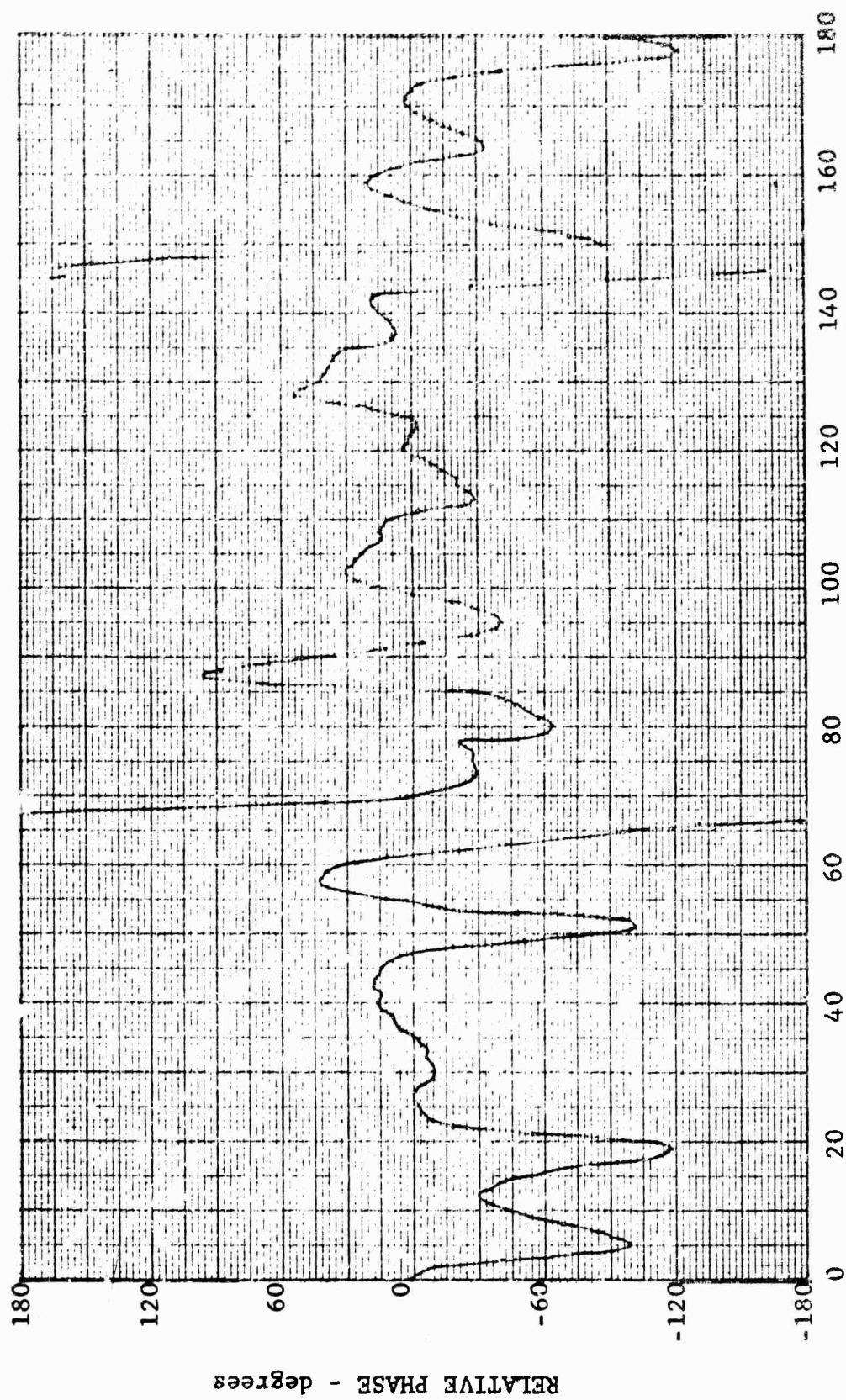
AZIMUTH - degrees

Fig. 96 RELATIVE PHASE PLOT BASED ON MODEL 1 DATA

RELATIVE PHASE - degrees

126
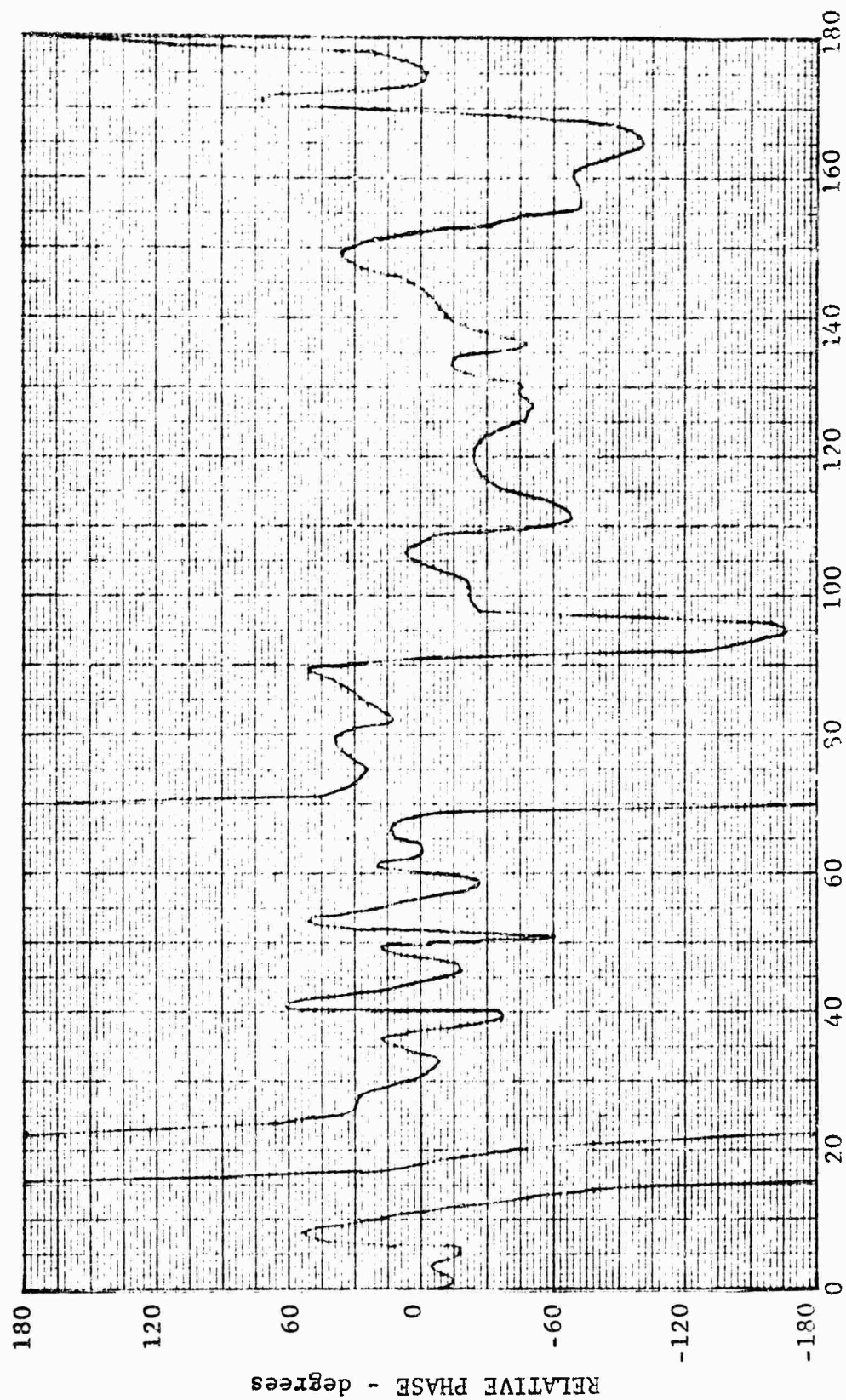
AZIMUTH - degrees

Fig. 97 RELATIVE PHASE PLOT BASED ON MODEL 2 DATA

RELATIVE PHASE - degrees

127

Fig. 98 RELATIVE PHASE PLOT BASED ON MODEL 3 DATA

AZIMUTH - degrees

RELATIVE PHASE - degrees

128

Additional information on the degradation of matrix performance could be obtained by investigation of (1) degradation versus constant phase error (calibration error), (2) degradation versus random phase and/or amplitude error, (3) a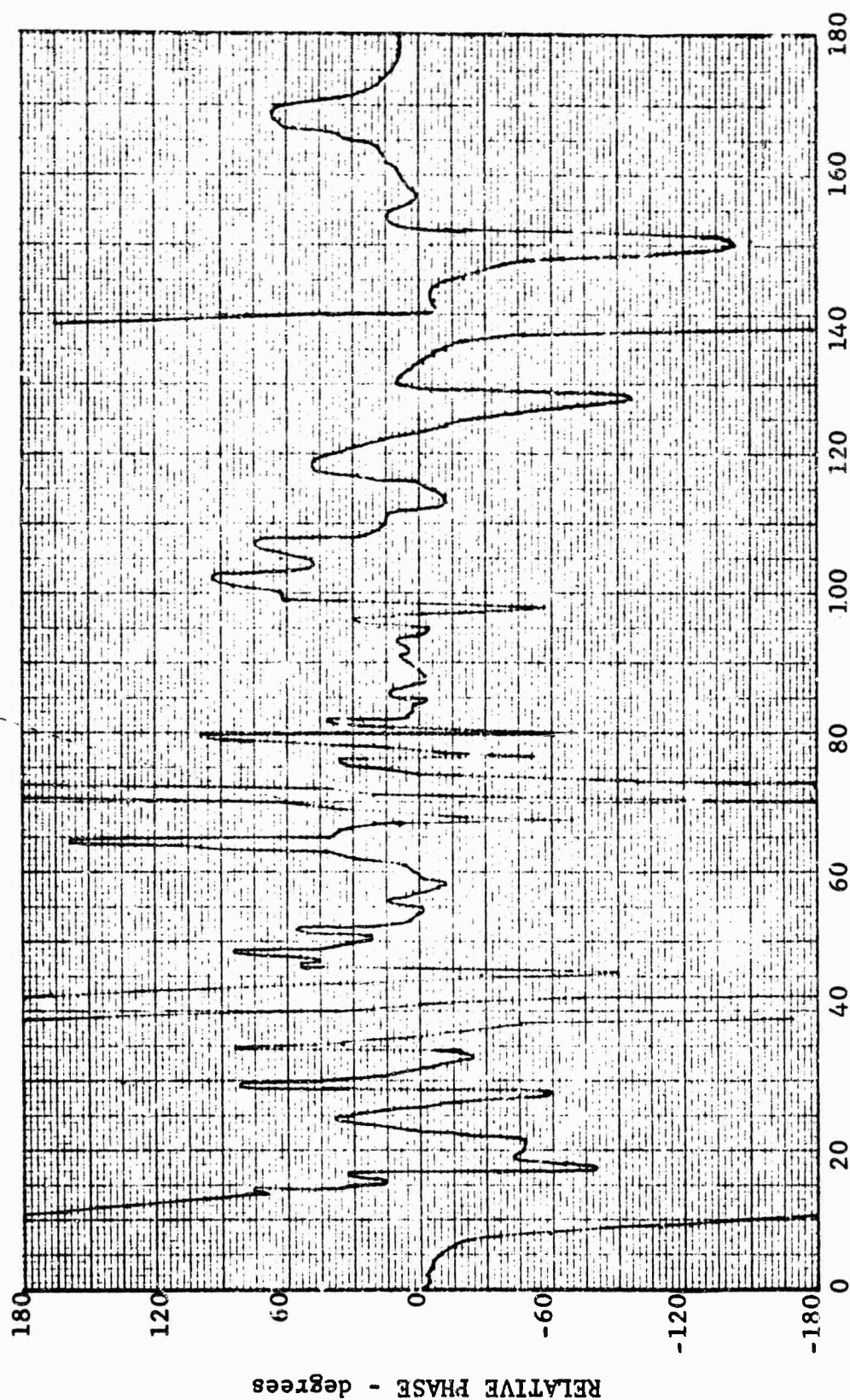cceptable S/N levels by using pattern comparison criteria based on statistical techniques, (4) degradation as a function of polarization, and (5) noise subtraction. There has been some investigation of degradation versus constant phase error (Reference 1); however, only a few matrices were used in the analysis (10) rather than the over 10 thousand matrices available from this program.

Investigation of degradation versus random phase and/or amplitude error would yield information similar to that generated by using the measured data obtained during this program at the lower S/N levels. In addition, results from these studies could be used to distinguish the amount of error caused by noise from that caused by measurement errors in the degradation data presented in Figures 68 through 79.

More studies relating to acceptable degradation levels by using different criterion are considered quite important in order to cover the class of potential uses of the scattering matrix. One such approach which has been considered is that of comparing degraded patterns with correct patterns by using statistical techniques for setting likeness confidence levels.

Although the polarizations used in this study were considered appropriate for generating general degradation curves, degradation curves as a function of polarization and type model would be of use in more specialized cases.

An investigation of subtracting noise from cross section data could be carried out using the measured data obtained at the lower S/N levels. The results of a study of this nature would indicate the amount of improvement over the degradation error curves presented in this report which could be expected by using analytical noise subtraction techniques.

All of the studies mentioned above can be conducted by using the scattering matrices generated during the program being reported, and they are related to the feasibility of using the scattering matrix in various programs. Studies related to potential uses of polarization versatility (scattering matrix transformations) which can be performed with the aid of a computer, and the data obtained under this program are (1) comparison of pattern recondition studies with and without the vehicle scattering matrix, (2) simulation of dynamic data by use of static data, (3) investigation of polarization stepping to reduce radar scintillation (analogous to frequency stepping). An example of the smoothing effect afforded by polarization stepping is shown in Figure 99. The data in Figure 99 was obtained using the scattering matrix of Model 3. Comparing the data in Figure 99 with that of Figures 24, 30, or 80 shows that polarization stepping produces a smoothing effect similar to that produced by frequency stepping (Reference 6). In addition to the averaging effect, the data obtained by polarization stepping preserves different characteristic lobes than would be preserved by frequency stepping at a fixed polarization. This fact might be quite useful in connection with (1) above.
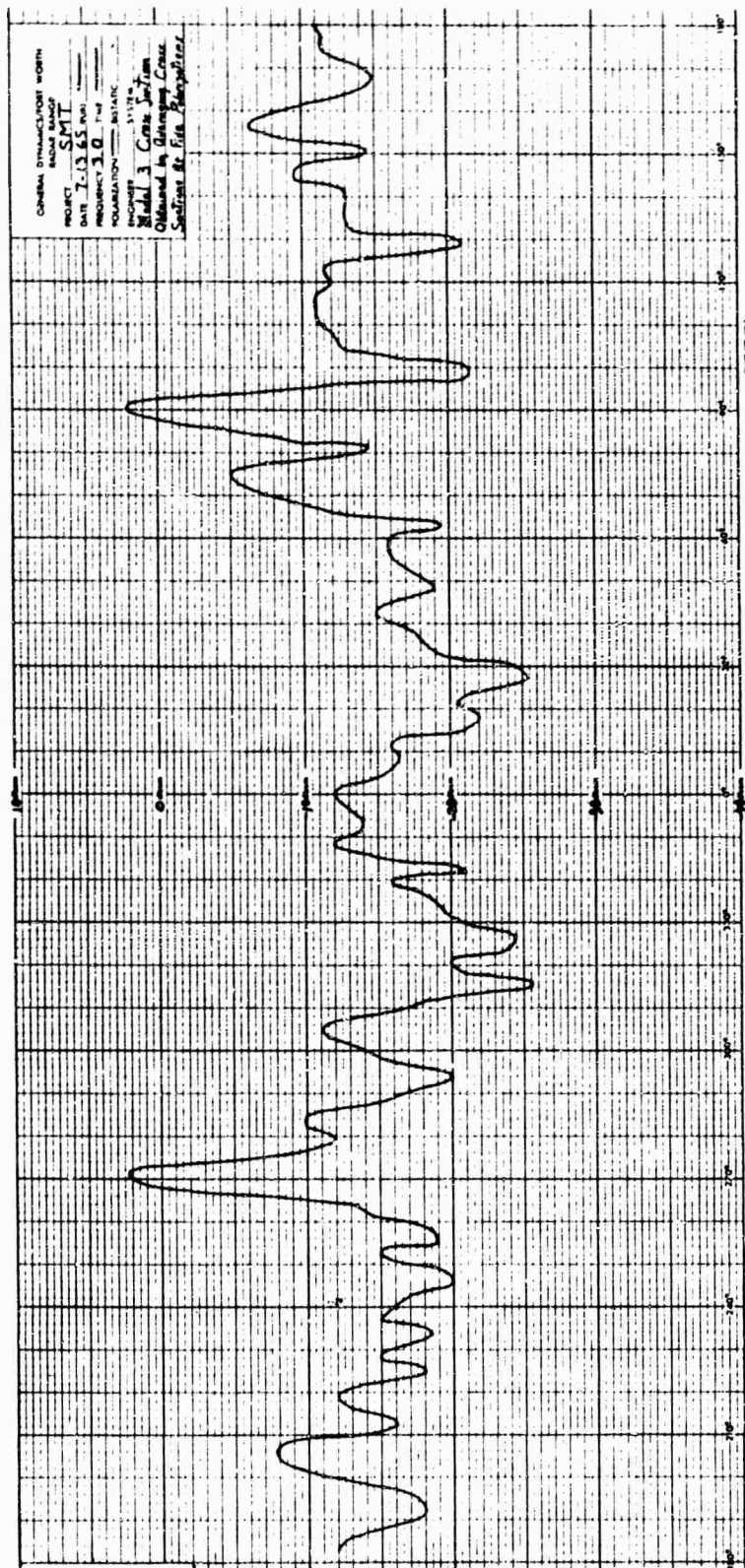
Fig. 99 POLARIZATION AVERAGED CROSS SECTION

130

REFERENCES

1. An Analysis of the Scattering Matrix Measurement Capabilities of a Ground Plane Radar Cross Section Range, Report No. RADC-TDR-64-317, June 1964.

2. Investigation of Measurement Errors of the RAT SCAT Cross Section Facility, Report No. RADC-TDR-64-397, July 1964.

3. RAT SCAT Phase Measurement System, Report No. FZE-344, General Dynamics/ Fort Worth.

4. Kouyoumjian, Robert G., "The Back Scattering From a Circular Loop," Applied Scientific Research, Section B, Vol. 6, April 1956, pp 165-179.

5. Skolnik, Merrill I., Introduction to Radar Systems, McGraw-Hill Book Co., Inc., New York, 1962.

6. A Theoretical Analysis and Experimental Results of a Frequency Stepping Method for Radar Scattering Measurements, Report No. RADC-TDR-64-150.

DOCUMENT CONTROL DATA - R&D

(Security classification of title, body of abstract and indexing annotation must be entered when the overall report is classified)

1. ORIGINATING ACTIVITY (Corporate author)	2a. REPORT SECURITY CLASSIFICATION
General Dynamics/Fort Worth	Unclassified
	2b. GROUP N/A

3. REPORT TITLE

Experimental and Analytical Investigation of Target Scattering Matrices

4. DESCRIPTIVE NOTES *(Type of report and inclusive dates)*

Final

5. AUTHOR(S) *(Last name, first name, initial)*

Freeny, C. C.

6. REPORT DATE	7a. TOTAL NO. OF PAGES	7b. NO. OF REFS
December 1965		6

8a. CONTRACT OR GRANT NO. AF30(602)-3716	9a. ORIGINATOR'S REPORT NUMBER(S)
b. PROJECT NO.	General Dynamics Report No. FZE-473
c. 6512	9b. OTHER REPORT NO(S) (Any other numbers that may be assigned this report)
d.	RADC-TR-65-298

10. AVAILABILITY/LIMITATION NOTICES This document is subject to special export controls and each transmittal to foreign governments or foreign nationals may be made only with prior approval of RADC (EMASF), GAFB, N. Y.

11. SUPPLEMENTARY NOTES	12. SPONSORING MILITARY ACTIVITY Rome Air Development Center Griffiss AFB New York 13442

13. ABSTRACT

Included in this report are the results of an investigation of scattering matrices of several types of targets. The primary purpose was to investigate the degradation of data resulting from cross section and phase computations by using a scattering matrix whose elements had been degraded by noise.

A review of the matrix representation of target scattering characteristics is presented along with a discussion of the measurement system and calibration procedure used to obtain the measured data. The measured data was obtained by using an absolute phase measuring radar system operating at 3 gigahertz. The scattering matrix of three targets, designed to exhibit distinctly different scattering characteristics, was measured at various signal-to-noise ratios. The measured data was then used as input data to an IBM 7090 which calculated cross sections and phase at five polarizations. The calculated data was used to generate degradation curves for each of the three types of targets. In addition, computed vs measured cross section and phase information on each of the three targets is presented for the case of 45-degree linear transmission and reception.

DD FORM 1473
1 JAN 54

14 KEY WORDS	LINK A		LINK B		LINK C	
	ROLE	WT	ROLE	WT	ROLE	WT
Scattering Matrix Radar Cross Section Signal to Noise Ratio						

INSTRUCTIONS

1. ORIGINATING ACTIVITY: Enter the name and address of the contractor, subcontractor, grantee, Department of Defense activity or other organization (corporate author) issuing the report.

2a. REPORT SECURITY CLASSIFICATION: Enter the overall security classification of the report. Indicate whether "Restricted Data" is included. Marking is to be in accordance with appropriate security regulations.

2b. GROUP: Automatic downgrading is specified in DoD Directive 5200.10 and Armed Forces Industrial Manual. Enter the group number. Also, when applicable, show that optional markings have been used for Group 3 and Group 4 as authorized.

3. REPORT TITLE: Enter the complete report title in all capital letters. Titles in all cases should be unclassified. If a meaningful title cannot be selected without classification, show title classification in all capitals in parenthesis immediately following the title.

4. DESCRIPTIVE NOTES: If appropriate, enter the type of report, e.g., interim, progress, summary, annual, or final. Give the inclusive dates when a specific reporting period is covered.

5. AUTHOR(S): Enter the name(s) of author(s) as shown on or in the report. Enter last name, first name, middle initial. If military, show rank and branch of service. The name of the principal author is an absolute minimum requirement.

6. REPORT DATE: Enter the date of the report as day, month, year; or month, year. If more than one date appears on the report, use date of publication.

7a. TOTAL NUMBER OF PAGES: The total page count should follow normal pagination procedures, i.e., enter the number of pages containing information.

7b. NUMBER OF REFERENCES: Enter the total number of references cited in the report.

8a. CONTRACT OR GRANT NUMBER: If appropriate, enter the applicable number of the contract or grant under which the report was written.

8b, 8c, & 8d. PROJECT NUMBER: Enter the appropriate military department identification, such as project number, subproject number, system numbers, task number, etc.

9a. ORIGINATOR'S REPORT NUMBER(S): Enter the official report number by which the document will be identified and controlled by the originating activity. This number must be unique to this report.

9b. OTHER REPORT NUMBER(S): If the report has been assigned any other report numbers (either by the originator or by the sponsor), also enter this number(s).

10. AVAILABILITY/LIMITATION NOTICES: Enter any limitations on further dissemination of the report, other than those imposed by security classification, using standard statements such as:

(1) "Qualified requesters may obtain copies of this report from DDC."

(2) "Foreign announcement and dissemination of this report by DDC is not authorized."

(3) "U. S. Government agencies may obtain copies of this report directly from DDC. Other qualified DDC users shall request through

_____."

(4) "U. S. military agencies may obtain copies of this report directly from DDC. Other qualified users shall request through

_____."

(5) "All distribution of this report is controlled. Qualified DDC users shall request through

_____."

If the report has been furnished to the Office of Technical Services, Department of Commerce, for sale to the public, indicate this fact and enter the price, if known.

11. SUPPLEMENTARY NOTES: Use for additional explanatory notes.

12. SPONSORING MILITARY ACTIVITY: Enter the name of the departmental project office or laboratory sponsoring (paying for) the research and development. Include address.

13. ABSTRACT: Enter an abstract giving a brief and factual summary of the document indicative of the report, even though it may also appear elsewhere in the body of the technical report. If additional space is required, a continuation sheet shall be attached.

It is highly desirable that the abstract of classified reports be unclassified. Each paragraph of the abstract shall end with an indication of the military security classification of the information in the paragraph, represented as (TS), (S), (C), or (U).

There is no limitation on the length of the abstract. However, the suggested length is from 150 to 225 words.

14. KEY WORDS: Key words are technically meaningful terms or short phrases that characterize a report and may be used as index entries for cataloging the report. Key words must be selected so that no security classification is required. Identifiers, such as equipment model designation, trade name, military project code name, geographic location, may be used as key words but will be followed by an indication of technical context. The assignment of links, rules, and weights is optional.